Living Rev. Solar Phys., **7**, (2010), 5
http://www.livingreviews.org/lrsp-2010-5

LIVING REVIEWS
in solar physics

Coronal Loops: Observations and Modeling of Confined Plasma

Fabio Reale
Dipartimento di Scienze Fisiche & Astronomiche,
Università di Palermo, Sezione di Astronomia,
Piazza Parlamento 1, 90134 Palermo, Italy
email: reale@astropa.unipa.it
http://www.astropa.unipa.it/~reale/

Accepted on 28 October 2010
Published on 8 November 2010

Abstract

Coronal loops are the building blocks of the X-ray bright solar corona. They owe their brightness to the dense confined plasma, and this review focuses on loops mostly as structures confining plasma. After a brief historical overview, the review is divided into two separate but not independent parts: the first illustrates the observational framework, the second reviews the theoretical knowledge. Quiescent loops and their confined plasma are considered, and therefore topics such as loop oscillations and flaring loops (except for non-solar ones which provide information on stellar loops) are not specifically addressed here. The observational section discusses loop classification and populations, and then describes the morphology of coronal loops, its relationship with the magnetic field, and the concept of loops as multi-stranded structures. The following part of this section is devoted to the characteristics of the loop plasma and of its thermal structure in particular, according to the classification into hot, warm, and cool loops. Then, temporal analyses of loops and the observations of plasma dynamics and flows are illustrated. In the modeling section some basics of loop physics are provided, supplying some fundamental scaling laws and timescales, a useful tool for consultation. The concept of loop modeling is introduced and models are distinguished between those treating loops as monolithic and static, and those resolving loops into thin and dynamic strands. Then, more specific discussions address modeling the loop fine structure and the plasma flowing along the loops. Special attention is devoted to the question of loop heating, with separate discussion of wave (AC) and impulsive (DC) heating. Finally, a brief discussion about stellar X-ray emitting structures related to coronal loops is included and followed by conclusions and open questions.

Imprint / Terms of Use

Living Reviews in Solar Physics is a peer reviewed open access journal published by the Max Planck Institute for Solar System Research, Max-Planck-Str. 2, 37191 Katlenburg-Lindau, Germany. ISSN 1614-4961.

Because a *Living Reviews* article can evolve over time, we recommend to cite the article as follows:

Fabio Reale,
"Coronal Loops: Observations and Modeling of Confined Plasma",
Living Rev. Solar Phys., **7**, (2010), 5. [Online Article]: cited [<date>],
http://www.livingreviews.org/lrsp-2010-5

The date given as <date> then uniquely identifies the version of the article you are referring to.

Article Revisions

Living Reviews supports two ways of keeping its articles up-to-date:

Fast-track revision A fast-track revision provides the author with the opportunity to add short notices of current research results, trends and developments, or important publications to the article. A fast-track revision is refereed by the responsible subject editor. If an article has undergone a fast-track revision, a summary of changes will be listed here.

Major update A major update will include substantial changes and additions and is subject to full external refereeing. It is published with a new publication number.

For detailed documentation of an article's evolution, please refer to the history document of the article's online version at http://www.livingreviews.org/lrsp-2010-5.

Contents

List of Tables

1 Introduction

The corona is the outer part of the solar atmosphere. Its name derives from the fact that, since it is extremely tenuous with respect to the lower atmosphere, it is visible in the optical band only during the solar eclipses as a faint crown (corona in Latin) around the black moon disk. When inspected through spectroscopy the corona reveals unexpected emission lines, which were first identified as due to a new element (coronium) but which were later ascertained to be due to high excitation states of iron (e.g., Golub and Pasachoff, 1997, 2001). It became then clear that the corona is made of very high temperature gas, hotter than 1 MK. Almost all the gas is fully ionized there and thus interacts effectively with the ambient magnetic field. It is for this reason that the corona appears so inhomogeneous when observed in the X-ray band, in which plasma at million degrees emits most of its radiation. In particular, the plasma is confined inside magnetic flux tubes which are anchored on both sides to the underlying photosphere. When the confined plasma is heated more than the surroundings, its pressure and density increase. Since the tenuous plasma is optically thin, the intensity of its radiation is proportional to the square of the density, and the tube becomes much brighter than the surrounding ones and looks like a bright closed arch: a coronal loop.

When observed in the X-ray band, the bright corona appears to be made entirely by coronal loops that can, therefore, be considered as the building blocks of X-ray bright corona. This review specifically addresses coronal loops as bright structures confining plasma. It first provides an observational framework that is the basis for the second part dealing with modeling and interpretation. There have been several earlier books (Bray *et al.*, 1991; Golub and Pasachoff, 1997; Aschwanden, 2004) and reviews (Vaiana and Rosner, 1978; Peres and Vaiana, 1990; Golub, 1996; Aschwanden *et al.*, 2001; Reale, 2005), in particular on coronal heating (Zirker, 1993; Cargill, 1995; Klimchuk, 2006), that have in general a larger or different scope but include information about coronal loops. Interested readers are urged to survey these other reviews in order to complement and fill in any gaps in topical coverage of the present paper.

2 Historical Keynotes

First evidence of magnetic confinement came from rocket missions in the 1960s. In particular, in 1965, arcmin angular resolution was achieved with grazing incidence optics (Giacconi *et al.*, 1965). The data analysis led to the first density and temperature diagnostics with wide band filters, to derive high pressure in compact regions with intense bipolar magnetic fields and to propose the magnetic confinement (Reidy *et al.*, 1968). The first coronal loop structures were identified properly after a rocket launch in 1968 which provided for the first time an image of an X-ray flare (Vaiana *et al.*, 1968), with a resolution of a few arcsec.

In the course of collecting the results of all rocket missions of the American Science and Engineering (AS&E) program, Vaiana *et al.* (1973) proposed a classification of the morphology of the X-ray corona as fundamentally consisting of arch-like structures connecting regions of opposite magnetic polarity in the photosphere. The classification was based on the loop size, on the physical conditions of the confined plasma, and on the underlying photospheric regions. They distinguished active regions, coronal holes, active regions interconnection, filament cavities, bright points, and large-scale structures (Vaiana and Rosner, 1978; Peres and Vaiana, 1990).

The magnetic structuring of the solar corona is evident. However, the magnetic field lines can be traced only indirectly because direct measurements are feasible generally only low in the photosphere through the Zeeman effect on spectral lines. It is anyhow possible to extrapolate the magnetic field in a volume. This was done to derive the magnetic field structure of a relatively stable active region by Poletto *et al.* (1975) using the Schmidt (1964) method, under the assumption of negligible currents in the corona. This was also useful to derive sufficient magnetic field intensities for hot plasma confinement. Later on, even more reliable magnetic field topologies were derived assuming force-free fields (e.g., Sakurai, 1981), i.e., with currents everywhere parallel to the magnetic field as it is expected in coronal loops.

The rocket missions lacked good time coverage and the information about the evolution of coronal loops was only limited, mostly available from the Orbiting Solar Observatory-IV (OSO-IV) mission (Krieger *et al.*, 1972). This satellite had an angular resolution in the order of the arcmin and could not resolve individual loops. In 1973 the X-ray telescope S-054 on-board Skylab monitored the evolution of coronal loops for several months, taking 32 000 X-ray photographs with a maximum resolution of 2 arcsec and an extended dynamic range. It was possible to study the whole evolution of an active region, from the emergence as compact loops filled with dense plasma to its late spreading, a few solar rotations later, as progressively longer and longer loops filled with less and less dense plasma (Golub *et al.*, 1982). It was confirmed that the whole X-ray bright corona consists of magnetic loops, whose lifetime is typically much longer than the characteristic cooling times (Rosner *et al.*, 1978). No exception is made by the coronal holes where the magnetic field opens radially to the interplanetary space and the plasma streams outwards with practically no X-ray emission.

In the same mission, coronal loops were also detected in the UV band at temperatures below 1 MK, by Extreme UltraViolet (EUV) telescopes S-055 (Reeves *et al.*, 1977) and S-082 (Tousey *et al.*, 1977; Bartoe *et al.*, 1977). These loops are invisible in the X-ray band and many of them depart from sunspots, appear coaxial and are progressively thinner for progressively lower temperature ions (Foukal, 1975, 1976), suggesting nested loops hotter toward outer shells, although this suggestion has never been validated. The apparent scale height of the emission is larger than that expected from a static model, but the loops appear to be steady for long times. Foukal (1976) proposed a few explanations including siphon flows and thermal instability of the plasma at the loop apex. New observations of such cool loops were performed several years later with the SOlar and Heliospheric Observatory (SoHO) mission and provided new details and confirmations (Section 3.5).

A different target was addressed by the Solar Maximum Mission (SMM, 1980 – 1989, Bohlin

et al., 1980; Acton *et al.*, 1980), which included high-resolution spectrometers in several X-ray lines, i.e., the Bent Crystal Spectrometer (BCS) and the Flat Crystal Spectrometer (FCS), mostly devoted to obtain time-resolved spectroscopy of coronal flares (e.g., MacNeice *et al.*, 1985). Similarly, the Hinotori mission (1981 – 1991, Tanaka, 1983) was dedicated mainly to solar flare observations in the X-ray band. This was also the scope of the later Yohkoh mission, (1991 – 2001, Ogawara *et al.*, 1991) by means of high resolution X-ray spectroscopy, adding the monitoring and imaging of the hot and flaring corona. Hara *et al.* (1992) found first indications of plasma at 5 – 6 MK in active regions with the Soft X-ray Telescope (SXT, Tsuneta *et al.*, 1991).

Normal incidence optics have been developed in the late 1980s. An early experiment was the Normal Incidence X-ray Telescope (NIXT, Golub and Herant, 1989), which provided a few high resolution coronal images in the EUV band.

More recent space missions dedicated to study the corona have been the Solar and Heliospheric Observatory (SoHO, Domingo *et al.*, 1995), launched in 1995 and still operative, and the Transition Region and Coronal Explorer (TRACE, Handy *et al.*, 1999), launched in 1998 and replaced in 2010 by the Solar Dynamic Observatory instruments. Both SoHO and TRACE were tailored to observe the quiet corona (below 2 MK). SoHO images the whole corona (Extreme ultraviolet Imaging Telescope, EIT, Delaboudinière *et al.*, 1995) and performs wide band spectroscopy (Solar Ultraviolet Measurements of Emitted Radiation, SUMER, Wilhelm *et al.*, 1995) and (Coronal Diagnostic Spectrometer, CDS, Harrison *et al.*, 1995) in the EUV band; TRACE imaged the EUV corona with high spatial (0.5 arcsec) and temporal (30 s) resolution. Both SoHO/EIT and TRACE are based on normal incidence optics and contain three different EUV filters that provide limited thermal diagnostics.

Thanks to their capabilities, both missions allowed to address finer diagnostics, in particular to investigate the fine transverse structuring of coronal loops, both in its geometric and thermal components, and the plasma dynamics and the heating mechanisms at a higher level of detail. SoHO and TRACE have been complementary in many respects and several studies attempted to couple the information from them.

Among other relevant missions, we mention the CORONAS series (Ignatiev *et al.*, 1998; Oraevsky and Sobelman, 2002), with instruments like SPectroheliographIc X-Ray Imaging Telescope (SPIRIT, Zhitnik *et al.*, 2003), Rentgenovsky Spektrometr s Izognutymi Kristalami (ReSIK, Sylwester *et al.*, 1998), and Solar Photometer in X-rays (SPHINX, Sylwester *et al.*, 2008), which have contributed to the investigation of coronal loops.

In late 2006, two other major solar missions started, namely Hinode (Kosugi *et al.*, 2007) and the Solar TErrestrial Relations Observatory (STEREO) (e.g., Kaiser *et al.*, 2008). On-board Hinode, two instruments address particularly the study of coronal loops: the X-Ray Telescope (XRT, Golub *et al.*, 2007) and the Extreme-ultraviolet Imaging Spectrometer (EIS, Culhane *et al.*, 2007). Both these instruments offer considerable improvements on previous missions. The XRT has a spatial resolution of about 1 arcsec, a very low scattering, and the possibility to switch among nine filters and combinations of them. EIS combines well spectral ($\sim$ 2 mA), spatial (2"), and temporal ($\sim$ 10 s) resolution to obtain accurate diagnostics of plasma dynamics and density. One big achievement of the STEREO mission is that, since it consists of two separate spacecrafts getting farther and farther from each other, it allows – through, for instance, its Sun-Earth Connection Coronal and Heliospheric Investigation (SECCHI) package – a first 3D reconstruction of coronal loops (Aschwanden *et al.*, 2009; Kramar *et al.*, 2009).

Hinode and STEREO represent the state-of-art for coronal loop observations, and the coronal loop studies including recent findings of these missions will be overviewed. In 2010, the new big solar mission Solar Dynamic Observatory (SDO) has been launched and new interesting results about the solar corona are expected soon, with instruments like the Atmospheric Imaging Assembly (AIA).

3 The Observational Framework

3.1 General properties

Although coronal loops are often well defined and studied in the EUV band, detected by many space mission spectrometers like those on board SoHO and Hinode, and by high resolution imagers such as NIXT and TRACE, the bulk of coronal loops is visible in the X-ray band (Figure 1). Also, the peak of the coronal emission measure of active regions – where the loops are brightest – is above 2 MK, which is best observed in X-rays (e.g., Peres *et al.*, 2000; Reale *et al.*, 2009a).

Coronal loops are characterized by an arch-like shape that recalls typical magnetic field topology. This shape is replicated over a wide range of dimensions. Referring, for the moment, to the soft X-ray band, the main properties of coronal loops are listed in Table 1. The length of coronal loops spans over at least 4 orders of magnitude: bright points ($\sim 10^8$ cm), small Active Region (AR) loops ($\sim 10^9$ cm), AR loops ($\sim 10^{10}$ cm), giant arches ($\sim 10^{11}$ cm) (Figure 2). As already mentioned, the loops owe their high luminosity and variety to their nature of magnetic flux tubes where the plasma is confined and isolated from the surroundings. Magnetized fully-ionized plasma conducts thermal energy mostly along the magnetic field lines. Due to the high thermal insulation, coronal loops can have different temperatures, from $\sim 10^5$ K (cool loops), to a few 10^6 (X-ray loops), up to a few 10^7 K (flaring loops). A density of the confined plasma below $10^7 - 10^8$ cm^{-3} can be difficult to detect, while more typical values of bright loops are $10^9 - 10^{10}$ cm^{-3} in quiescent and active regions loops. Flaring loops can be easily a factor 10 denser. The corresponding plasma pressure can typically vary between 10^{-3} and 10 dyne cm^{-2} for non-flaring loops, corresponding to confining magnetic fields of the order of $0.1 - 10$ G. One characterizing feature of coronal loops is that typically their cross-section is constant along their length above the transition region, at variance from the topology of potential magnetic fields. There is evidence that the cross-section varies across the transition region, as documented in Gabriel (1976).

Table 1: Typical X-ray coronal loop parameters

Type	Length [10^9 cm]	Temperature [MK]	Density [10^9 cm^{-3}]	Pressure [dyne cm^{-2}]
Bright points	$0.1 - 1$	2	5	3
Active region	$1 - 10$	3	$1 - 10$	$1 - 10$
Giant arches	$10 - 100$	$1 - 2$	$0.1 - 1$	0.1
Flaring loops	1–10	> 10	> 50	> 100

3.1.1 Classification

Myriads of loops populate the solar corona and constitute statistical ensembles. Attempts to define and classify coronal loops were never easy, and no finally established result exists to-date. Early attempts were based on morphological criteria, i.e., bright points, active region loops, and large scale structures Vaiana *et al.* (1973), largely observed with instruments in the X-ray band. In addition to such classification, more recently, the observation of loops in different spectral bands and the suspicion that the difference lies not only in the band, but also in intrinsic properties, have stimulated another classification based on the temperature regime, i.e., *cool, warm*, and *hot* loops (Table 2). *Cool loops* are generally detected in UV lines at temperatures between 10^5 and 10^6 K. They were first addressed by Foukal (1976) and later explored more with SoHO observations (Brekke *et al.*, 1997). *Warm loops* are well observed by EUV imagers such as SoHO/EIT and TRACE, and confine plasma at temperature around $1 - 1.5$ MK Lenz *et al.* (1999). *Hot loops* are

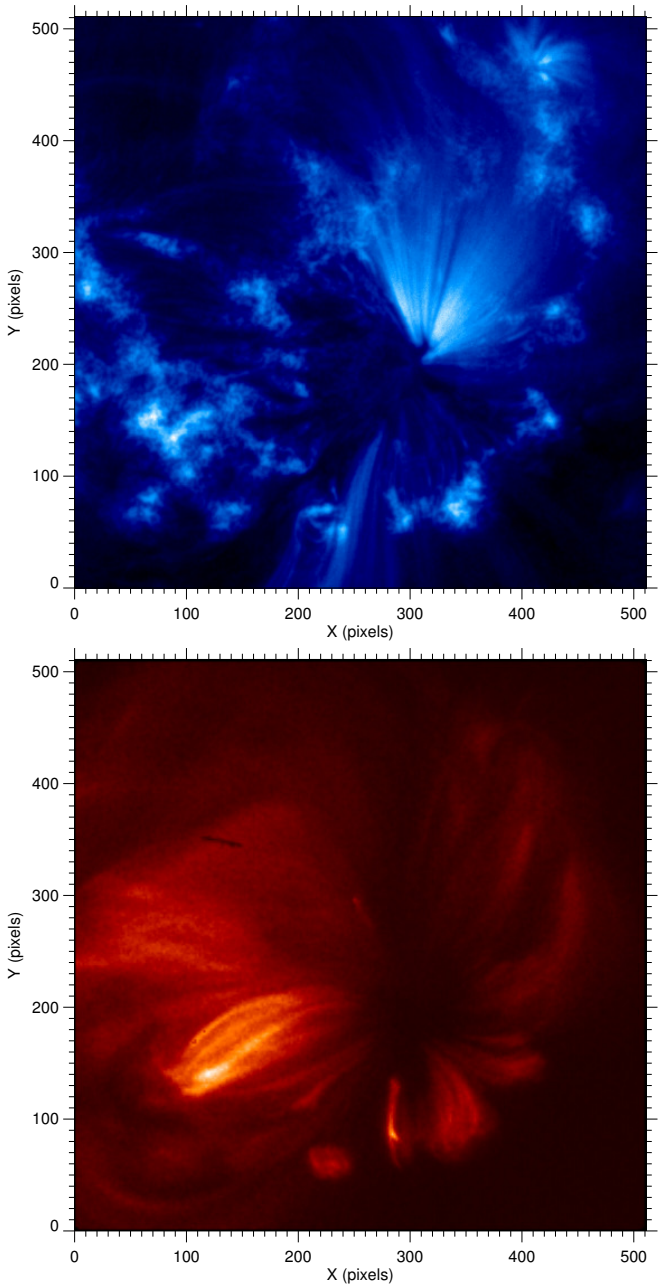

Figure 1: Images of the same active region, taken in the EUV band with TRACE (top) and in the X-ray band with Hinode/XRT (bottom), on 14 November 2006. The X-ray image shows more clearly that the active region is densely populated with coronal loops.

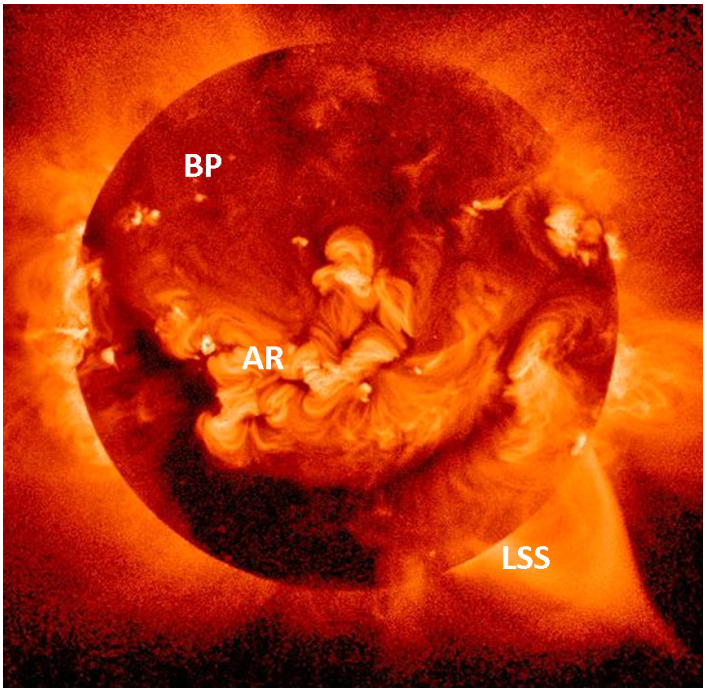

Figure 2: The X-ray corona contains loops with different spatial scales, e.g., bright points (BP), active region loops (AR), large scale structures (LSS). Credit: Yohkoh mission, ISAS, Japan.

those typically observed in the X-ray band and hot UV lines (e.g., Fe XVI), with temperatures around or above 2 MK (Table 1). These are the coronal loops already identified, for instance, in the early rocket missions Vaiana *et al.* (1973). This distinction is not only due to observation with different instruments and in different bands, but there are hints that it may be more substantial and physical, i.e., there may be two or more classes of loops that may be governed by different regimes of physical processes. For instance, the temperature along warm loops appears to be distributed uniformly and the density to be higher than that predicted by equilibrium conditions. Does this make such loops intrinsically different from hot loops, or is it just the signature that warm loops are a transient conditions of hot loops?

Table 2: Thermal coronal loop classification

Type	Temperature [MK]
Cool	$0.1-1$
Warm	$1-1.5$
Hot	≥ 2

A real progress in the insight into coronal loops is expected from the study of large samples of loops or of loop populations. Systematic studies of coronal loops suffer from the problem of the sample selection and loop identification, because, for instance, loops in active regions overlap along the line sight. Attempts of systematic studies have been performed in the past on Yohkoh and TRACE data (e.g., Porter and Klimchuk, 1995; Aschwanden *et al.*, 2000). A large number of loops were analyzed and it was possible to obtain meaningful statistics. However, it is difficult to generalize the results because of limited samples and/or selection effects, e.g., best observed

loops, specific instrument. One basic problem for statistical studies of coronal loops is that it is very difficult to define an objective criterion for loop identification. In fact, loops are rarely isolated; they coexist with other loops which intersect or even overlap along the line of sight. This is especially true in active regions where most of the loops are found. In order to make a real progress along this line, we should obtain loop samples and populations selected on totally objective and unbiased criteria, which is difficult due to the problems outlined above. Some steps are coming in this direction and we will see results in the future.

3.2 Morphology and fine structuring

3.2.1 Geometry

Coronal loops are magnetic structures and might therefore be mapped easily and safely by mapping reliably the coronal magnetic field. Unfortunately, it is well-known that it is very difficult to measure the magnetic field in the corona, and it can only be done in very special conditions, e.g., very strong local field (White *et al.*, 1991). In some cases it is possible to use coronal seismology (first proposed by Uchida, 1970) to determine the average magnetic field strength in an oscillating loop first used by Nakariakov *et al.* (1999) and Nakariakov and Ofman (2001) on TRACE loops, and recently investigated in a number of studies. The accuracy of this method depends on the correct detection of the temporally and spatially resolved mode of oscillation, and on the details of the loop geometry.

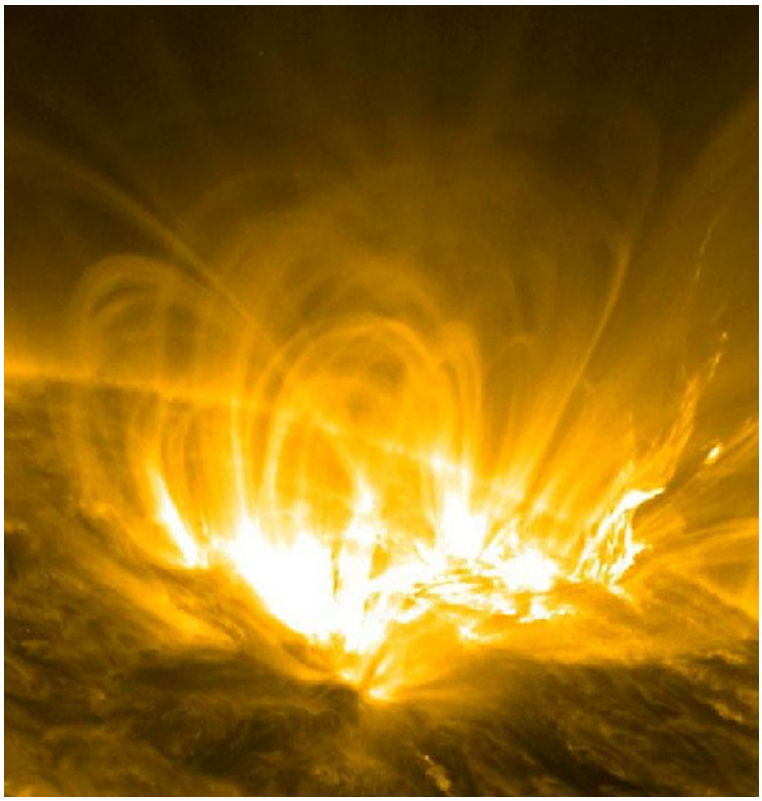

Figure 3: Coronal loops have approximately a semicircular shape. Image: SDO/AIA, 171 A filter, 9 July 2010. Credit: NASA/SDO.

Since we cannot well determine the coronal magnetic field, coronal loop geometry deserves specific analysis. As a good approximation, loops generally have a semicircular shape (Figure 3). The loop aspect, of course, depends on the loop orientation with respect to the line of sight: loops with the footpoints on the limb more easily appear as semicircular, as well as loops very inclined on the surface near the center of the disk. The assumption of semicircular shape can be useful to measure the loop length even in the presence of important deformations due to projection effects: the de-projected distance of the loop footpoints is the diameter of the arc. However, deviations from circularity are rather common and, in general, the detailed analysis of the loop geometry is not a trivial task. The accurate determination of the loop geometry is rather important for the implications on the magnetic field topology and reconstruction. It is less important for the structure and evolution of the confined plasma, which follow the field lines whatever shape they have and change little also with moderate changes of the gravity component along the field lines. First works on the accurate determination of the loop geometry date back to the sixties (Saito and Billings, 1964). More specific ones take advantage of stereoscopic views allowed by huge loops during solar rotation, with the aid of magnetic field reconstruction methods. These studies find deviations from ideal circularity and symmetry, not surprising for such large structures (Berton and Sakurai, 1985). The geometry of a specific loop observed with TRACE was measured in the framework of a complete study including time-dependent hydrodynamic modeling (Reale *et al.*, 2000b,a). In that case, the discrepancy between the length derived from the distance of the footpoints taken as loop diameter and the length measured along the loop itself allowed to assess the loop as elongated. Later, a reconstruction of loop geometry was applied to TRACE observation of medium-sized oscillating loops, to derive the properties of the oscillations. In this case, a semicircular pattern was applied (Aschwanden *et al.*, 2002). The importance of the deviations from circularity on constraining loop oscillations was remarked later (Dymova and Ruderman, 2006).

The STEREO mission is actually contributing much to the analysis of loop morphology and geometry, thanks to its unique capability to observe the Sun simultaneously from different positions. Feng *et al.* (2007) presented a first stereoscopic reconstruction of the three-dimensional shape of magnetic loops in an active region from two different vantage points based on simultaneously recorded STEREO/SECCHI images. They derived parameters of five relatively long loops and constraints on the local magnetic field, and found reconstructed loops to be non-planar and more curved than field lines extrapolated from SoHO/MDI measurements, probably due to the inadequacy of the linear force-free field model used for the extrapolation. A misalignment of 20 – 40 deg between theoretical model and observed loops has been quantified from STEREO results and discussed (Sandman *et al.*, 2009; DeRosa *et al.*, 2009). Aschwanden *et al.* (2008b) presented triangulations and 3D reconstructions of 30 coronal loops, using the Extreme UltraViolet Imager (EUVI) telescopes of both STEREO spacecrafts and deriving a series of loop characteristics, such as the loop plane inclination angles, and the coplanarity and circularity. They derived the parameters of seven complete and quite inclined loops and found deviations from circularity within 30%, and less significant from coplanarity. Aschwanden *et al.* (2009) applied a reconstruction method to an active region observed with STEREO by combining stereoscopic triangulation of 70 loops and addressing mainly density and temperature modeling with a filling factor equivalent to tomographic volume rendering.

Another interesting issue regarding coronal loop geometry is the analysis of the loop cross-section, which also provides information about the structure of the coronal magnetic field. Yohkoh / SXT allowed for systematic and quantitative studies of loop morphology and showed that the cross-section of coronal loops is approximately constant along their length and do not increase significantly. More in detail, a systematic analysis of a sample of ten loops showed that the loops tend to be only slightly ($\sim$ 30%) wider at their midpoints than at their footpoints, while for a bipolar field configuration we would expect expansions by factors. One possible explanation of this effect is the presence of significant twisting of the magnetic field lines, and therefore the

development of electric currents and strong deviations from a potential field. The effect might be seen either as a twisting of a single loop or as a "braiding" of a bundle of unresolved thin loops. At the same time it was found that the variation of width along each loop tends to be modest, implying that the cross section has an approximately circular shape (Klimchuk *et al.*, 1992). Implications of these results on the theory of coronal heating are discussed in Klimchuk (2000), but the conclusion is that none of the current models alone is able to explain all observed properties.

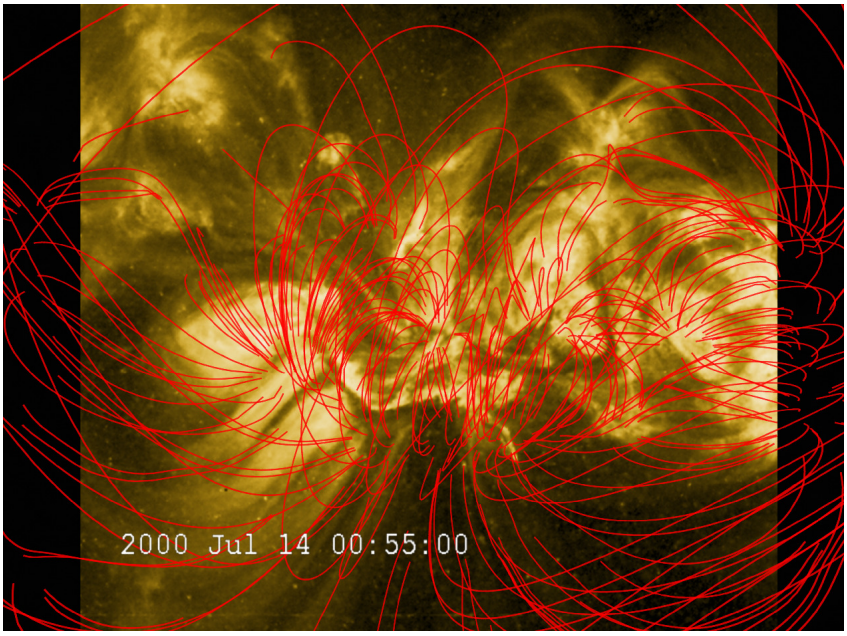

Figure 4: Magnetic field lines extrapolated from optical magnetogram superposed on a TRACE image. Credit: NASA/ESA/LMSAL.

Important information about the internal structuring of coronal loops comes from the joint analysis of the photospheric and coronal magnetic field (Figure 4). An analysis of the magnetic field at the footpoints of hot and cool loops showed, among other results, that the magnetic filling factor is lower in hot loops (0.05 – 0.3 out of sunspots) than in warm loops (0.2 – 0.6) (Katsukawa and Tsuneta, 2005). López Fuentes *et al.* (2006) investigated the magnetic structure of loops observed with TRACE, applying a linear force-free extrapolation model to SoHO/MDI data and comparing the resulting configuration of the magnetic field directly with TRACE images of the same region. They confirmed that, whereas the model predicts a significant expansion of the magnetic field structures, at least a factor two, from the footpoints to the corona, and a significant asymmetry of the structures, because the magnetic field lines starting from the same footpoint can diverge to different other end footpoints, these features are not observed: also TRACE loops are quite symmetric and their cross-section is constant to a good degree of approximation, as it had been already found for Yohkoh loops (Klimchuk *et al.*, 1992). The results in López Fuentes *et al.* (2006) suggest that the tangling of the magnetic flux strands driven by the photospheric convection might be very strong, and confirm, therefore, that the magnetic field structure is far more complicated than it can be modelled even with linear force-free extrapolation. Schrijver (2007) studied braiding-induced interchange reconnection of the magnetic field and the width of solar coronal loops and showed that loop width observations support the hypothesis that granular braiding is countered statistically by frequent coronal reconnections, which in turn explain the general absence of entangled coronal field structures in high-resolution observations of the quiescent

solar corona. DeForest (2007) addressed the apparent uniform cross section of bright threadlike structures in the corona, long apparent scale height, and the inconsistency between loop densities derived by spectral and photometric means. They found that, if coronal loops are interpreted as a mixture of diffuse background and very dense, unresolved stranded structures, this requires a combination of high plasma density within the structures, which greatly increases the emissivity of the structures, and geometric effects that attenuate the apparent brightness of the feature at low altitudes.

New methods to improve the morphological analysis of loops are being developed. For instance, Dudok de Wit and Auchère (2007) made multispectral analysis of solar EUV images and explored the possibility of separating the different solar structures from a linear combination of images. They found source images with more contrast than the original ones.

3.2.2 Fine structuring

It has been long claimed (e.g., Gomez *et al.*, 1993) that coronal loops consist of bundles of thin strands, to scales below the current instrumental resolution. The task to investigate this substructuring is not easy because the thickness of the elementary components may be as small as a few km, according to some nanoflare models (e.g., Vekstein, 2009), and the measured one goes down to the resolution limit of the most powerful imaging instruments (e.g., Gomez *et al.*, 1993). First limited evidence of fine structuring was the low filling factor inferred for loops observed with NIXT (Di Matteo *et al.*, 1999) (see Section 3.3.2). The high spatial resolution achieved by the TRACE normal incidence telescope allowed to address the transverse structure of the imaged coronal loops. TRACE images visibly show that coronal loops are substructured (Figure 5).

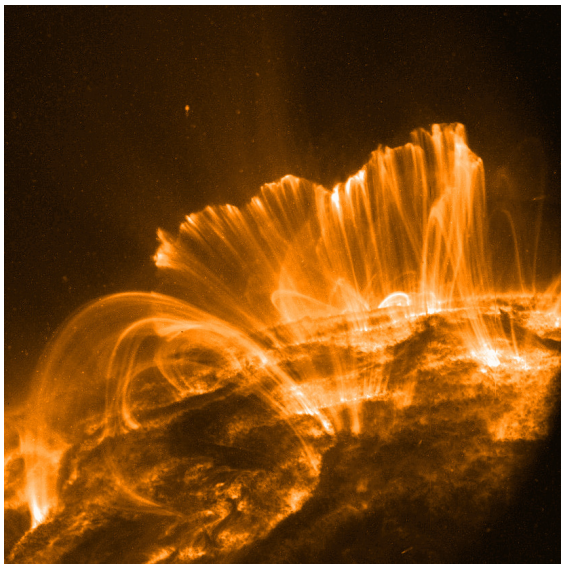

Figure 5: TRACE image including a system of coronal loops (9 November 2000, 2 UT). Bundles of strands are clearly visible.

There were some early attempts to study the structure along the single strands in TRACE observations (Testa *et al.*, 2002). Later, it was shown that in many cases, hot loop structures observed with the Yohkoh/SXT are not exactly co-spatial with warm structures observed with the SoHO/EIT, which is sensitive in the same bands as TRACE, nor they cool down to become visible to the EIT (Nagata *et al.*, 2003; Schmieder *et al.*, 2004).

The detailed morphological comparison of an active region showed that hot loops seen in SXT ($T > 3$ MK) and warm loops seen in the SoHO/EIT 195 Å band ($T \sim 1-2$ MK) are located in almost alternating manner (Nagata *et al.*, 2003). The anti-coincidence of the hot and the warm loops is conserved for a duration longer than the estimated cooling timescale. These results suggest that loops are not isothermal in the transverse direction, rather they have a differential emission measure distribution of modest but finite width that peaks at different temperatures for different loops (see Section 3.3).

In apparent alternative, Winebarger and Warren (2005) showed that hot monolithic loops visible with the Yohkoh/SXT are later resolved as stranded cooler structures with TRACE. However, this occurs with a time delay of 1 to 3 hours, much longer than the plasma cooling times, and, therefore, correlation can be hardly established between the plasma detected by Yohkoh and that detected by TRACE. Direct density measurements of loop plasma made from multi-line observations at the solar limb indicate not very dense plasma and relatively high plasma filling factor (0.2 – 0.9, Ugarte-Urra *et al.*, 2005). This is in the direction of a moderate structuring of the loops.

Aschwanden and Nightingale (2005) analyzed specifically and systematically TRACE images to search for the thinnest coherent structures that can be resolved with TRACE. They found that about 10% of the positions can be fitted with an isothermal model and proposed that, since the corresponding structures have a uniform thermal distribution, they should be elementary loop components, with an average width of about 2000 km. Aschwanden *et al.* (2007) studied statistically a large set of coronal loops and found further evidence of elementary loop strands resolved by TRACE.

Other studies based both on models and on analysis of observations independently suggest that elementary loop components should be even finer, with typical cross-sections of the strands to be of the order of 10 – 100 km (Beveridge *et al.*, 2003; Cargill and Klimchuk, 2004; Vekstein, 2009).

3.3 Diagnostics and thermal structuring

The investigation of the thermal structure of coronal loops is very important for their exhaustive physical comprehension and to understand the underlying heating mechanisms. For instance, one of the classifications outlined above is based on the loop thermal regime, and, we remark, it is debated whether the classification indicates a real physical difference.

Diagnostics of temperature are not trivial in the corona. No direct measurements are available. Since the plasma is optically thin, we receive information integrated on all the plasma column along the line of sight. The problem is to separate the distinct contributing thermal components and reconstruct the detailed thermal structure along the line of sight. However, even the determination of global and average values deserves great attention.

Moderate diagnostic power is allowed by imaging instruments, by means of multifilter observations. Filter ratio maps provide information about the spatial distribution of temperature and emission measure (e.g., Vaiana *et al.*, 1973). The emission of an optically thin isothermal plasma as measured in a j-th filter passband is

$$I_j = EM \;\; G_j(T), \tag{1}$$

where T is the temperature and EM is the emission measure, defined as

$$EM = \int_V n^2 dV,$$

where n is the particle density and V the plasma volume. The ratio R_{ij} of the emission in two different filters i, j is then independent of the density, and only a function of the temperature:

$$R_{ij} = \frac{I_i}{I_j} = \frac{G_i(T)}{G_j(T)}. \tag{2}$$

The inversion of this relationship provides a value of temperature.

The limitations of this method are substantial. In particular, one filter ratio value provides one temperature value for each pixel; this is a reliable measurement, within experimental errors, as long as the assumption of isothermal plasma approximately holds for the plasma column in the pixel along the line of sight. If the plasma is considerably multithermal, the temperature value is an average weighted for the instrumental response. Since the response is a highly non-linear function of the emitting plasma temperature, it is not trivial to interpret the related maps correctly. In addition, it is fundamental to know the instrument response with high precision, in order to avoid systematic errors, which propagate dangerously when filter ratios are evaluated. In this sense, broadband filters provide robust thermal diagnostics, because they are weakly dependent on the details of the atomic physics models, e.g., on the presence of unknown or not well-known spectral lines, on the choice of element abundances. Narrowband filters can show non-unique dependencies of filter ratio values on temperature (e.g., Patsourakos and Klimchuk, 2007), due to the presence of several important spectral lines in the bands, but a more general problem can be the bias to detect narrow ranges of temperatures forced by the specific instrument characteristics. This problem can be important especially when the distribution of the emission measure along the line of sight is not simple and highly non-linear (e.g., Reale *et al.*, 2009b). The problem of diagnostics of loop plasma from filter ratios and, more in general, the whole analysis of loop observations, are made even more difficult by the invariable presence of other structures intersecting along the line of sight. A uniform diffuse background emission also affects the temperature diagnostics, by adding systematic offsets which alter the filter ratio values. The task of subtracting this "background emission" from the measured emission is non-trivial and can affect seriously the results of the whole analysis. This problem emerged dramatically when the analysis of the same large loop structure observed with Yohkoh/SXT on the solar limb led to three different results depending mostly on the different ways to treat the background (Priest *et al.*, 2000; Aschwanden, 2001; Reale, 2002b). The amount of background depends on the instrument characteristics, such as the passband and the point response function: it is most of the signal in TRACE UV filterbands, for instance, and its subtraction becomes a very delicate issue (e.g., Del Zanna and Mason, 2003; Reale and Ciaravella, 2006; Aschwanden *et al.*, 2008a; Terzo and Reale, 2010). The problem can be mitigated if one analyzes loops as far as possible isolated from other loops, but this is not easy, for instance, in active regions. If this is not the case, broadband filters may also include contamination from many structures at relatively different temperature and make the analysis of single loops harder. The problem of background subtraction in loop analysis has been addressed by several authors, who apply different subtraction ranging from simple offset, to emission in nearby pixels or subregions, to values interpolated between the loop sides, to whole images at times when the loop is no longer (or not yet) visible (Testa *et al.*, 2002; Del Zanna and Mason, 2003; Schmelz *et al.*, 2003; Aschwanden and Nightingale, 2005; Reale and Ciaravella, 2006; Aschwanden *et al.*, 2008a; Terzo and Reale, 2010).

More accurate diagnostics, although with less time and space resolution, is in principle provided by spectrometers and observations in temperature-sensitive spectral lines, which are being constantly improved to provide better and better spatial information. Early results from UV spectroscopy already recognized the link between transition region and coronal loops, for instance, from Skylab mission (Feldman *et al.*, 1979; Mariska *et al.*, 1980). Together with background subtraction, one major difficulty met by spectroscopic analysis is that, in the UV band, the density of lines is so high that they are often blended and, therefore, it is hard to separate the contribution of the single lines, especially the weak ones. Fine diagnostics, such as Doppler shifts and line broadening, can become very tricky in these conditions and results are subject to continuous revisitation and warnings from the specialized community. The problem of background subtraction is serious also for spectral data, because their lower spatial and temporal resolution determines the presence of more structures, and therefore more thermal components, along the line of sight in the same spatial

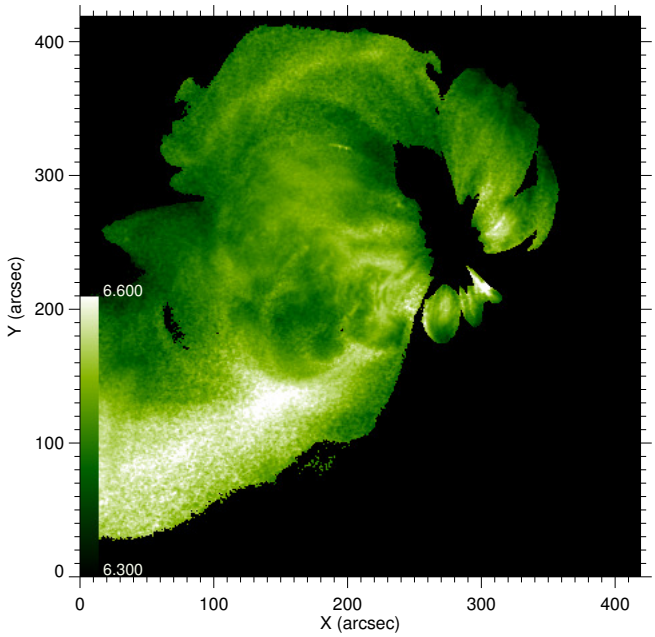

Figure 6: Temperature map of an active region obtained from the ratio of two images in different broadband filters with Hinode/XRT (12 November 2006, 12 UT).

element.

Care should be paid also when assembling information from many spectral lines into a reconstruction of the global thermal structure along the line of sight. Methods are well-established (e.g., Gabriel and Jordan, 1975) and several approaches are available. The so-called method of the emission measure loci (Jordan *et al.*, 1987) is able to tell whether plasma is isothermal of multithermal along the line of sight (Figure 7), but less able to add details. Detailed emission measure distributions can be obtained from differential emission measure (DEM) reconstruction methods (e.g., Brosius *et al.*, 1996; Kashyap and Drake, 1998), but this is an ill-posed mathematical problem and, therefore, results are not unique and are subject to systematic and unknown errors. Forward modeling and simulations can be ways to escape from these problems, but they require non-trivial computational efforts and programming, and it is not always possible to provide accurate confidence levels. All these approaches are constantly improved and probably the best way to proceed is to combine different approaches and multiband observations and to finally obtain a global consistency.

In addition to the problems intrinsic to diagnostic techniques, we have to consider that loops appear to have different properties in different bands, as mentioned in Section 3.1.1. It is still debated whether such differences originate from an observational bias due to the instruments or from intrinsic physical differences, or both. In view of this uncertainty, in the following we will make a distinction between hot and warm loops, which will generally correspond to loops observed in the X-ray (and hot UV lines, e.g., Yohkoh/SXT, Hinode/XRT, SoHO/CDS Fe XVI line) and in the UV band (e.g., SoHO/EIT, TRACE), respectively. Cool loops are also observed in the UV band. The boundary between hot and warm loops is, of course, not sharp, and it is not even clear whether they are aspects of the same basic structure, or they really are physically different and are heated differently (see also Section 3.3.3). We will devote attention to the comparison between hot and warm loops.

3.3.1 Hot loops

After the pioneering analyses driven by the Skylab X-ray instruments (Section 2), Yohkoh/SXT allowed to conduct large scale studies on the thermal and structure diagnostics of hot loops, and the comparison with other instruments, for instance on-board SoHO, allowed to obtain important cross-checks and additional information. Filter ratio maps of flaring loops were shown early after the mission launch (Tsuneta *et al.*, 1992).

Systematic measurements of temperature, pressure, and length of tens of quiescent and active region coronal loops were conducted on Yohkoh observations (Porter and Klimchuk, 1995) using the filter ratio method. For this sample of loops, selected to be steady and isolated, the lengths were measured with assumptions on the loop geometry and ranged in a decade between $5 \times 10^9 < 2L < 5 \times 10^{10}$ cm. The temperature measurements were averaged over about half of the loops and also ranged in a decade ($2 < T < 30$ MK), with a mean of about 6 MK. Therefore, it appears as a sample of particularly hot loops, although the uncertainties in the hot tail of the distribution are very large, probably due to the flat dependence of the temperature on the filter ratio at high temperature. Pressures were derived from the equation of state, after derivation of the density, from the emission measure and from the volume inferred from the length and assumptions on the loop aspect. They ranged in two decades ($0.1 < p < 20$ dyne cm^{-2}). Overall, it was shown that the temperature and length of this sample of hot loops are uncorrelated, that pressure varies inversely with length (as overall expected for a thermally homogeneous sample from loop scaling laws, see Section 4.1.1), although with a large spread. Such distributions were used as constraints on the loop heating through the derivation of the dependence of the magnetic field intensity on the loop length (Klimchuk and Porter, 1995). They also led to accurate analysis of data uncertainties (Klimchuk and Gary, 1995). Another systematic analysis was made on a sample of about 30 bright steady Yohkoh loops located in active regions (Kano and Tsuneta, 1995). The temperatures were measured after averaging several images and taking the value at the loop top. While this analysis confirmed some of the correlations found in Porter and Klimchuk (1995), it found a correlation between the loop length and the temperature, and showed deviations from RTV scaling laws (Section 4.1.1). It cannot be excluded that correlations between parameters depend on the loop sample, as a single scaling law links three parameters. Yohkoh/SXT loops hotter than 3 MK were found also in another study, the hottest ones with shorter lifetimes (less than few hours), and often exhibiting cusps (Yoshida and Tsuneta, 1996).

A big effort has recently been devoted to the possible detection of hot plasma outside of evident flares. This would be a conclusive evidence of nanoflaring activity in coronal loop (e.g., Klimchuk, 2006, see Section 4.4). Hinode instruments appear to be able to provide new interesting contributions to this topic. The analysis of spectroscopic observations of hot lines in solar active regions from Hinode/EIS allows to construct emission measure distributions in the 1 – 5 MK temperature range, and shows that the distributions are flat or slowly increasing up to approximately 3 MK and then fall off rapidly at higher temperatures (Patsourakos and Klimchuk, 2009). Evidence of emission from hot lines has been found also in other Hinode/EIS observations, and in particular from the analysis of the emission from the Ca XVII at 192.858 Å, formed near a temperature of 6×10^6 K, which has been found in several parts of active regions (Ko *et al.*, 2009). Using Fe lines, Young *et al.* (2009) has shown very accurate density measurements ($\approx 5\%$) across an active region, with values in the range $8.5 \leq \log(N_e/\mathrm{cm}^{-3}) \leq 11.0$. A smaller density range (from $10^{8.5}$ to $10^{9.5}$ cm^{-3} has been found by Watanabe *et al.* (2009) using the Fe XIII line group, although one pair has been found to reach the high density limit. Density sensitive lines have been used to measure the filling factor of coronal structures. Dere (2008, 2009) has used spectra and images obtained with EIS and comparison with TRACE to determine the volumetric filling factor of bright points. The emission measure and bright point widths have been compared with the electron densities and with TRACE data. The plasma-filling factor has been found to vary from 3×10^{-3} to 0.3 with a

median value of 0.04, which may indicate considerable subresolution structure, or the presence of a single completely-filled unresolved loop with subarcsec width.

Thanks to its multifilter observations, also Hinode/XRT is providing useful information about the thermal structure of the bright X-ray corona. Temperature maps derived with combined filter ratios show fine structuring to the limit of the instrument resolution and evidence of multithermal components (Reale *et al.*, 2007). This kind of temperature diagnostics is supported by the evidence of warm structures bright in the TRACE images. Observations including flare filters show evidence of a hot component in active regions outside of flares (Schmelz *et al.*, 2009b) and data in the medium thickness filters appear to constrain better this component of hot plasma as widespread, although minor, and peaking around $\log T \sim 6.8-6.9$, with a tail above 10 MK (Reale *et al.*, 2009b). This may support the hypothesis that active regions are heated impulsively. Evidence of a persistent although small hot plasma component outside of flare is shown also by RHESSI data (McTiernan, 2009), and the comparison between RHESSI and XRT data seem to support this scenario in a consistent way (Reale *et al.*, 2009a). The topic of coronal active region heating is debated. Evidence interpreted in the direction of more gradual heating has been obtained by Warren *et al.* (2010) (see Section 4.4).

3.3.2 Comparison of hot and warm loops

Before the SoHO/EIT and TRACE observations, warm loops had been imaged in a similar spectral band and with similar optics by the rocket NIXT mission (see Section 2). Studies of NIXT loops including the comparison with hydrostatic loop models (Section 4.1.1) pointed out that bright spots also visible in Hα band were the footpoints of hot high-pressure loops (Peres *et al.*, 1994). This result was confirmed by the comparison of the temperature structure obtained from Yohkoh with NIXT data (Yoshida *et al.*, 1995) (see also Section 3.3.3).

Another comparison of loops imaged with NIXT and Yohkoh/SXT showed that the compact loop structures (length $\sim 10^9$ cm) have a good general morphological correspondence, while larger scale NIXT loops ($\sim 10^{10}$ cm) have no obvious SXT counterpart (Di Matteo *et al.*, 1999). Comparison with static loop models (see Section 4.1.1) allowed to derive estimates of the loop filling factors, important for the loop fine structure (Section 3.2.2). In the NIXT band, the filling factor of short loops was found to be very low ($10^{-3}-10^{-2}$), but of the order of unity in the SXT band and for the largest structure. Information about the loop filling factor was derived also from the analysis of simultaneous SoHO and Yohkoh observations of a small solar active region, suggesting a volume filling factor decreasing with increasing density and possible differences between emitting material in active regions and the quiet Sun (Griffiths *et al.*, 2000).

Some similarity between loops observed in the TRACE EUV band and Yohkoh X-ray band was found out of the core of active region loops Nitta (2000) and interpreted as evidence of loops with a broad range of temperatures. Core loops were instead observed only in the X-rays and found to be variable, indicating that probably they are not steady.

The thermal distribution across the loop structures, i.e., along the line of sight, can be investigated with the analysis of observations in several spectral lines, as obtained, for instance, with the SoHO/CDS. Information on the validity of the data analysis and of the loop diagnostics can be obtained from the comparison with simultaneous and co-spatial data from imaging instruments.

Density and temperatures in two active regions were accurately determined from SOHO-CDS observations (Mason *et al.*, 1999) and it was confirmed quantitatively that the AR cores are hotter than larger loop structures extending above the limb. From the analysis of a single loop observed on the solar limb with SoHO/CDS, Schmelz *et al.* (2001) found a bias to obtain flat temperature distributions along the loop from ratios of single lines or narrow band filters (TRACE), while a careful DEM reconstruction at selected points along the loop is inconsistent with isothermal plasma both across and along the loop. A whole line of works started from this study reconsidering and

questioning the basic validity of the temperature diagnostics with TRACE and emphasizing the importance of the background subtraction, but also the need to obtain accurate spectral data (Schmelz, 2002; Martens *et al.*, 2002; Aschwanden, 2002; Schmelz *et al.*, 2003). Similar results but different conclusions were reached by Landi and Landini (2004); Landi and Feldman (2004) who analyzed a loop observed with SoHO and, finding it nearly isothermal, considered this evidence as real and invoked a non-constant cross-section to explain it. On the other hand, evidence of non-uniform temperature along loops observed with TRACE was also found (Del Zanna and Mason, 2003; Reale and Ciaravella, 2006), emphasizing that the temperature diagnostics with narrow band instruments is a delicate issue.

An interesting debate has focussed on the question whether the loops observed with TRACE and CDS have a uniform transverse thermal distribution, i.e., a narrow DEM, or a multi-thermal distribution, i.e., a wide DEM which may group together warm and hot loops. Although tackled from a different perspective, this question also concerns the fine longitudinal structuring of the loops and of their heating and is therefore strictly connected to the subject of Sections 3.2.2 and 4.4. Del Zanna and Mason (2003) found a loop detected with TRACE to be isothermal (with temperatures below 1 MK) along the line of sight from diagnostics of spectral lines obtained with SoHO/CDS. Schmelz *et al.* (2005) analyzed another loop on the limb observed with SoHO/CDS, with a DEM reconstruction and a careful analysis of background subtraction, and found a multi-thermal distribution across the loop. From the comparison with the isothermal structure of hot loops derived from CDS data (Di Giorgio *et al.*, 2003; Landi and Landini, 2004), they concluded that there may be two different classes of loops, multi-thermal and isothermal, which they found to be confirmed by a systematic inspection of the CDS atlas (Figure 7).

Multiband observations allow to obtain even more information and constraints. Reale and Ciaravella (2006) analyzed a well-defined loop system detected in a time-resolved observation in several spectral bands, namely three TRACE UV filters, one Yohkoh/SXT filter, two rasters taken with SoHO/CDS in twelve relevant lines ($5.4 \leq \log T \leq 6.4$). The data analysis supported a coherent scenario across the different bands and instruments, indicating a globally cooling loop and the presence of thermal structuring. The study overall indicated that the loop analysis can be easily affected by a variety of instrumental biases and uncertainties, for instance due to gross background subtraction. The fact that the loop that could be well analyzed across several bands and lines is a cooling loop may not be by chance (see end of Section 3.3.3).

Specific analyses of SoHO spectrometric data have continued to contribute much to the study of the loop thermal structure up to recently. A Differential Emission Measure (DEM) analysis of coronal loops using a forward-folding technique on SoHO/CDS data has shown different results for two loops, one to be isothermal and the other to have a broad DEM (Schmelz *et al.*, 2007b). Landi and Feldman (2008) have analyzed an extensive active region spectrum observed by the SUMER instrument on board SOHO and found that the plasma is made of three distinct isothermal components, whose physical properties are similar to coronal hole, quiet-Sun, and active region plasmas.

Hinode/EIS observations of active region loops certify that structures which are clearly discernible in cooler lines ($\sim$ 1 MK) become fuzzy at higher temperatures ($\sim$ 2 MK, Tripathi *et al.*, 2009, Figure 8) as already pointed out by Brickhouse and Schmelz (2006).

Comparative studies of active region loops in the transition region and the corona Ugarte-Urra *et al.* (2009) observed with Hinode seem to point out the presence of two dominant loop populations, i.e., core multitemperature loops that undergo a continuous process of heating and cooling in the full observed temperature range 0.4 – 2.5 MK shown by the X-Ray Telescope, and peripheral loops which evolve mostly in the temperature range 0.4 – 1.3 MK.

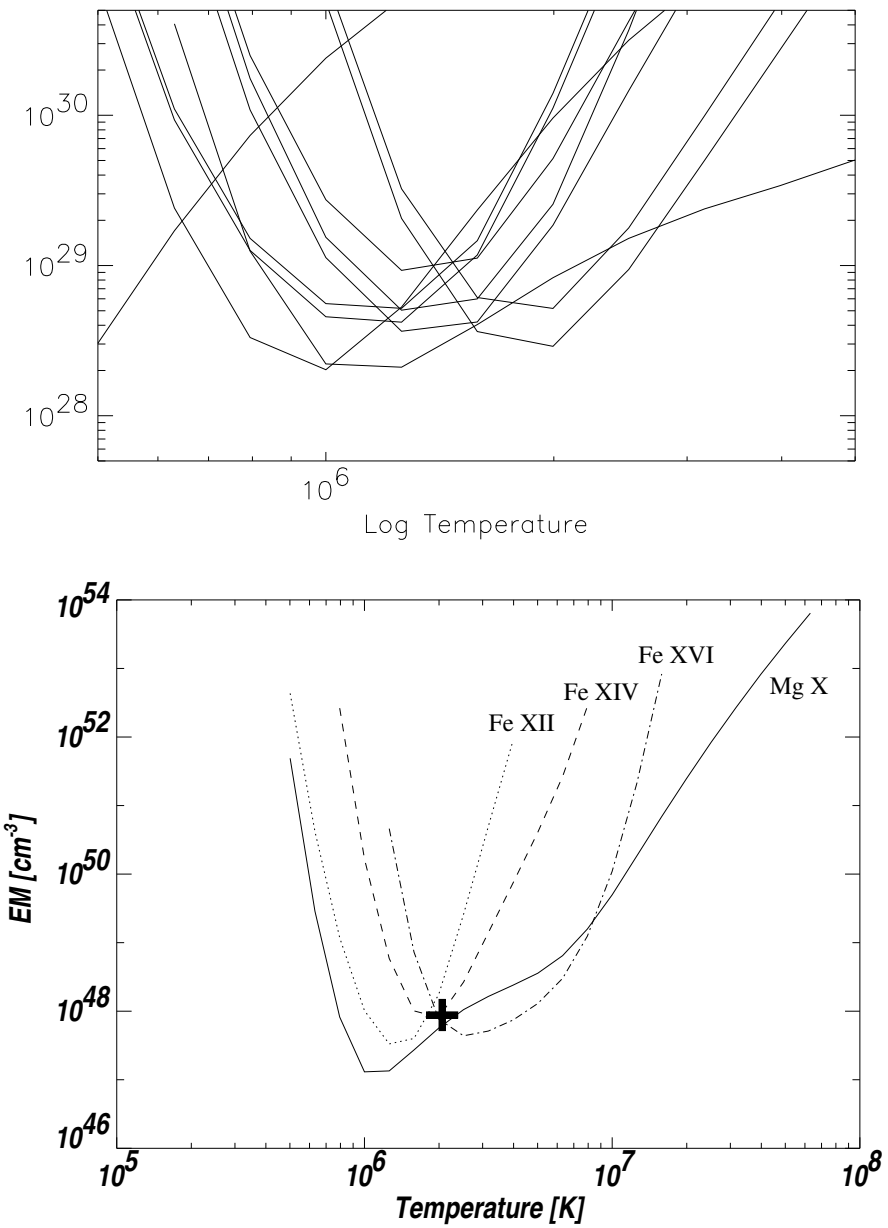

Figure 7: EM-loci plots for two different loop systems, one showing a multi-thermal structure (top, from Schmelz *et al.*, 2005, reproduced by permission of the AAS), the other an almost isothermal one (bottom, from Di Giorgio *et al.*, 2003). The EM is per unit area in the top panel.

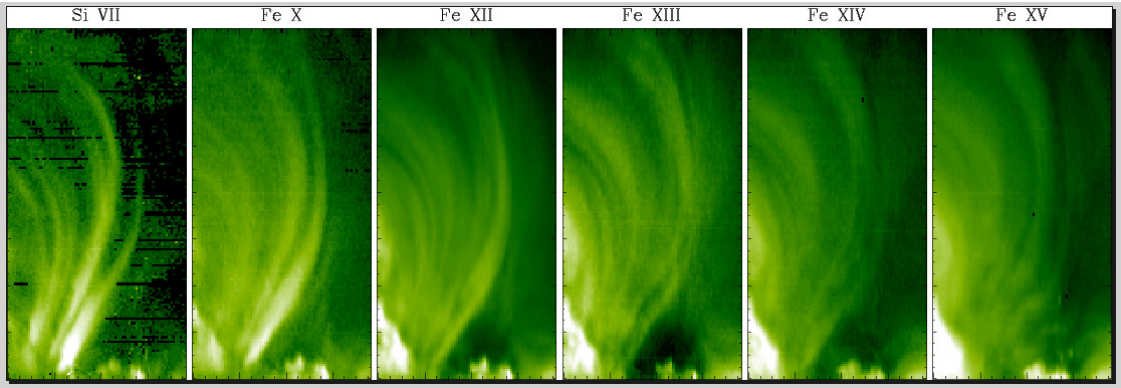

Figure 8: Loop system observed in several EUV spectral lines with Hinode/EIS (19 May 2007, 11:41 – 16:35 UT). The loops become less and less contrasted, i.e., fuzzier and fuzzier, at higher and higher temperature (courtesy of D. Tripathi).

3.3.3 Warm loops

The TRACE mission opened new intriguing questions because the data showed new features, e.g., stranded bright structures mostly localized in active regions, name "the moss", and because the narrow band filters offered some limited thermal diagnostics, but not easy to interpret. Reliable temperatures are in fact found in a very narrow range, and many coronal loops are found to be isothermal in that range.

As mentioned in Section 3.3.2, first loop diagnostics with normal incidence telescopes were obtained from data collected with NIXT Peres *et al.* (1994). The bright spots with Hα counterparts were identified with the footpoints of high pressure loops, invisible with NIXT because not sensitive to plasma hotter than 1 MK. They have been later addressed as the *moss* in the TRACE images, which undergo the same effect. Interactions of moss with underlying chromospheric structures were first described by Berger *et al.* (1999a). Comparison of SOHO/CDS and TRACE observations led to establish that the plasma responsible for the moss emission has a temperature range of about 1 MK and is associated with hot loops at 1 – 2 MK, with a volume filling factor of order 0.1 (Fletcher and De Pontieu, 1999). It was also found that the path along which the emission originates is of order 1000 km long. According to an analytical loop model, a filling factor of about 0.1 is in agreement with the hypothesis of moss emission from the legs of 3 MK loops (Martens *et al.*, 2000).

As for temperature diagnostics with narrow band filters, loops soon appeared to be mostly isothermal with ratios of TRACE filters (Lenz *et al.*, 1999; Aschwanden *et al.*, 2000). Is this a new class of loops? Equivalent SoHO/EIT filter ratios provided analogous results (Aschwanden *et al.*, 1999b). This evidence is intriguing and many investigations have addressed it (see also Section 3.3.2). From the diagnostic perspective, Schmelz *et al.* (2001) reconstructed DEM distributions along the line of sight from spectral SoHO/CDS data and synthesized EIT count rates from them, which led to almost uniform temperatures along the loop, pointing again to an instrumental bias. Weber *et al.* (2005) confirmed that, provided they are flat, i.e., top-hat-shaped, even broad DEMs along the line of sight produce constant TRACE filter ratio values. However, we learn from DEM studies made both with spectrometers and from multi-wideband imagers that the DEM of coronal loops is most probably neither isothermal nor broad and flat, instead peaked with components extending both to low and high temperatures (e.g., Peres *et al.*, 2000; Reale *et al.*, 2009b). The critical point becomes the DEM width and its range of variation.

Later, Schmelz *et al.* (2007a) found that even TRACE triple-filter data cannot, in general, con-

strain the temperature distribution for plasma in warm loops. On the other hand, Patsourakos and Klimchuk (2007) studied the cross-field thermal structure of a sample of coronal loops from triple-filter TRACE observations, and found that the observations are compatible with multithermal plasma with significant emission measure throughout the range 1 – 3 MK. Schmelz *et al.* (2009a) used TRACE filter ratios, emission measure loci, and two methods of differential emission measure analysis to examine the temperature structure of three different loops. In agreement with previous studies, they found both isothermal and multithermal cases. This might not be a contradiction, in the view of the presence of at least three possible conditions of warm loops, as discussed at the end of this section. Noglik *et al.* (2008) compared TRACE to CDS data to measure the temperature along a coronal loop in an active region on the solar limb. Their double filter ratio temperature analysis technique led to temperatures between 1.0 and 1.3 MK. Emission measure loci from CDS lines were consistent with a line-of-sight isothermal structure which increases in temperature from $\sim$ 1.20 to 1.75 MK along the loop, in contrast with the nearby multithermal background.

Another puzzling issue, certainly linked to the loop isothermal appearance, is that warm loops are often diagnosed to be overdense with respect to the equilibrium values predicted by loop scaling laws (Lenz *et al.*, 1999; Winebarger *et al.*, 2003a, Section 4.1.1). To explain both these pieces of evidence, several authors claimed that the loops cannot be at equilibrium and that they must be filamented and cooling from a hotter state, probably continuously subject to heating episodes (nanoflares, Warren *et al.*, 2002, 2003, Sections 4.2 and 4.4). Other authors proposed that part of the effect might be due to inaccurate background subtraction (Del Zanna and Mason, 2003).

The Hinode mission is stimulating new analyses of warm coronal structures, mostly based on its high quality EIS spectral data. Modeling observations of coronal moss with Hinode/EIS confirmed that the moss intensities predicted by steady, uniformly heated loop models are too intense relative to the observations (Warren *et al.*, 2008b). A nonuniform filling factor is required and must vary inversely with the loop pressure. Observations of active region loops with EIS indicate that isolated coronal loops that are bright in Fe XII generally have very narrow temperature distributions (3×10^5 K), but are not properly isothermal and have a volumetric filling factors of approximately 10% (Warren *et al.*, 2008a).

Schmelz *et al.* (2008) studied temperatures of loops identified in a TRACE image in three density-sensitive line ratios. While emission measure loci plots indicated that the loop plasma is not isothermal, a more detailed differential emission measure analysis showed that two broad components can reproduce the background-subtracted intensities. They proposed that the two-component DEM distribution represents two ensembles of strands, one for each of the loops seen in the TRACE image.

Density diagnostics through density-sensitive line ratio also led to measure directly density values, for instance in active regions (e.g., Doschek *et al.*, 2007b). Tripathi *et al.* (2008) found that the hot core of the active region is densest with values as high as $10^{10.5}$ cm^{-3}. The electron density estimated in specific regions in the active region moss decreases with increasing temperature. The density within the moss region was highest at $\log T = 5.8 – 6.1$, with a value around 10^{10} cm^{-3}.

In a cooler regime ($4.15 < \log T < 5.45$) observed in coordination by SOHO spectrometers and imagers, STEREO/EUVI, and Hinode/EIS, active region plasma at the limb has been found to cool down from a coronal hole status with temperatures in the $5.6 < \log T < 5.9$ range (Landi *et al.*, 2009).

The loop reconstruction analysis described in Aschwanden *et al.* (2009) was used mainly for density and temperature modeling of the warm loops of an active region observed with STEREO. The rendering reduces the problem of background subtraction. Although based on simple model assumptions, the derived density and temperature distributions are able to reproduce the total observed fluxes within 20%. The modeling extrapolates results quite outside of the range of sensitivity of the STEREO EUV filters, anyhow finding emission measure distributions not very different from those obtained from spectroscopic observations (Brosius *et al.*, 1996) and deviations

from hydrostatic values in agreement with other previous studies (Lenz *et al.*, 1999; Winebarger *et al.*, 2003a).

In summary, the current observational framework and loop analysis seems to indicate that for a coherent scenario warm loops are manifestations of at least three different loop conditions: i) in loops consisting of bundles of thin independently-heated strands, few cooling strands of steady hot X-ray loops might be detected as warm overdense loops in the UV band. These warm loops would coexist with hot loops and would show a multithermal emission measure distribution (Patsourakos and Klimchuk, 2007; Warren *et al.*, 2008a; Tripathi *et al.*, 2009); ii) we might have warm loops as an obvious result of a relatively low average heating input in the loop. These loops would be much less visible in the X-rays and thus would not be cospatial with hot loops, and would also be much less multithermal (Di Giorgio *et al.*, 2003; Landi and Landini, 2004; Aschwanden and Nightingale, 2005; Noglik *et al.*, 2008); iii) warm loops might be globally cooling from a status of hot X-ray loop (Reale and Ciaravella, 2006). These loops would also be overdense and cospatial with hot loops but with a time shift of the X-ray and UV light curves, i.e., they would be bright in the X-rays before they are in the UV band. Also these loops would have a relatively narrow thermal distribution along the line of sight.

3.4 Temporal analysis

The solar corona is the site of a variety of transient phenomena. Coronal loops sometimes flare in active regions (see the review by Benz, 2008). However, most coronal loops are well-known to remain in a steady state for most of their life, much longer than the plasma characteristic cooling times (Rosner *et al.*, 1978, see Section 4.1.1). This is taken as an indication that a heating mechanism must be on and steady long enough to bring the loop to an equilibrium condition, and keep it there for a long time. Nevertheless, the emission of coronal loops is found to vary significantly on various timescales, and the temporal analyses of coronal loop data have been used to obtain different kinds of information, and as a help to characterize the dynamics and heating mechanisms. The time variability of loop emission is generally not trivial to interpret. The problem is that the emission is very sensitive to density and less to temperature. Therefore, variations are not direct signatures of heating episodes, not even of local compressions, because the plasma is free to flow along the magnetic field lines. Variations must therefore be explained in the light of the evolution of the whole loop. This typically needs accurate modeling, or, at least, care must be paid to many relevant and concurrent effects.

Another important issue is the band in which we observe. The EUV bands of the normal incidence telescopes are quite narrow. Observations are then more sensitive to variations because cooling or heating plasma is seen to turn on and off rapidly as it crosses the band sensitivity. On the other hand, telescopes in the X-ray band detect hotter plasma which is expected to be more sensitive to heating and, therefore, to vary more promptly, but the bandwidths are large and do not take as much advantage of the temperature sensitivity as the narrow bands. Finally, spectroscopic observations are, in principle, very sensitive to temperature variations because they observe single lines, but their time cadence is typically low and able to follow variations only on large timescales. Time analysis studies can be classified to address two main classes of phenomena: temporal variability of steady structures and single transient events, such as flare-like brightenings.

In spite of limited time coverage, the instrument S-054 on-board Skylab already allowed for early studies of variability of hot X-ray loops. Decay times were studied by Krieger (1978) who found evidence of continued evaporation of coronal plasma in slowly-decaying structures. Sheeley Jr (1980) and Habbal *et al.* (1985) found timescales of moderate variability of a few hours over a substantial steadiness for observations of active region loops in 2 MK lines such as Fe XV and Si XII. Substantial (but non-flaring) temporal variability was reported by Haisch *et al.* (1988) in two active region loops observed with SMM in a few relatively hot X-ray lines ($\sim$ 5 MK) on time scales of

some minutes. Cooler loops (< 1 MK) first studied in detail by Foukal (1976) (see Section 3.5) were found to be more variable and dynamic (e.g., Kopp *et al.*, 1985).

The high time coverage and resolution of Yohkoh triggered studies of brightenings on short time scales. The Yohkoh/SXT resolution and dynamic range allowed to study the interaction of differently bright hot loops and to show, for instance, that X-ray bright points often involve loops considerably larger than the bright points themselves, and that they vary on timescales from minutes to hours (Strong *et al.*, 1992). The analysis of a large set (142) of macroscopic transient X-ray brightenings indicated that they derive from the interaction of multiple loops at their footpoints (Shimizu *et al.*, 1994). Some other more specific loop variations were also observed, e.g., the shrinkage of large-scale non-flare loops (Wang *et al.*, 1997). This was interpreted not as an apparent motion but as a real contraction of coronal loops that brighten due to heating at footpoints followed by gradual cooling. Fine-scale motions and brightness variations of the emission were found on timescales of 1 minute or less, with dark inclusions corresponding to jets of chromospheric plasma seen in the wings of Hα. Such small scale variations are associated with the fine structure and dynamics of the conductively heated upper transition region between the solar chromosphere and corona (Berger *et al.*, 1999b).

Loop variability was specifically studied in several UV spectral lines observed with SoHO/CDS for about 3 hours by Di Giorgio *et al.* (2003). In the hottest lines, within the limited time resolution of about 10 minutes, a few brightenings of a hot loop (~ 2 MK) were detected but they are minor perturbations over a steadily high emission level. The observation of the whole life of a cool loop ($\log T \sim 5.3$) on a time lapse of a few hours confirmed the highly transient nature of cool loops, probably linked to the presence of substantial flows (Section 3.5).

Variability analyses have been conducted also on warm loops present in TRACE data. The brightening of a single coronal loop was analyzed in detail by Reale *et al.* (2000b) in an observation of more than 2 hours with a cadence of about 30 s. The loop evolves coherently in the rise phase and brightens from the footpoints to the top, allowing for detailed hydrodynamic modeling (Reale *et al.*, 2000a) (see also Section 4.4). Active region transient events, i.e., short-lived brightenings in small-scale loops, were observed with TRACE with a high cadence of 35 s over half an hour (Seaton *et al.*, 2001). Several brightenings detected over a neutral line in a region of emerging flux were interpreted as reconnection events associated with flux emergence, possible EUV counterparts to active region transient brightenings. The fast evolution probably implies high speed flows and high coronal densities. Shimojo *et al.* (2002) noticed apparent shrinking and expansion of brightening warm loops and proposed heating and cooling of different concentric strands, leading to coronal rain visible in the Hα line. Plasma condensations in hot and warm loops were detected also in the analysis of line intensity and velocity in temporal series data from SOHO/CDS (O'Shea *et al.*, 2007). Antiochos *et al.* (2003) found no significant variability of the moss regions observed with TRACE. This has been taken as part of the evidence toward steady coronal heating in active region cores (Warren *et al.*, 2010, Section 4.4).

The analysis of temporal series from various missions has been used, more recently, to investigate the possible presence of continuous impulsive heating by nanoflares. The temporal evolution of hot coronal loops was studied in data taken with GOES Solar X-ray Imager (SXI), an instrument with moderate spatial resolution and spectral band similar to Yohkoh/SXT (López Fuentes *et al.*, 2007). The durations and characteristic timescales of the emission rise, steady, and decay phases were found to be much longer than the cooling time and indicate that the loop-averaged heating rate increases slowly, reaches a maintenance level, and then decreases slowly (Figure 9), not in contradiction with the early results of Skylab (Section 2). This slow evolution is taken as an indication of a single heating mechanism operating for the entire lifetime of the loop. If so, the timescale of the loop-averaged heating rate might be roughly proportional to the timescale of the observed intensity variations.

Joint TRACE and SOHO/CDS observations allowed to study temperature as a function of time

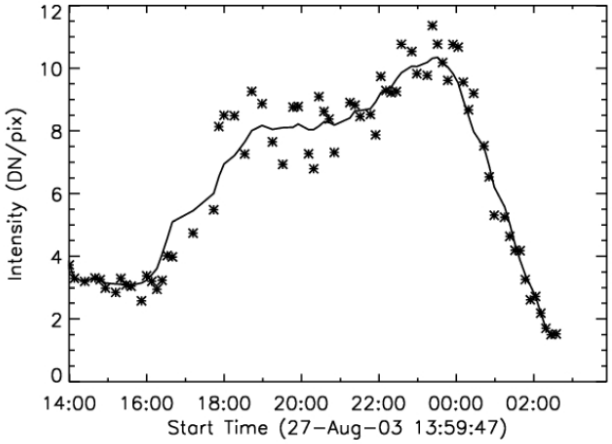

Figure 9: X-ray light curve observed with the SXI telescope on board GOES. The loop lifetime is much longer than the characteristic cooling times (courtesy of J.A. Klimchuk and M.C. Lòpez Fuentes).

in active region loops (Cirtain *et al.*, 2007). In many locations along the loops, the emission measure loci were found consistent with an isothermal structure, but the results also indicated significant changes in the loop temperature (between 1 and 2 MK) over the 6 h observing period. This was interpreted as one more indication of multistranded loops, substructured below the resolution of the imager and of the spectrometer. Further support to fine structuring comes from the analysis of the auto-correlation functions in SXT and TRACE loop observations (Sakamoto *et al.*, 2008). The duration of the intensity fluctuations for the hot SXT loops was found to be relatively short because of the significant photon noise, but that for the warm TRACE loops agrees well with the characteristic cooling timescale. This may support loops to be continuously heated by impulsive nanoflares. The energy of nanoflares is estimated to be 10^{25} erg for SXT loops and 10^{23} erg for TRACE loops. The occurrence rate of nanoflares is about 0.4 and 30 nanoflares s^{-1} in a typical hot SXT loop and a typical warm TRACE loop, respectively.

A recent study on time series has been performed on data taken with the Hinode mission. Hinode's Solar Optical Telescope (SOT) magnetograms and high-cadence EIS spectral data were taken to study the relationship between chromospheric, transition region, and coronal emission and the evolution of the magnetic field (Brooks *et al.*, 2008). The data have allowed to distinguish hot, relatively steadily emitting warm coronal loops from isolated transient brightenings and to find that they are both associated with highly dynamic magnetic flux regions. Brightenings have been typically found in regions of flux collision and cancellation, while warm loops are generally rooted in magnetic field regions that are locally unipolar with unmixed flux. The authors suggest that the type of heating (transient vs. steady) is related to the structure of the magnetic field, and that the heating in transient events may be fundamentally different from that in warm coronal loops.

3.5 Flows

Diagnosing the presence of significant flows in coronal loops is not an easy task. Apparently moving brightness variations may not be a conclusive evidence of plasma motion, since the same effect may be produced by the propagation of thermal fronts or waves. Conclusive evidence of plasma motion comes from measurements of Doppler shifts in relevant spectral lines. However, the detection

of significant Doppler shifts requires several conditions to be fulfilled altogether, e.g., significant component along the line of sight, amount of moving plasma larger than amount of static plasma, plasma motion comparable to typical line broadening effects.

In general, we can distinguish two main classes of mass bulk motions inside coronal loops: siphon flows, due to a pressure difference between the footpoints, and loop filling or draining, due to transient heating and subsequent cooling, respectively. Some other evidence of bulk motions, such as systematic redshifts in UV lines, has been difficult to interpret.

Siphon flows have been mainly invoked to explain motions in cool loops. The existence of cold loops has been known for a long time (Foukal, 1976) (see Section 2) and SoHO has collected high-quality data showing the presence of dynamic cool loops (Brekke *et al.*, 1997). A well-identified detection was found in SoHO/SUMER data, i.e., a small loop showing a supersonic siphon-like flow (Teriaca *et al.*, 2004) and in SoHO/CDS data (Di Giorgio *et al.*, 2003).

Redshifts in transition region UV lines have been extensively observed on the solar disk (e.g., Doschek *et al.*, 1976; Gebbie *et al.*, 1981; Dere, 1982; Feldman *et al.*, 1982; Klimchuk, 1987; Rottman *et al.*, 1990; Brekke, 1993; Peter, 1999). Some mechanisms have been proposed to explain these redshifts: downward propagating acoustic waves (Hansteen, 1993), downdrafts driven by radiatively-cooling condensations in the solar transition region (Reale *et al.*, 1996, 1997b), nanoflares (Teriaca *et al.*, 1999b); a conclusive word is still to be given with the better and better definition of the observational framework.

Blue-shifts in the transition region are also studied but not necessarily associated with coronal loops (e.g., Dere *et al.*, 1986). More localized and transient episodes of high velocity outflows, named explosive events, have been observed in the transition lines such as C IV, formed at 100 000 K (e.g., Dere *et al.*, 1989; Chae *et al.*, 1998b; Winebarger *et al.*, 1999, 2002a,b). However, Teriaca *et al.* (2002) found indications that such EUV explosive events are not directly relevant in heating the corona, are characteristic of structures not obviously connected with the upper corona, and have a chromospheric origin.

Chae *et al.* (1998a) found Doppler shifts increasing and then decreasing with increasing temperature and explained them by the dominance of emission from plasma flowing downward from the upper hot region to the lower cool region along flux tubes with varying cross section (a factor about 30). Teriaca *et al.* (1999a) confirmed these results with the exception of blueshifts at higher temperature.

EUV spectra of coronal loops above an active region show clear evidence of strong dynamical activity. In the O V 629 Å line, formed at 240 000 K, line-of-sight velocities greater than 50 km s^{-1} have been measured with the shift extending over a large fraction of a loop (Brekke *et al.*, 1997). Active region loop structures appear to be extremely time variable and dynamic at transition region temperatures, with large Doppler-shifts (Brekke, 1999). Di Giorgio *et al.* (2003) showed the direct observation and identification of the birth, evolution, and cooling of one of such transient cool loops, and measured a blue-shifted up-flow all along the loop, probably a one-direction siphon flow.

Winebarger *et al.* (2002c) analyzed co-aligned TRACE and the SoHO/SUMER observations of warm active region loops. Although these loops appear static in the TRACE images, SUMER detects line-of-sight flows along the loops of up to 40 km s^{-1}. Apparent motions were also detected in TRACE images (Winebarger *et al.*, 2001).

In SoHO/EIT high-cadence 304 Å images, De Groof *et al.* (2004) analyzed systematic intensity variations along an off-limb half loop structure propagating from the top towards the footpoint and reported several arguments supporting that these intensity variations are due to flowing/falling plasma blobs and not to slow magneto-acoustic waves (Section 4.4). This evidence has been the object of modeling studies (see Section 4.3).

The high spectral resolution of Hinode/EIS is allowing for very detailed studies of persistent loop plasma motions, which are very important to assess whether the loops are to be treated

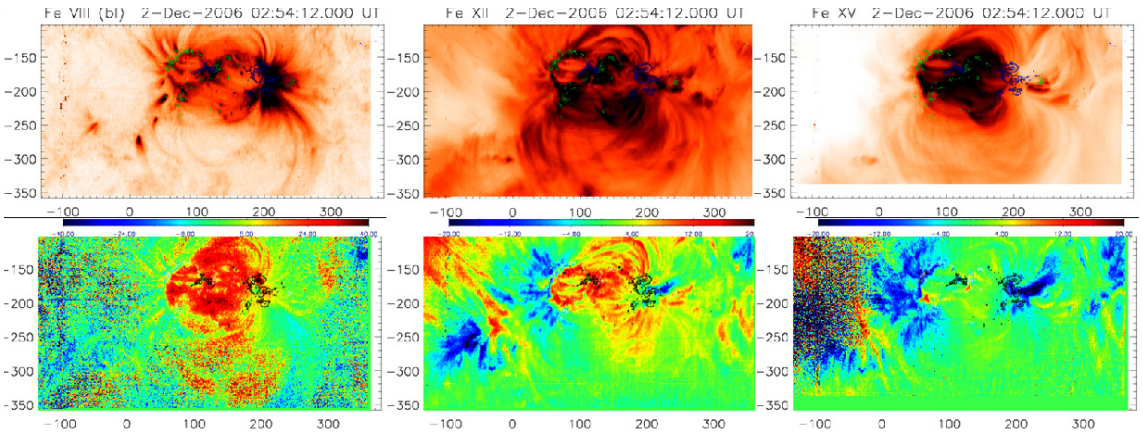

Figure 10: Monochromatic (negative) images and dopplergrams (km s^{-1}) of an active region (NOAA 10926) observed with Hinode/EIS in Fe VIII, Fe XII, Fe XV lines (courtesy of G. Del Zanna).

more as static or dynamic structures as a whole. More specifically, nonthermal velocities were detected in solar active regions (Doschek *et al.*, 2007a). The largest widths seem to be located more in relatively faint zones, some of which also show Doppler outflows. Doppler flows in active region loops observed by Hinode EIS were explicitly addressed by Del Zanna (2008), who found a multifaceted scenario (Figure 10). Persistent redshifts, stronger in cooler lines (about $5-10$ km s^{-1} in Fe XII and $20-30$ km s^{-1} in Fe VIII), were observed in most loop structures. Persistent blueshifts, stronger in the hotter lines (typically $5-20$ km s^{-1} in Fe XII and $10-30$ km s^{-1} in Fe XV), were present in areas of weak emission, in a sharp boundary between the low-lying "hot" 3 MK loops and the higher "warm" 1 MK loops. Strong localized outflows (~ 50 km s^{-1}) in a widespread downflow region were clearly visible in Doppler-shifts maps obtained with EIS (Doschek *et al.*, 2008). The outflows might be tracers of long loops and/or open magnetic fields.

Ofman and Wang (2008) used the high resolution Hinode SOT observations and detected cool plasma flowing in multi-threaded coronal loops with speeds in the range $74-123$ km s^{-1}. In addition to flows, the loops exhibited transverse oscillations.

Further analysis of coronal plasma motions near footpoints of active region loops showed again a strong correlation between Doppler velocity and nonthermal velocity (Hara *et al.*, 2008). Significant deviations from a single Gaussian profile were found in the blue wing of the line profiles for the upflows. These may suggest that there are unresolved high-speed upflows. Tripathi *et al.* (2009) found that an active region was comprised of redshifted emissions (downflows) in the core and blueshifted emissions (upflows) at the boundary. All these results have to be matched with the recent finding of extensive blueshifts correlated with spicules upflows and with coronal emission intensity (De Pontieu *et al.*, 2009) (Section 4.4).

4 Loop Physics and Modeling

4.1 Basics

The basics of loop plasma physics are well established since the 1970s (e.g., Priest, 1978). In typical coronal conditions, i.e., ratio of thermal and magnetic pressure $\beta \ll 1$, temperature of a few MK, density of $10^8 - 10^{10}$ cm^{-3}, the plasma confined in coronal loops can be assumed as a compressible fluid moving and transporting energy only along the magnetic field lines, i.e., along the loop itself (e.g., Rosner *et al.*, 1978; Vesecky *et al.*, 1979). In this configuration, the magnetic field has only the role of confining the plasma. It is also customary to assume constant loop cross-section (see Section 3.2.1). In these conditions, neglecting gradients across the direction of the field, effects of curvature, and transverse waves, the plasma evolution can be described by means of the one-dimensional hydrodynamic equations for a compressible fluid, using only the coordinate along the loop (Figure 11).

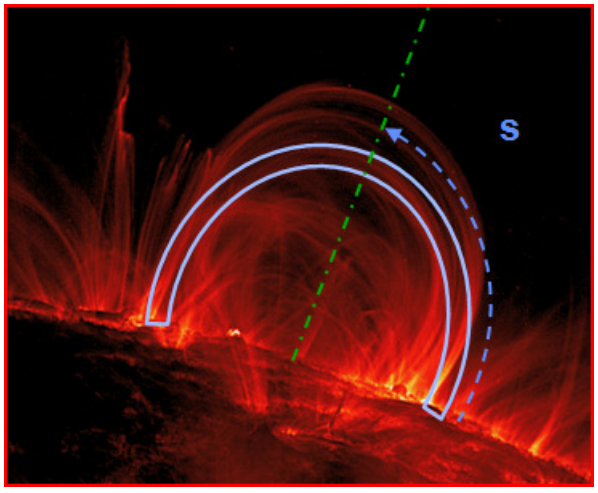

Figure 11: The plasma confined in a loop can be described with one-dimensional hydrodynamic modeling, with a single coordinate (s) along the loop (image: TRACE, 6 November 1999, 2 UT).

The time-dependent equations of mass, momentum, and energy conservation typically include the effects of the gravity component along the loop, the radiative losses from an optically thin plasma, the plasma thermal conduction, an external heating input, the plasma compressional viscosity:

$$\frac{dn}{dt} = -n\frac{\partial v}{\partial s}, \tag{3}$$

$$nm_{\rm H}\frac{dv}{dt} = -\frac{\partial p}{\partial s} + nm_{\rm H}g + \frac{\partial}{\partial s}(\mu\frac{\partial v}{\partial s}), \tag{4}$$

$$\frac{d\epsilon}{dt} + (p+\epsilon)\frac{\partial v}{\partial s} = H - n^2\beta_i P(T) + \mu\left(\frac{\partial v}{\partial s}\right)^2 + F_c, \tag{5}$$

with p and ϵ defined by

$$p = (1+\beta_i)nk_{\rm B}T \qquad \epsilon = \frac{3}{2}p + n\beta_i\chi, \tag{6}$$

and the conductive flux

$$F_c = \frac{\partial}{\partial s}\left(\kappa T^{5/2}\frac{\partial T}{\partial s}\right), \tag{7}$$

where n is the hydrogen number density, s the spatial coordinate along the loop, v the plasma velocity, $m_{\rm H}$ the mass of hydrogen atom, μ the effective plasma viscosity, $P(T)$ the radiative losses function per unit emission measure (e.g., Raymond *et al.*, 1976), β_i the fractional ionization, i.e., $n_{\rm e}/n_{\rm H}$, F_c the conductive flux, κ the thermal conductivity (Spitzer Jr, 1962), $k_{\rm B}$ the Boltzmann constant, and χ the hydrogen ionization potential. $H(s,t)$ is a function of both space and time which describes the heat input in the loop.

These equations can be solved numerically and several specific codes have been used extensively to investigate the physics of coronal loops and of X-ray flares (e.g., Nagai, 1980; Peres *et al.*, 1982; Doschek *et al.*, 1982; Nagai and Emslie, 1984; Fisher *et al.*, 1985a,b,c; MacNeice, 1986; Gan *et al.*, 1991; Hansteen, 1993; Betta *et al.*, 1997; Antiochos *et al.*, 1999; Müller *et al.*, 2003; Ofman and Wang, 2002; Bradshaw and Mason, 2003; Bradshaw and Cargill, 2006).

The concept of numerical loop modeling is to use simulations, first of all, to get insight into the physics of coronal loops, i.e., the reaction of confined plasma to external drivers, to describe plasma evolution, and to derive predictions to compare with observations. One major target of modeling is, of course, to discriminate between concurrent hypotheses, for instance, regarding the heating mechanisms and to constrain the related parameters.

The models require to be provided with initial loop conditions and boundary conditions. In view of our ignorance of the specific heating mechanisms (see Section 4.4), the models require to define an input heating function, specifying its time-dependence, for instance it can be steady, slowly or impulsively changing, and its position in space. The output typically consists of distributions of temperature, density, and velocity along the loop evolving with time. From simulation results, some modelers derive observables, i.e., the plasma emission, which can be compared directly to data collected with the telescopes. The model results are, in this case, to be folded with the instrumental response. This forward-modeling allows to obtain constraints on model parameters and, therefore, quantitative information about the questions to be solved, e.g., the heating rate and location (e.g., Reale *et al.*, 2000a).

Loop codes are typically based on finite difference numerical methods. Although they are one-dimensional, and therefore typically less demanding than other multi-dimensional codes that study systems with more complex geometry, and although they do not include the explicit description of the magnetic field, as full MHD codes, loop codes require some special care. One of the main difficulties consists in the appropriate resolution of the steep transition region ($1-100$ km thick) between the chromosphere and the corona, which can easily drift up and down depending on the dynamics of the event to be simulated. The temperature gradient there is very large due to the local balance between the steep temperature dependence of the thermal conduction and the peak of the radiative losses function (Serio *et al.*, 1981). The density is steep as well so to maintain the pressure balance. The transition region can become very narrow during flares.

Also a fine temporal resolution is extremely important, because the highly efficient thermal conduction in a hot magnetized plasma can lead to a very small time step and make execution times not so small even nowadays. Another important issue is the necessary presence of a relatively thick, cool, and dense region under the transition region, i.e., a chromosphere, otherwise the atmosphere gets unstable. The main role of the chromosphere in this context is only that of a mass reservoir and, therefore, in several codes, it is chosen to treat it as simply as possible, e.g., an isothermal inactive layer which neither emits, nor conducts heat. In other cases, a more accurate description is chosen, e.g., to include a detailed model (e.g., Vernazza *et al.*, 1981) and to maintain a simplified radiative emission and a detailed energy balance with an *ad hoc* heat input (Peres *et al.*, 1982; Reale *et al.*, 2000a).

In recent years, time-dependent loop modeling has revived in the light of the observations with SoHO and TRACE for the investigation of the loop dynamics and heating. The upgrade driven by the higher quality of the data has consisted in the introduction of more detailed mechanisms for the heating input, for the momentum deposition, or others, e.g., the time-dependent ionization and the

saturated thermal conduction (Bradshaw and Cargill, 2006; Reale and Orlando, 2008). Some codes have been upgraded to include adaptive mesh refinement for better resolution in regions of high gradients, such as in the transition region, or during impulsive events (e.g., Betta *et al.*, 1997). Another form of improvement has been the description of loops as collections of thin strands. Each strand is a self-standing, isolated and independent atmosphere, to be treated exactly as a single loop. This approach has been adopted both to describe loops as static (Reale and Peres, 2000) (Figure 12) and as impulsively heated by nanoflares (Warren *et al.*, 2002). On the same line, collections of loop models have been applied to describe entire active regions (Warren and Winebarger, 2006).

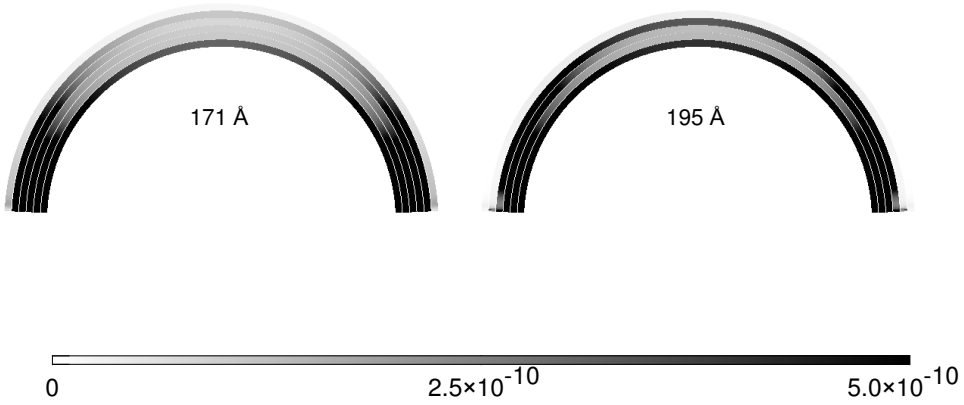

Figure 12: Emission in two TRACE filterbands predicted by a model of loop made by several thin strands (from Reale and Peres, 2000).

One limitation of current 1D loop models is that they are unable to treat conveniently the tapering expected going down from the corona to the chromosphere (or expansion upwards) through the transition region. This effect can be neglected in many circumstances, but it is becoming increasingly important with the finer and finer level of diagnostics allowed by upcoming observational data. For instance, the presence of tapering changes considerably the predicted distribution of emission measure in the low temperature region (Section 4.1.1).

Possible deviations from pure 1D evolution might be driven by intense oscillations or kinks, as described in Ofman (2009). The effect of the three-dimensional loop structure should then be taken into account to describe the interaction with excited MHD waves (McLaughlin and Ofman, 2008; Pascoe *et al.*, 2009; Selwa and Ofman, 2009).

However, the real power of 1D loop models, that makes them still on the edge, is that they fully exploit the property of the confined plasma to evolve as a fluid and practically independently of the magnetic field, and that they can include the coronal part, the transition region, and the photospheric footpoint in a single model with thermal conduction. In this framework, we may even simulate a multi-thread structure only by collecting many single loop models together, still with no need to include the description and interaction with the magnetic field. We should however be aware that the magnetic confinement of the loop material is not as strong and the thermal conduction is not as anisotropic below the coronal part of the loop as it is in the corona.

Klimchuk *et al.* (2008) illustrate a new efficient model of dynamic coronal loops called "Enthalpy-Based Thermal Evolution of Loops" (EBTEL), which accurately describes the evolution of the average temperature, pressure, and density along a coronal strand with a "0-D", very fast approach. This model is particularly useful for the description of loops as collections of myriads of strands.

In more detailed modeling, it has been recently shown that non-local thermal conduction may lengthen considerably the conduction cooling times and may enhance the chances of observing hot nanoflare-heated plasma (West *et al.*, 2008).

Alternative approaches to single or multiple loop modeling have been developed more recently, thanks also to the increasing availability of high performance computing systems and resources. A global "ab initio" approach was presented by Gudiksen and Nordlund (2005) and by Hansteen *et al.* (2007) (see also Yokoyama and Shibata, 2001, for the case of a flare model). They model a small part of the solar corona in a computational box using a three-dimensional MHD code that span the entire solar atmosphere from the upper convection zone to the lower corona. These models include non-grey, non-LTE (Local Thermodynamic Equilibrium) radiative transport in the photosphere and chromosphere, optically thin radiative losses, as well as magnetic field-aligned heat conduction in the transition region and corona. Although such models still cannot resolve well fine structures, such as current sheets and the transition region, they certainly represent the first important step toward fully self-consistent modeling of the magnetized corona.

4.1.1 Monolithic (static) loops: scaling laws

The Skylab mission remarked, and later missions confirmed (Figure 9), that many X-ray emitting coronal loops persist mostly unchanged for a time considerably longer than their cooling times by radiation and/or thermal conduction (Rosner *et al.*, 1978, and references therein). This means that, for most of their lives, they can be well described as systems at equilibrium and has been the starting point for several early theoretical studies (Landini and Monsignori Fossi, 1975; Gabriel, 1976; Jordan, 1976; Vesecky *et al.*, 1979; Jordan, 1980). Rosner *et al.* (1978) devised a model of coronal loops in hydrostatic equilibrium with several realistic simplifying assumptions: symmetry with respect to the apex, constant cross section (see Section 3.2.1), length much shorter than the pressure scale height, heat deposited uniformly along the loop, and low thermal flux at the base of the transition region, i.e., the lower boundary of the model. In these conditions, the pressure is uniform all along the loop, which is then described only by the energy balance between the heat input and the two main losses mentioned above. From the integration of the equation of energy conservation, one obtains the well-known scaling laws

$$T_{0,6} = 1.4\,(pL_9)^{1/3} \tag{8}$$

and

$$H_{-3} = 3p^{7/6}L_9^{-5/6}, \tag{9}$$

where $T_{0,6}$, L_9, and H_{-3} are the loop maximum temperature T_0, length L and heating rate per unit volume H, measured in units of 10^6 K (MK), 10^9 cm, and 10^{-3} erg cm^{-3} s^{-1}, respectively. These scaling laws were found in agreement with Skylab data within a factor 2.

Analogous models were developed in the same framework (Landini and Monsignori Fossi, 1975) and equivalent scaling laws were found independently by Craig *et al.* (1978), and more general ones by Hood and Priest (1979). They have been derived with a more general formalism by Bray *et al.* (1991). Although scaling laws could explain several observed properties, some features such as the emission measure in UV lines and the cool loops above sunspots could not be reproduced and, although the laws have been questioned a number of times (e.g., Kano and Tsuneta, 1995) in front of the acquisition of new data, such as those by Yohkoh and TRACE, they anyhow provide a basic physical reference frame to interpret any loop feature. For instance, they provide reference equilibrium values even for studies of transient coronal events, they have allowed to constrain that many loop structures observed with TRACE are overdense (e.g., Lenz *et al.*, 1999; Winebarger *et al.*, 2003a, Section 4.1.2) and, as such, these loops must be cooling from hotter status (Winebarger and Warren, 2005) (see Section 3.3.3, and so on). They also are useful for

density estimates when closed with the equation of state, and for coronal energy budget when integrated on relevant volumes and times.

Scaling laws have been extended to loops higher than the pressure scale height (Serio *et al.*, 1981) and limited by the finding that very long loops become unstable (Wragg and Priest, 1981). According to Antiochos and Noci (1986), the cool loops belong to a different family and are low-lying, and may eventually explain an evidence of excess of emission measure at low temperature.

The numerical solution of the complete set of hydrostatic equations allowed to obtain detailed profiles of the physical quantities along the loop, including the steep transition region. Figure 13 shows two examples of solution for different values of heating uniformly distributed along the loop.

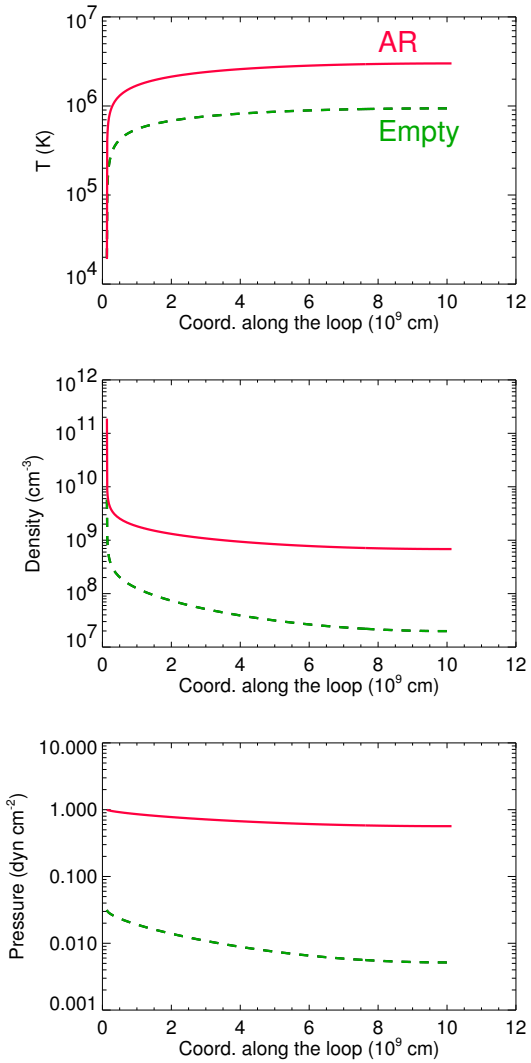

Figure 13: Distributions of temperature, density, and pressure along a hydrostatic loop computed from the model of Serio *et al.* (1981) for a high pressure loop (AR) and a low pressure one (Empty) with heating uniformly distributed along the loop.

Reale (1999) and Aschwanden and Nitta (2000) investigated in detail the effect of hydrostatic weighting on the loop visibility and on the vertical temperature structure of the solar corona.

From the comparison of SOHO-CDS observations of active region loops with a static, isobaric loop model (Landini and Landi, 2002), Brković *et al.* (2002) showed that a classical model is not able to reproduce the observations, but ad hoc assumptions might be needed. Further improvements of this approach including flows did not improve the agreement between the model and the observations (Landi and Landini, 2004). Using static models, Landi and Feldman (2004) found that the loop models overestimate the footpoint emission by orders of magnitude and proposed that non-uniformity in the loop cross section, more specifically a significant decrease of the cross section near the footpoints, is the most likely solution to the discrepancy (Section 4.1). On the same line, Winebarger *et al.* (2008) modelled X-ray loops and EUV moss in an active region core with steady uniform heating and found that a filling factor of 8% and loops that expand with height provide the best agreement with the intensity in two X-ray filters, though maintaining still some discrepancies with observations. Gontikakis *et al.* (2008) studied the distribution of coronal heating in a solar active region using a simple electrodynamic model and attributed the observed small coronal-loop width expansion to both the preferential heating of coronal loops of small cross-section variation and the cross-section confinement due to the random electric currents flowing along the loops.

The strength of scaling laws is certainly their simplicity and their easy and general application, even in the wider realm of stellar coronae. However, increasing evidence of dynamically heated, fine structured loops is indicating the need for improvements.

4.1.2 Structured (dynamic) loops

In the scenario of loops consisting of bundles of thin strands, each strand behaves as an independent atmosphere and can be described as an isolated loop itself. If the strands are numerous and heated independently, a loop can be globally maintained steady with a sequence of short heat pulses, each igniting a single or a few strands (nanoflares). In this case, although the loop remains steady on average for a long time, each strand has a continuously dynamic evolution. The evolution of a loop structure under the effect of an impulsive heating is well-known and studied from observations and from modeling (e.g., Nagai, 1980; Peres *et al.*, 1982; Cheng *et al.*, 1983; Nagai and Emslie, 1984; Fisher *et al.*, 1985a,b,c; MacNeice, 1986; Betta *et al.*, 2001), since it resembles the evolution of single coronal flaring loops. We have to mention here that there have been attempts to model even flaring loops as consisting of several flaring strands (Hori *et al.*, 1997, 1998; Reeves and Warren, 2002; Warren, 2006).

The evolution of single coronal loops or single loop strands subject to impulsive heating has been recently summarized in the context of the diagnostics of stellar flares (Reale, 2007). A heat pulse injected in an inactive tenuous strand makes chromospheric plasma expand in the coronal section of the strand, and become hot and dense, X-ray bright, coronal plasma. After the end of the heat pulse, the plasma begins to cool slowly. In general, the plasma cooling is governed by the thermal conduction to the cool chromosphere and by radiation from optically thin conditions. In the following we outline the evolution of the confined heated plasma into four phases, according to Reale (2007). Figure 14 tracks this evolution which maps on the path drawn in the density-temperature diagram of Figure 15 (see also Jakimiec *et al.*, 1992).

Phase I: From the start of the heat pulse to the temperature peak (*heating*). If the heat pulse is triggered in the coronal part of the loop, the heat is efficiently conducted down to the much cooler and denser chromosphere. The temperature rapidly increases in the whole loop, with a time scale given by the conduction time in a low density plasma (see below). This evolution changes only slightly if the heat pulse is deposited near the loop footpoints: the conduction front then propagates mainly upwards and on timescales not very different from the evaporation time scales, also because the heat conduction saturates (e.g., Klimchuk, 2006; Reale and Orlando, 2008). In this case the distinction from Phase II is not clearly marked.

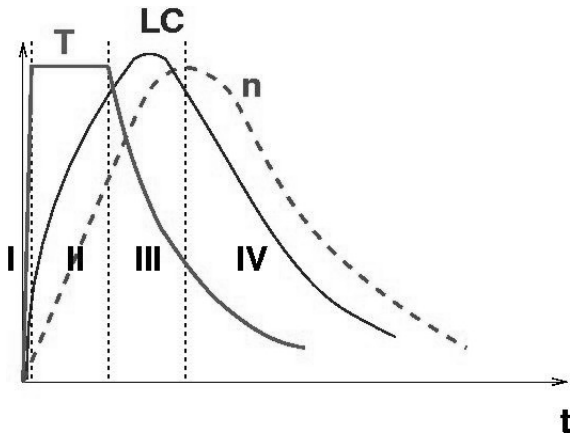

Figure 14: Scheme of the evolution of temperature (T, thick solid line), X-ray emission, i.e., the light curve (LC, thinner solid line) and density (n, dashed line) in a loop strand ignited by a heat pulse. The strand evolution is divided into four phases (I, II, III, IV, see text for further details) (from Reale, 2007).

Phase II: From the temperature peak to the end of the heat pulse (*evaporation*). The temperature settles to the maximum value (T_0). The chromospheric plasma is strongly heated, expands upwards, and fills the loop with much denser plasma. This occurs both if the heating is conducted from the highest parts of the corona and if it released directly near the loop footpoints. The evaporation is explosive at first, with a timescale given by the isothermal sound crossing time (s), since the temperature is approximately uniform in the highly conductive corona:

$$\tau_{sd} = \frac{L}{\sqrt{2k_B T_0/m}} \approx 80 \frac{L_9}{\sqrt{T_{0,6}}}, \tag{10}$$

where m is the average particle mass. After the evaporation front has reached the loop apex, the loop continues to fill more gently. The time scale during this more gradual evaporation is dictated by the time taken by the cooling rate to balance the heat input rate.

Phase III: From the end of the heat pulse to the density peak (*conductive cooling*). When the heat pulse stops, the plasma immediately starts to cool due to the efficient thermal conduction (e.g., Cargill and Klimchuk, 2004), with a time scale (s):

$$\tau_c = \frac{3 n_c k_B T_0 L^2}{2/7 \kappa T_0^{7/2}} = \frac{10.5 n_c k_B L^2}{\kappa T_0^{5/2}} \approx 1500 \frac{n_9 L_9^2}{T_6^{5/2}}, \tag{11}$$

where n_c ($n_{c,10}$) is the particle density (10^{10} cm^{-3}) at the end of the heat pulse, the thermal conductivity is $\kappa = 9 \times 10^{-7}$ (c.g.s. units). Since the plasma is dense, we expect no saturation effects in this phase.

The heat stop time can be generally traced as the time at which the temperature begins to decrease significantly and monotonically. While the conduction cooling dominates, the plasma evaporation is still going on and the density increasing. The efficiency of radiation cooling increases as well, while the efficiency of conduction cooling decreases with the temperature.

Phase IV: From the density peak afterwards (*radiative cooling*). As soon as the radiation cooling time becomes equal to the conduction cooling time (Cargill and Klimchuk, 2004), the density reaches its maximum, and the loop depletion starts, slowly at first and then progressively faster. The pressure begins to decrease inside the loop, and is no longer able to sustain the

plasma. The radiation becomes the dominant cooling mechanism, with the following time scale (s):

$$\tau_r = \frac{3k_B T_M}{n_M P(T)} = \frac{3k_B T_M}{bT_M^{\alpha} n_M} \approx 3000 \frac{T_{M,6}^{3/2}}{n_{M,9}}, \tag{12}$$

where T_M ($T_{M,6}$) is the temperature at the time of the density maximum (10^7 K), n_M ($n_{M,9}$) the maximum density (10^9 cm^{-3}), and $P(T)$ the plasma emissivity per unit emission measure, expressed as:

$$P(T) = bT^{\alpha},$$

with $b = 1.5 \times 10^{-19}$ and $\alpha = -1/2$. The density and the temperature both decrease monotonically.

The presence of significant residual heating could make the decay slower. In single loops, this can be diagnosed from the analysis of the slope of the decay path in the density-temperature diagram (Sylwester *et al.*, 1993; Reale *et al.*, 1997a). The free decay has a slope between 1.5 and 2 in a log density vs log temperature diagram; heated decay path is flatter down to a slope ~ 0.5. In non-flaring loops, the effect of residual heating can be mimicked by the effect of a strong gravity component, as in long loops perpendicular to the solar surface. The dependence of the decay slope on the pressure scale height has been first studied in Reale *et al.* (1993) and, more recently, in terms of enthalpy flux by Bradshaw and Cargill (2010).

As clear from Figure 15 the path in this phase is totally below, or at most approaches, the QSS curve. This means that for a given temperature value the plasma density is higher than that expected for an equilibrium loop at that temperature, i.e., the plasma is "overdense". Evidence of such overdensity (Section 3.3.3) has been taken as an important indication of steadily pulse-heated loops.

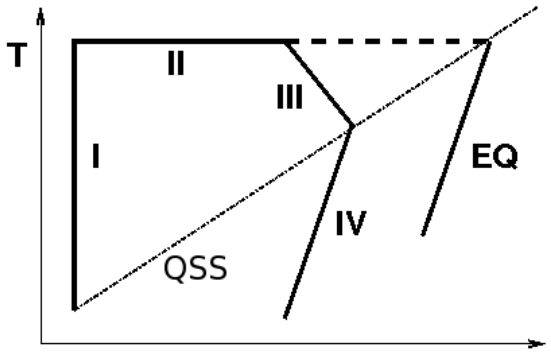

Figure 15: Scheme of the evolution of pulse-heated loop plasma of Figure 14 in a density-temperature diagram (*solid line*). The four phases are labeled. The locus of the equilibrium loops is shown (*dashed-dotted line*, marked with QSS), as well as the evolution path with an extremely long heat pulse (*dashed line*) and the corresponding decay path (marked with EQ) (adapted from Reale, 2007).

This is the evolution of a loop strand ignited by a transient heat pulse. Important properties of the heated plasma can be obtained from the analysis of the evolution after the heating stops, i.e., when the plasma cools down.

Serio *et al.* (1991) derived a global thermodynamic time scale for the pure cooling of heated plasma confined in single coronal loops, which has been later (Reale, 2007) refined to be (s):

$$\tau_s = 4.8 \times 10^{-4} \frac{L}{\sqrt{T_0}} = 500 \frac{L_9}{\sqrt{T_{0,6}}}. \tag{13}$$

This decay time was obtained assuming that the decay starts from equilibrium conditions, i.e., departing from the locus of the equilibrium loops with a given length (hereafter QSS line, Jakimiec *et al.*, 1992) in Figure 15. It is, therefore, valid as long as there is no considerable contribution from the plasma draining to the energy balance. The link between the assumption of equilibrium and the plasma evolution is shown in Figure 15: if the heat pulse lasts long enough, Phase II extends to the right, and the heated loop asymptotically reaches equilibrium conditions, i.e., the horizontal line approaches the QSS line. If the decay starts from equilibrium conditions, Phase III is no longer present, and Phase II links directly to Phase IV. Therefore, there is no delay between the beginning of the temperature decay and the beginning of the density decay: the temperature and the density start to decrease simultaneously. Also, the decay will be dominated by radiative cooling, except at the very beginning (Serio *et al.*, 1991).

The presence of Phase III implies a delay between the temperature peak and the density peak. This delay is often observed both in solar flares (e.g., Sylwester *et al.*, 1993) and in stellar flares (e.g., van den Oord *et al.*, 1988; van den Oord and Mewe, 1989; Favata *et al.*, 2000; Maggio *et al.*, 2000; Stelzer *et al.*, 2002). The presence of this delay, whenever observed, is a signature of a relatively short heat pulse or, in other words, of a decay starting from non-equilibrium conditions.

According to Reale (2007), the time taken by the loop to reach equilibrium conditions under the action of a constant heating is much longer than the sound crossing time (Equation (10)), which rules the very initial plasma evaporation. As already mentioned, in the late rise phase the dynamics become much less important and the interplay between cooling and heating processes becomes dominant. The relevant time scale is, therefore, that reported in Equation (13).

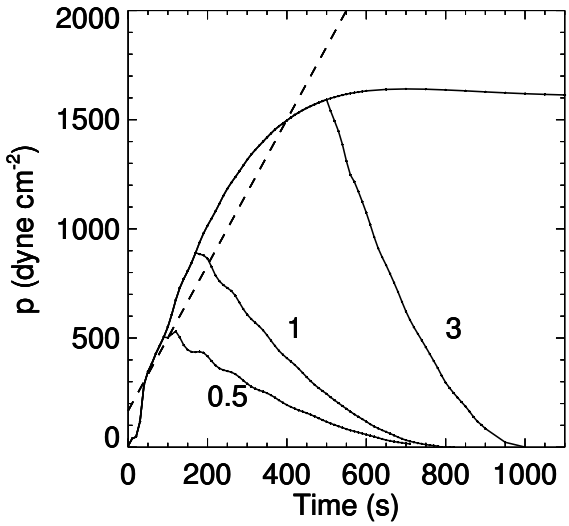

Figure 16: Pressure evolution obtained from a hydrodynamic simulation of a loop strand ignited by heat pulses of different duration (0.5, 1, 3 times the loop decay time, see text) and with a continuous heating. Most of the rise phase can be reasonably described with a linear trend (dashed lines) (from Reale, 2007).

Hydrodynamic simulations confirm that the time required to reach full equilibrium scales as the loop cooling time (τ_s) and, as shown for instance in Figure 16 (see also Jakimiec *et al.*, 1992), the time to reach flare steady-state equilibrium is

$$t_{eq} \approx 2.3\tau_s. \tag{14}$$

For $t \geq t_{eq}$, the density asymptotically approaches the equilibrium value

$$n_0 = \frac{T_0^2}{2a^3 k_B L} = 1.3 \times 10^6 \ \frac{T_0^2}{L}, \tag{15}$$

where $a = 1.4 \times 10^3$ (c.g.s. units), or

$$n_9 = 1.3 \frac{T_{0,6}^2}{L_9}. \tag{16}$$

If the heat pulse stops before the loop reaches equilibrium conditions, the loop plasma maximum density is lower than the value at equilibrium, i.e., the plasma is underdense (Cargill and Klimchuk, 2004, Section 4.4). Figure 16 shows that, after the initial impulsive evaporation on a time scale given by Equation (10), the later progressive pressure growth can be approximated with a linear trend. Since the temperature is almost constant in this phase, we can approximate that the density increases linearly for most of the time. We can then estimate the value of the maximum density at the loop apex as

$$n_M \approx n_0 \frac{t_M}{t_{eq}}, \tag{17}$$

where t_M is the time at which the density maximum occurs.

Phase III ranges between the time at which the heat pulse ends and the time of the density maximum. The latter is also the time at which the decay path crosses the locus of the equilibrium loops (QSS curve). According to Reale (2007), the temperature T_M at which the maximum density occurs is

$$T_M = 9 \times 10^{-4} (n_M L)^{1/2} \tag{18}$$

or

$$T_{M,6} = 0.9 (n_{M,9} L_9)^{1/2} \quad .$$

We can also derive the duration of Phase III, i.e., the time from the end of the heat pulse to the density maximum, as

$$\Delta t_{0-M} \approx \tau_c \ln \psi, \tag{19}$$

where

$$\psi = \frac{T_0}{T_M}$$

and τ_c (Equation (11)) is computed for an appropriate value of the density n_c. A good consistency with numerical simulations is obtained for $n_c = (2/3) n_M$.

By combining Equations (19) and (17) we obtain

$$\frac{\Delta t_{0-M}}{t_M} \approx 1.2 \ln \psi, \tag{20}$$

which ranges between 0.2 and 0.8 for typical values of ψ (1.2 – 2).

These scalings are related to the evolution of a single strand under the effect of a local heat pulse. The strands are below the current instrument spatial resolution and, therefore, we have to consider that, if this scenario is valid, we see the envelope of a collection of small scale events. The characteristics of the single heat pulses become, therefore, even more difficult to diagnose, and the question of their frequency, distribution, and size remains open. Also from the point of view of the modeling, a detailed description of a multistrand loop implies a much more complex and demanding effort. A possible approach is to literally build a collection of 1-D loop models,

each with an independent evolution (Guarrasi *et al.*, 2010). One common approach so far has been to simulate anyhow the evolution of a single strand and to assume that, in the presence of a multitude of such strands, in the steady state we would see at least one strand at any step of the strand evolution. In other words, a collection of nanoflare-heated strands can be described as a whole with the time-average of the evolution of a single strand (Warren *et al.*, 2002, 2003; Winebarger *et al.*, 2003a,b, see also Section 4.2). Another issue to be explored is whether it is possible, and to what extent, to describe a collection of independently-evolving strands as a single effective evolving loop. For instance, how does the evolution of a single loop where the heating is decreasing slowly compare to the evolution of a collection of independently heated strands, with a decreasing rate of ignition? To what extent do we expect coherence and how is it connected to the degree of global coherence of the loop heating? Is there any kind of transverse coherence or ordered ignition of the strands? It is probably reasonable to describe a multi-stranded loop as a single "effective" loop if we can assume that the plasma loses memory of its previous history. This certainly occurs in late phases of the evolution when the cooling has been going on for a long time.

4.2 Fine structuring

The description and role of fine structuring of coronal loops is certainly a challenge for coronal physics, also on the side of modeling, essentially because we have few constraints from observations (Section 3.2.2). One of the first times that the internal structuring of coronal loops have been invoked in a modeling context was for the problem of the interpretation of the uniform filter ratio distribution detected with TRACE *along* warm loops. Lenz *et al.* (1999) claimed that standard hydrostatic loop models with uniform heating could not explain such indication of uniform temperature distribution. Reale and Peres (2000) showed that a uniform filter ratio could be produced by the superposition of several thin strands described by standard static models of loops at different temperatures. In alternative, Aschwanden (2001) showed that long loops heated at the footpoints result to be mostly isothermal. The problem with this model is that footpoint-heated loops (with heating scale height less than 1/3 of the loop half-length) had been shown to be thermally unstable and, therefore, they cannot be long-lived, as instead observed. A further alternative is to explain observations with steady non-static loops, i.e., with significant flows inside (Winebarger *et al.*, 2001, 2002c, see below). Also this hypothesis does not seem to answer the question (Patsourakos *et al.*, 2004).

A first step to modeling fine-structured loops is to use multistrand static models. Such models show some substantial inconsistencies with observations, e.g., in general they predict too large loop cross sections (Reale and Peres, 2000). Such strands are conceptually different from the thin strands predicted in the nanoflare scenario (Parker, 1988), which imply a highly dynamic evolution due to pulsed-heating. The nanoflare scenario is approached in multi-thread loop models, convolving the independent hydrodynamic evolution of the plasma confined in each pulse-heated strand (see Section 4.3). These are able to match some more features of the evolution of warm loops observed with TRACE (Warren *et al.*, 2002, 2003; Winebarger *et al.*, 2003a,b). By means of detailed hydrodynamic loop modeling, Warren *et al.* (2002) found that an ensemble of independently heated strands can be significantly brighter than a static uniformly heated loop and would have a flat filter ratio temperature when observed with TRACE. As an extension, time-dependent hydrodynamic modeling of an evolving active region loop observed with TRACE showed that a loop made as a set of small-scale, impulsively heated strands can generally reproduce the spatial and temporal properties of the observed loops, such as a delay between the appearance of the loop in different filters (Warren *et al.*, 2003). As an evolution of this approach, Warren and Winebarger (2006) modelled an entire active region for comparison with a SoHO/EIT observation. They made potential field extrapolations to compute magnetic field lines and populate these field lines with solutions to the hydrostatic loop equations assuming steady, uniform heating. As a result, they

constrained the link between the heating rate and the magnetic field and size of the structures. However, they also found significant discrepancies with the observed EIT emission.

More recently modeling a loop system as a collection of thin unresolved strand with pulsed heating has been used to explain why active regions look fuzzier in harder energy bands, i.e., X-rays, and/or hotter spectral lines, e.g., Fe XVI (Tripathi *et al.*, 2009, Section 3.3.2). The basic reason is that in the dynamic evolution of each strand, the plasma spends a relatively longer time and with a high emission measure at temperature about 3 MK (Guarrasi *et al.*, 2010).

Although multistrand models appear much more complex than single loop models and need further refinements to match all the observational constraints, as mentioned in Section 4.1.2, they certainly represent an important issue for the future of coronal loop comprehension.

4.3 Flows

A generalization of static models of loops (Section 4.1.1) is represented by models of loops with stationary flows, driven by a pressure imbalance between the footpoints (siphon flows). The properties of siphon flows have been studied by several authors (Cargill and Priest, 1980; Priest, 1981; Noci, 1981; Borrini and Noci, 1982; Antiochos, 1984; Thomas, 1988; Montesinos and Thomas, 1989; Noci *et al.*, 1989; Thomas and Montesinos, 1990; Spadaro *et al.*, 1990; Thomas and Montesinos, 1991; Peres *et al.*, 1992; Montesinos and Thomas, 1993). Orlando *et al.* (1995a) developed a complete detailed model of loop siphon flows and used it to explore the space of the solutions and to derive an extension of RTV scaling laws to loops containing subsonic flows.

Orlando *et al.* (1995b) explored the conditions for the presence of stationary shocks in critical and supersonic siphon flows in coronal loops (Figure 17), finding that the shock position depends on the volumetric heating rate of the loop, and devising related scaling laws. The presence of massive flows may alter the line emission with respect to static plasma, because of the delay of the moving plasma to settle to ionization equilibrium (Golub *et al.*, 1989). Spadaro *et al.* (1990) modelled that, even including the effect of ionization non-equilibrium, the UV lines are predicted to be blue-shifted by loop models. So non-equilibrium emission from flows cannot explain the observed dominant redshifts (Section 3.5). The effects of non-equilibrium of ionization in UV line emission from shocked siphon flows are further discussed in Orlando and Peres (1999).

Modeling efforts were devoted in the 1990s to explain specifically the extensive evidence of redshifted UV lines on the solar disk. Hansteen (1993) used a hydrodynamic loop model including the effects of non-equilibrium of ionization to show that the redshifts might be produced by downward propagating acoustic waves, possibly stimulated by nanoflares. By means of two-dimensional hydrodynamic simulations, Reale *et al.* (1996, 1997b) proposed that the UV redshifts might be due to downdrafts driven by radiatively-cooling condensations in the solar transition region. In the exploration of the parameter space, they found redshifted components at speeds of several km s^{-1} for ambient pressure values ranging from those typical of quiet Sun to active regions and predicted that redshifts may occur more easily in the higher pressure plasma, typical of active regions.

Teriaca *et al.* (1999b) explored the idea that the occurrence of nanoflares in a magnetic loop around the O VI formation temperature could explain the observed redshift of mid-low transition region lines as well as the blueshift observed in low coronal lines ($T > 6 \times 10^5$ K). Observations were compared to numerical simulations of the response of the solar atmosphere to an energy perturbation of 4×10^{24} erg, including non-equilibrium of ionization. Performing an integration over the entire period of simulations, they found a redshift in C IV, and a blueshift in O VI and Ne VIII, of a few km s^{-1}, in reasonable agreement with observations. A similar idea was applied by Patsourakos and Klimchuk (2006) to make predictions about the presence or absence of nonthermal broadening in several spectral lines (e.g., Ne VIII, Mg X, Fe XVII) due to nanoflare-driven chromospheric evaporation. Clearly, the occurrence of such effects in the lines depends considerably on the choice of the heat pulse parameters. Therefore, more constraints are needed to make the whole

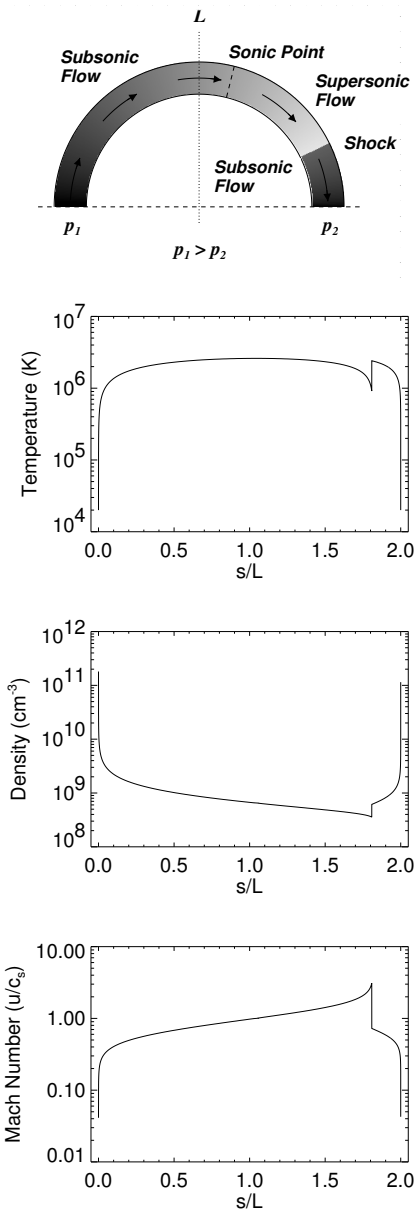

Figure 17: Example of solutions of a siphon flow loop model including a shock (from Orlando and Peres, 1999).

model more consistent. In other words, modeling should address specific observations to provide more conclusive results.

Theoretical reasons indicate that flows should be invariably present in coronal loop systems, although they may not be necessarily important in the global loop momentum and energy budget. For instance, it has been shown that the presence of, at least, moderate flows is necessary to explain why we actually see the loops (Lenz, 2004). The loop emission and detection is in fact due to the emission from heavy ions, like Fe. In hydrostatic equilibrium conditions, gravitational settlement should keep the emitting elements low on the solar surface, and we should not be able to see but the loop footpoints. Instead, detailed modeling shows that flows of few km s^{-1} are enough to drag ions high in the corona by Coulomb coupling and to enhance coronal ion abundances by orders of magnitudes. Incidentally, the same modeling shows that, for the same mechanisms, no chemical fractionation of coronal plasma with respect to photospheric composition as a function of the element First Ionization Potential (FIP) should be present in coronal loops.

Other studies point instead to the relative unimportance of flows in coronal loops. In particular, as already mentioned in Section 3.2.2, by means of steady hydrodynamic loop modeling (i.e., assuming equilibrium condition and, therefore, dropping the time-dependent terms in Equations (3), (4), and (5), Patsourakos *et al.* (2004) showed that flows may not be able to explain the evidence of isothermal loops, as instead proposed by Winebarger *et al.* (2002c). They found that a heating deposited asymmetrically in a loop is able to drive significant flows in the loop and to enhance its density to the levels typically diagnosed from TRACE observations, but it also produces an inversion of the temperature distribution and, consequently, a highly structured distribution of the relevant filter ratio along the loop, which is not observed.

Plasma cooling is a mechanism that may drive significant downflows in a loop (e.g., Bradshaw and Cargill, 2005, 2010). As an extension of studies on modeling catastrophic cooling in loops (Müller *et al.*, 2004), Müller *et al.* (2005) tried to explain the evidence of propagating intensity variations observed in the He II 304 Å line with SoHO/EIT (De Groof *et al.*, 2004, Section 3.5). Two possible driving mechanisms had been proposed: slow magnetoacoustic waves or blobs of cool downfalling plasma. A model of cool downfalling blob triggered in a thermally-unstable loop heated at the footpoints gave a qualitative agreement with measured speeds and predicted a significant braking in the high-pressure transition region, to be checked in future high cadence observations in cool lines.

Plasma waves have been more recently proposed to have an important role in driving flows within loops. Acoustic waves excited by heat pulses at the chromospheric loop footpoints and damped by thermal conduction in corona are possible candidates (Taroyan *et al.*, 2005). Even more attention received the propagation of Alfvén waves in coronal loops. Hydrodynamic loop modeling O'Neill and Li (2005) showed that Alfvén waves deposit significant momentum in the plasma, and that steady state conditions with significant flows and relatively high density can be reached. Analogous results were independently obtained with a different approach: considering a wind-like model to describe a long isothermal loop, Grappin *et al.* (2003, 2005) showed that the waves can drive pressure variations along the loop which trigger siphon flows. Alfvén disturbances have been recently shown to be amplified by the presence of loop flows (Taroyan, 2009).

As listed above, models predict the development of flows inside coronal loops in a wide variety of situations, namely evaporation, draining, siphon flows, waves. The challenge will be to distinguish clearly among them and to assess the appropriate weight and importance to them both in the spatial and temporal distribution.

4.4 Heating

The problem of what heats coronal loops is essentially the problem of coronal heating, and is a central issue in the whole solar physics. Although the magnetic origin of coronal heating has been

well-established since the very first X-ray observations of the corona, the detailed mechanism of conversion of magnetic energy into thermal energy is still under intense debate, because a series of physical effects conspire to make the mechanism intrinsically elusive.

Klimchuk (2006) splits the heating problem into six steps: the identification of the source of energy, its conversion into heat, the plasma response to the heating, the spectrum of the emitted radiation, the final signature in observables. Outside of analytical approaches, the source and conversion of energy are typically studied in detail by means of multi-dimensional full MHD models (e.g., Gudiksen and Nordlund, 2005), which, however, are still not able to provide exhaustive predictions on the plasma response and complete diagnostics on observables. On the other hand, the plasma response is the main target of loop hydrodynamic models, which, instead, are not able to treat the heating problem in a self-consistent way (Section 4.1).

In the investigation of the source of energy, Golub *et al.* (1980) already pointed out that the magnetic field plays an active role in heating the coronal loops. They assumed that the field lines are wound continuously by the photospheric convective motions and the generated non-potential component is dissipated into heating. Several following studies were devoted to the connection and scaling of the magnetic energy to the coronal energy content (Golub *et al.*, 1982) and to the rate of energy release through reconnection (Galeev *et al.*, 1981). The photospheric motions are, therefore, the ultimate energy source and stress the field or generate waves depending on whether the timescale of the motion is long or short compared to the end-to-end Alfvén travel time. Following Klimchuk (2006), dissipation of magnetic stresses can be referred to as Direct Current (DC) heating, and dissipation of waves as Alternating Current (AC) heating.

The question of the conversion of the magnetic energy into heat is also challenging, because dissipation is predicted to occur on very small scales or large gradients in the corona by classical theory, unless anomalous dissipation coefficients are invoked. As reviewed by Klimchuk (2006), large gradients may be produced in various ways, involving either magnetic field patterns and their evolution, magnetic instabilities such as the kink instability, or velocity pattern, such as turbulence. For waves, resonance absorption and phase mixing may be additional viable mechanisms.

The problem of plasma response to heating has been kept historically well separated from the primary heating origin, although some attempts have been made to couple them. For instance, in Reale *et al.* (2005) the time-dependent distribution of energy dissipation along the loop obtained from a hybrid shell model was used as heating input of a time-dependent hydrodynamic loop model (see below). A similar concept was applied to search for signatures of turbulent heating in UV spectral lines (Parenti *et al.*, 2006).

As already mentioned, studies using steady-state or time-dependent purely hydrodynamic loop modeling have addressed primarily the plasma response to heating, and also its radiative emission and the detailed comparison with observations. A forward-modeling including all these steps was performed by Reale *et al.* (2000b,a). They first analyzed a TRACE observation of a brightening coronal loop (see also Section 3.4). The analysis was used to set up the parameters for the forward modeling, and to run loop hydrodynamic simulations with various assumptions on the heating location and time dependence. The comparison of the TRACE emission predicted by the simulations with the measured one constrained the heat pulse to be short, much less than the observed loop rise phase, and intense, appropriate for a 3 MK loop, and its location to be probably midway between the apex and one of the footpoints.

The investigation of the heating mechanisms through the plasma response is made difficult by a variety of reasons. For instance, the problem of background subtraction can be crucial in the comparison with observations, as shown by the three analyses of the same large loop structure observed with Yohkoh/SXT on the solar limb, mentioned in Section 3.3. More specifically, Priest *et al.* (2000) tried to deduce the form of the heating from Yohkoh observed temperature profiles and found that a uniform heating best describes the data, if the temperature is obtained from the ratio of the total filter intensities, with no background subtraction. Aschwanden (2001) splitted the

measured emission into two components and found a better agreement with heating deposited at the loop footpoints. Reale (2002b) revisited the analysis of the same loop system, considering conventional hydrostatic single-loop models and accounting accurately for an unstructured background contribution. With forward-modeling, i.e., synthesizing from the model observable quantities to be compared directly with the data, background-subtracted data are fitted with acceptable statistical significance by a model of relatively hot loop (~ 3.7 MK) heated at the apex, but it was pointed out the importance of background subtraction and the necessity of more specialized observations to address this question. More diagnostic techniques to compare models with observations were proposed afterwards (e.g., Landi and Landini, 2005).

Independently of the adopted numerical or theoretical tool, many studies have been addressing the mechanisms of coronal loop heating clearly distinguishing between the two main classes, i.e., DC heating through moderate and frequent explosive events, named nanoflares (e.g., Parker, 1988) and AC heating via Alfvén waves (e.g., Litwin and Rosner, 1998).

4.4.1 DC heating

Heating by nanoflares has a long story as a possible candidate to explain the heating of the solar corona and, in particular, of the coronal loops (e.g., Peres *et al.*, 1993; Cargill, 1993; Kopp and Poletto, 1993; Shimizu, 1995; Judge *et al.*, 1998; Mitra-Kraev and Benz, 2001; Katsukawa and Tsuneta, 2001; Warren *et al.*, 2002, 2003; Spadaro *et al.*, 2003; Cargill and Klimchuk, 1997, 2004; Müller *et al.*, 2004; Testa *et al.*, 2005; Reale *et al.*, 2005; Vekstein, 2009).

More specifically, Cargill (1994) provided detailed predictions from a model of loops made of thousands of nanoflare-heated strands. In particular, whereas the loop total emission measure distribution should steepen above the canonical $T^{1.5}$ (Jordan, 1980; Orlando *et al.*, 2000; Peres *et al.*, 2001) dependence for temperature above 1 MK. Moreover, it was stressed the importance of the dependence of effects such as the plasma dynamics (filling and draining) on the loop filling factor driven by the elemental heat pulse size (Section 4.1.2). In Cargill and Klimchuk (1997) the nanoflare model was applied to the heating of coronal loops observed by Yohkoh. A good match was found only for hot (4 MK) loops, with filling factors less than 0.1, so that it was hypothesized the existence of two distinct classes of hot loops.

Although there is evidence of intermittent heating episodes, it has been questioned whether and to what extent nanoflares are able to provide enough energy to heat the corona (e.g., Aschwanden, 1999). On the other hand, loop models with nanoflares and, in particular, those considering a prescribed random time distribution of the pulses deposited at the footpoints of multi-stranded loops have been able to explain several features of loop observations, for instance, of warm loops from TRACE (Warren *et al.*, 2002, 2003), (see Section 3.2.2).

Hydrodynamic loop modeling showed also that different distributions of the heat pulses along the loop have limited effects on the observable quantities (Patsourakos and Klimchuk, 2005), because most of the differences occur at the beginning of the heat deposition, when the emission measure is low, while later the loop loses memory of the heat distribution (see also Winebarger and Warren, 2004). Patsourakos and Klimchuk (2008) applied both static and impulsive models to solar active regions and showed that the latter ones are able to simultaneously reproduce EUV and SXR loops in active regions, and to predict radial intensity variations consistent with the localized core and extended emissions. Cargill and Klimchuk (2004) showed with a semi-analytical loop model that the cycle of loop heating/cooling naturally leads to hot-underdense/warm-overdense loop (Section 4.1.2), as observed (Winebarger *et al.*, 2003b, Section 3.3.3), and that the width of the DEM of a nanoflare-heated loop can depend on the number of strands which compose the loop: a relatively flat DEM or a peaked (isothermal) DEM are obtained with strands of diameter about 15 km or about 150 km, respectively. This is of relevance for the diagnostics both of the loop fine structure (Section 3.2.2) and of the DEM reconstruction (Section 3.3). As a further improvement,

Warren and Winebarger (2007) added an impulsive heating model to the simulation of an entire active region and found that it is possible to reproduce the total observed soft X-ray emission in all of the Yohkoh/SXT filters. However, once again, at EUV wavelengths the agreement between the simulation and the observation is only partial.

Nanoflares have been studied also in the framework of stellar coronae. Testa *et al.* (2005) showed that intermittent heating by relatively intense nanoflares deposited at the loop footpoints make the loop stable on long time scales (loops continuously heated at the footpoints are unstable) and, on the other hand, produces a well-defined peak in the average DEM of the loop, similar to that derived from the DEM reconstruction of active stars, and also to those shown in Cargill (1994). Therefore, this is an alternative way to obtain a steep temperature dependence of the loop emission measure distribution in the low temperature range.

An alternative approach to study nanoflare heating is to analyze intensity fluctuations (Shimizu and Tsuneta, 1997; Vekstein and Katsukawa, 2000; Katsukawa and Tsuneta, 2001; Vekstein and Jain, 2003) and to derive their occurrence distribution (Sakamoto *et al.*, 2008, 2009). From the width of the distributions and autocorrelation functions, it has been suggested that nanoflare signatures are more easily found in observations of warm TRACE loops than of hot Yohkoh/SXT loops. It is to be investigated whether the results change after relaxing the assumption of temperature-independent distribution widths. Also other variability analysis of TRACE observations was found able to put constraints on loop heating. In particular, according to Antiochos *et al.* (2003), in TRACE observations, the lack of observable warm loops and of significant variations in the moss regions implies that the heating in the hot moss loops should not be truly flare-like, but instead quasi-steady and that the heating magnitude is only weakly varying. Further evidence in this direction has been found more recently by Warren *et al.* (2010).

An analogous approach is to analyze the intensity distributions. The distribution of impulsive events vs their number in the solar and stellar corona is typically described with a power law. The slope of the power law is a critical parameter to establish weather such events are able to heat the solar corona (Hudson, 1991). In particular, a power law index of 2 is the critical value above or below which flare-like events may be able or unable, respectively, to power the whole corona (e.g., Aschwanden, 1999). Unfortunately, due to the faintness of the events, the distribution of weak events is particularly difficult to derive and might even be separate from that of proper flares and microflares. Parenti and Young (2008) used a hydrodynamic model to simulate the UV emission of a loop system heated by nanoflares on small, spatially unresolved scales. The simulations confirm previous results that several spectral lines have an intensity distribution that follows a power-law, in a similar way to the heating function (Hudson, 1991). However, only the high temperature lines best preserve the heating function's power law index (especially Fe XIX).

4.4.2 AC heating

Loop oscillations, modes, and wave propagation deserve a review by themselves, and are outside of the scope of the present one. Here we account for some aspects which are relevant for the loop heating. A recent review of coronal waves and oscillations can be found in Nakariakov and Verwichte (2005). New observations from SDO AIA provide ample evidence of wave activity in the solar corona (Title, 2010). These observations are currently the subject of intensive analysis and will be reported on in the future.

As reviewed by Klimchuk (2006), MHD waves of many types are generated in the photosphere, e.g., acoustic, Alfvén, fast and slow magnetosonic waves. Propagating upwards, the waves may transfer energy to the coronal part of the loops. The question is what fraction of the wave flux is able to pass through the very steep density and temperature gradients in the transition region. Acoustic and slow-mode waves form shocks and are strongly damped, fast-mode waves are strongly refracted and reflected (Narain and Ulmschneider, 1996).

Ionson (1978, 1982, 1983) devised an LRC equivalent circuit to show the potential importance of AC processes to heat the corona. Hollweg (1984) used a dissipation length formalism to propose resonance absorption of Alfvén waves as a potential coronal heating mechanism. A loop may be considered as a high-quality resonance cavity for hydromagnetic waves. Turbulent photospheric motions can excite small-scale waves. Most Alfvén waves are strongly reflected in the chromosphere and transition region, where the Alfvén speed increases dramatically with height. Significant transmission is possible only within narrow frequency bands centered on discrete values where loop resonance conditions are satisfied (Hollweg, 1981, 1984; Ionson, 1982). The waves resonate as a global mode and dissipate efficiently when their frequency is near the local Alfvén waves frequency $\omega_A \approx 2\pi v_A/L$. By solving the linearized MHD equations Davila (1987) showed that this mechanism can potentially heat the corona, as further supported by numerical solution of MHD equations for low beta plasma (Steinolfson and Davila, 1993), and although Parker (1991) argued that Alfvén waves are difficult to be generated by solar convection.

Evidence for photospheric Alfvén waves was obtained from magnetic and velocity fluctuations in regions of strong magnetic field (Ulrich, 1996) and from granular motions in the quiet Sun (Muller *et al.*, 1994) with fluxes of the order of 10^7 erg cm^{-2} s^{-1}, which might contribute to heating if transmitted efficiently to the corona.

Hollweg (1985) estimated that enough flux may pass through the base of long ($> 10^{10}$ cm) active region loops to provide their heating, but shorter loops are a problem, since they have higher resonance frequencies and the photospheric power spectrum is believed to decrease exponentially with frequency in this range. Litwin and Rosner (1998) suggested that short loops may transmit waves with low frequencies, as long as the field is sufficiently twisted. Hollweg and Yang (1988) proposed that Alfvén resonance can pump energy out of the surface wave into thin layers surrounding the resonant field lines and that the energy can be distributed by an eddy viscosity throughout large portions of coronal active region loops.

Waves may be generated directly in the corona and evidence for their presence was found (e.g., Nakariakov *et al.*, 1999; Aschwanden *et al.*, 1999a; Berghmans and Clette, 1999; De Moortel *et al.*, 2002). It is unclear whether coronal waves carry a sufficient energy flux to heat the plasma (Tomczyk *et al.*, 2007). Ofman *et al.* (1995) studied the dependence on the wavenumber for comparison with observations of loop oscillations and found partial agreement with velocity amplitudes measured from nonthermal broadening of soft X-ray lines. The observed nonthermal broadening of transition region and coronal spectral lines implies fluxes that may be sufficient to heat both the quiet Sun and active regions, but it is unclear whether the waves are efficiently dissipated (Porter *et al.*, 1994). Furthermore, the nonthermal line broadening could be produced by unresolved loop flows that are unrelated to waves (Patsourakos and Klimchuk, 2006). Ofman *et al.* (1998) included inhomogeneous density structures and found that a broadband wave spectrum becomes necessary for efficient resonance and that it fragments the loop into many density layers that resemble the multistrand concept. The heat deposition by the resonance of Alfvén waves in a loop was investigated by O'Neill and Li (2005) By assuming a functional form first proposed by Hollweg (1986), hydrodynamic loop modeling showed that, depending on the model parameters, heating by Alfvén waves leads to different classes of loop solutions, such as the isothermal cool loops indicated by TRACE, or the hot loops observed with Yohkoh/SXT. Specific diagnostics are still to be defined for the comparison with observations.

Efficient wave dissipation may be allowed by enhanced dissipation coefficients inferred from fast damping of flaring loop oscillations in the corona (Nakariakov *et al.*, 1999), but the same effect may also favor efficient magnetic reconnection in nanoflares. Alfvén waves required for resonant absorption are relatively high frequency waves. Evidence for lower frequency Alfvén waves has been found in the chromosphere with the Hinode SOT (De Pontieu *et al.*, 2007). Such waves may supply energy in the corona even outside of resonance with different mechanisms to be explored with modeling. Among dissipation mechanisms phase mixing with enhanced resistivity was suggested

by Ofman and Aschwanden (2002) and supported by the analysis of Ofman and Wang (2008). Also multistrand structures has been recognized to be important in possible wave dissipation and loop twisting, as recently modelled by Ofman (2009).

Intensity disturbances propagating along active region loops at speeds above 100 km s^{-1} were detected with TRACE and interpreted as slow magnetoacoustic waves (Nakariakov *et al.*, 2000). These waves probably originate from the underlying oscillations, i.e., the 3-minute chromospheric / transition-region oscillations in sunspots and the 5-minute solar global oscillations (p-modes). Slow magnetosonic waves might be good candidates as coronal heating sources according to quite a detailed model by Beliën *et al.* (1999), including the effect of chromosphere and transition region and of the radiative losses in the corona. Such waves might be generated directly from upward propagating Alfvén waves. Contrary conclusions, in favor of fast magnetosonic waves, have been also obtained, but with much simpler modeling (Pekünlü *et al.*, 2001). Slow magnetosonic waves with periods of about 5 minutes have been more recently detected in the transition region and coronal emission lines by Hinode/EIS at the footpoint of a coronal loop rooted at plage, but found to carry not enough energy to heat the corona (Wang *et al.*, 2009).

Investigation of AC heating has been made also through comparison with DC heating. Antolin *et al.* (2008) compared observational signatures of coronal heating by Alfvén waves and nanoflares using two coronal loop models and found that Hinode XRT intensity histograms display power-law distributions whose indices differ considerably, to be checked against observations. Lundquist *et al.* (2008a,b) applied a method for predicting active region coronal emissions using magnetic field measurements and a chosen heating relationship to 10 active regions. With their forward-modeling, they found a volumetric coronal heating rate proportional to magnetic field and inversely proportional to field-line loop length, which seems to point to, although not conclusively, the steady-state scaling of two heating mechanisms: van Ballegooijen's current layers theory (van Ballegooijen, 1986), taken in the AC limit, and Parker's critical angle mechanism (Parker, 1988), in the case where the angle of misalignment is a twist angle.

4.4.3 Modeling including the magnetic field

Some studies have investigated loop heating by including also the magnetic field in the analysis and modeling, and have tried to discriminate between different mechanisms using global approaches and scalings inferred from modeling. Based on a previous study of the plasma parameters and the magnetic flux density (Mandrini *et al.*, 2000), Démoulin *et al.* (2003) derived the dependence of the mean coronal heating rate on the magnetic flux density from the analysis of an active region. By using the scaling laws of coronal loops, they found that models based on the dissipation of stressed, current-carrying magnetic fields are in better agreement with the observations than models that attribute coronal heating to the dissipation of MHD waves injected at the base of the corona. Schrijver *et al.* (2004) considered a similar approach applied to the whole corona, by populating magnetic field lines taken from observed magnetograms with quasi-static loop atmospheres and obtaining the best match to X-ray and EUV observation with a heating that scales as it would be expected from DC reconnection at tangential discontinuities. These approaches will certainly be very useful when they will provide more detailed predictions and constraints.

Recent modeling has been able to explain the ignition of warm loops from primary energy release mechanisms, although it remains unclear how the same mechanisms could produce hot loops. A large scale approach (see also Section 4.1) is by "ab initio" modeling, i.e., with full MHD modeling of an entire coronal region (Gudiksen and Nordlund, 2005). Observed solar granular velocity pattern, a potential extrapolation of a SOHO/MDI magnetogram, and a standard stratified atmosphere were used as initial conditions. The simulation showed that, at steady state, the magnetic field is able to dissipate $(3-4) \times 10^6$ erg cm^{-2} s^{-1} in a highly intermittent corona, at an average temperature of $\sim 10^6$ K, adequate to reproduce typical warm loop populations observed

in TRACE images. Warm loops were also obtained with time-dependent loop modeling including the intermittent magnetic dissipation in MHD turbulence due to loop footpoint motions (Reale *et al.*, 2005). The dissipation rate along a loop predicted with a hybrid-shell model (Nigro *et al.*, 2004) was used as heating input (see Equation (5) in a proper time-dependent loop model, the Palermo-Harvard code (Peres *et al.*, 1982). It was shown that the most intense nanoflares excited in an ambient magnetic field of about 10 G can produce warm loops with temperatures of 1 – 1.5 MK in the corona of a 30 000 km long loop.

More recently, Rappazzo *et al.* (2007) used reduced MHD (rMHD) to identify MHD anisotropic turbulence as the physical mechanism responsible for the transport of energy from the large scales, where energy is injected by photospheric motions to the small scales, where it is dissipated. Strong turbulence was found for weak axial magnetic fields and long loops. The predicted heating rate is appropriate for warm loops, in agreement with Reale *et al.* (2005). Buchlin and Velli (2007) also used shell models of rMHD turbulence to analyze the case of a coronal loop heated by photospheric turbulence and found that the Alfvén waves interact non-linearly and form turbulent spectra. They derived an intermittent heating function, on average able to sustain the corona and proportional to the aspect ratio of the loop to the ~ 1.5 power. Buchlin *et al.* (2007) added in the modeling a profile of density and/or magnetic field along the loop, showing that differences are found in the heat deposition, in particular in the low part of the loop.

There are new efforts to include magnetic effects in the loop modeling. Haynes *et al.* (2008) studied observational properties of a kink unstable coronal loop, using a fluid code and finding potentially observable density effects. Browning *et al.* (2008) studied coronal heating by nanoflares triggered by a kink instability using three-dimensional magnetohydrodynamic numerical simulations of energy release for a cylindrical coronal loop model. Magnetic energy is dissipated, leading to large or small heating events according to the initial current profile.

Interesting perspectives are developing from models in which self-organized criticality triggers loop coronal heating. For Uzdensky (2007) and Cassak *et al.* (2008) coronal heating is self-regulating and keeps the coronal plasma roughly marginally collisionless. In the long run, the coronal heating process may be represented by repeating cycles that consist of fast reconnection events (i.e., nanoflares), followed by rapid evaporation episodes, followed by relatively long periods ($\sim$ 1 h) during which magnetic stresses build up and the plasma simultaneously cools down and precipitates. Morales and Charbonneau (2008) proposed an avalanche model for solar flares, based on an idealized representation of a coronal loop as a bundle of magnetic flux strands wrapping around one another. The system is driven by random deformation of the strands, and a form of reconnection is assumed to take place when the angle subtended by two strands crossing at the same lattice site exceeds some preset threshold. For a generic coronal loop of length 10^{10} cm and diameter 10^8 cm the mechanism leads to flare energies ranging between 10^{23} and 10^{29} erg, for an instability threshold angle of 11 degrees between contiguous magnetic flux strands.

4.4.4 New hints

Given the difficulty to find a conclusive answer about the heating of coronal loops, even in the presence of considerable observational and theoretical efforts, there has been recently the attempt to propose different or radically alternative scenarios. For instance, it has been suggested that warm and hot loops may be heated by different mechanisms, impulsive the former, much more steady the latter (Warren *et al.*, 2010). New evidence from Hinode satellite indicates the presence of significant upflows in the form of widespread spicules which have correspondence in coronal observations (De Pontieu *et al.*, 2009), This evidence suggests that the interaction between the chromosphere and the corona in the heating processes might be important and may receive support also by some modeling approaches (Gudiksen and Nordlund, 2005). These scenarios are intriguing but need additional investigation and support both from the observational and theoretical point

of view.

5 Stellar Coronal Loops

Non-solar X-ray missions since *Einstein* and European X-ray Observatory SATellite *EXOSAT* have established that most other stars have a confined corona, often much more active that the solar one. The level of activity is ruled by several factors but, first of all, the age of the star is important: young fast-rotating stars are more active (e.g., Telleschi *et al.*, 2005). The topic of stellar coronal loops deserves a review by itself (e.g., Rosner *et al.*, 1985) and here only a few relevant issues are discussed. A complete and more recent review of stellar coronae, with an extensive part regarding loops, is by Güdel (2004). In the framework of the solar-stellar connection, it is very important the comparison of what we know about the spatially resolved but single solar corona and what about the unresolved but numerous stellar coronae, which offer a variety of different environments. The lack of spatial resolution inhibits to obtain direct information about the size and appearance of the loops, and the general aspect of the corona. We, therefore, have to rely on indirect evidence. One possible approach to get information is to benefit from transient X-ray events, such as flares, which provide estimations of the loop scale length from their dependence on the decay and rise timescales (Reale, 2002a, 2003, and Section 4.1.2 for reviews). Detailed hydrodynamic modeling can provide even more constraints, for instance, on the heat deposition (e.g., Reale *et al.*, 1988, 2004). The study of stellar X-ray flares allowed, for instance, to constrain that most stellar flares involve plasma confined in closed structures (Reale *et al.*, 2002), and to infer the presence both of loops with size similar to those observed on the Sun (e.g., Reale *et al.*, 1988) and of giant loops (Favata *et al.*, 2005; Getman *et al.*, 2008), with length exceeding the stellar radius.

Another approach is to use the entire solar X-ray corona as a template and "Rosetta stone" to interpret stellar coronae. A detailed implementation of this approach was devised and applied extensively using Yohkoh data over its entire life, which covers a whole solar cycle (Orlando *et al.*, 2000; Peres *et al.*, 2000). It was shown that the solar corona indeed provides a pattern of components, i.e., quiet structures, active regions, active region cores, flares, which can be identified in stellar coronal data and which can explain stellar activity giving different weights to the components (Orlando *et al.*, 2001; Peres *et al.*, 2004). The method was also applied to describe stellar coronae in terms of loop populations and to extract general information and constraints on coronal heating (Peres *et al.*, 2004). It was applied to flares (Reale *et al.*, 2001) and to describe the evolution of active regions (Orlando *et al.*, 2004). More recently it was shown that a continuous unresolved flaring activity may explain the most active coronae, but also that the coronal heating appears to follow different scaling for quiet regions and for active and flaring regions across the cycle (Argiroffi *et al.*, 2008).

Cargill and Klimchuk (2006) realized that the strong hot peaks in the emission measure-temperature distributions in the coronae of some binary stars (Sanz-Forcada *et al.*, 2003) are similar to those expected for an impulsively-heated solar corona. A coronal model comprised of many impulsively heated strands shows that the evidence may be compatible with coronae made of many very small loops (length under 10^3 km) heated by microflares.

The recent deeper investigation of solar coronal heating mechanisms through the evidence of hot plasma and of variability makes even more important future tighter links to the study of stellar coronae, which show very strong evidence of very hot steady components (e.g., Schmitt *et al.*, 1990; Scelsi *et al.*, 2005).

6 Conclusions and Perspectives

Coronal loops have been the subject of in-depth studies for about 50 years. Since they owe their identity to the brightness of the confined plasma, most of the studies have addressed the physics of the confined plasma, i.e., its structure, dynamics, and evolution. Most of the basic laws that rule the confined plasma, such as scaling laws, were developed early after the discovery of loops and are now well-established. Although the observational scenario is ever-enriching with the progress of the solar coronal missions, a variety of questions remain still open, at all levels, starting from loop identification itself. The lack of operative definitions and automatic identification tools, and the difficulty to isolate loops from other surrounding and intersecting structures have prevented systematic studies on large and unbiased loop populations. Detailed morphological and theoretical analyses converge to a fine loop substructuring, which is critical to understand the basic mechanisms but is below the resolution limit of present-day instruments. Also the large scale structure of loops leaves room for further developments and, in particular, the link with the confining magnetic field, which is difficult to measure in the corona. One specific question to be addressed is the role of the loop tapering in the transition region.

Looking inside the loops, open questions involve the detailed thermal structure of the confined plasma. This issue is important to assess the basic loop heating mechanism: a broad multi-component thermal distribution would indicate a structured heating, a simpler distribution a monolithic mechanism. This question is still open for many reasons; spectroscopic methods provide very detailed thermal information, but mostly concentrated in the regime of warm loops. Moreover, the methods of analysis do not appear to provide unique answers yet. Also filter ratio diagnostics from broad-band X-ray and UV imaging telescopes have not been able to provide conclusive results so far. As a consequence, we are unable, right now, to assess the problem of the apparently different nature of warm (TRACE, SoHO/EIT) and hot (Yohkoh/SXT, Hinode/XRT) loops, and whether it is simply a matter of different heating rate or the heating mechanisms are radically different.

The role of the dynamics of plasma confined inside loops is also still under investigation. The measurement of plasma motions is made difficult by the possible ambiguity with the apparent motion of thermal fronts. It will be important in the future to evaluate the relative weight of the different flows, i.e., downflows, evaporation and draining, siphon flows, and their influence on the overall loop budget.

Also the investigation of temporal variations deserves attention. In particular, in narrow band instruments thermal variations might be confused with intensity variations, and make the interpretation difficult. On the other hand, the analysis of emission variations is very important, because it can potentially shed light on heating mechanisms based on short impulsive events (nanoflares) or on wave-like phenomena (Alfvén waves).

On the theoretical side, 1-D loop models are well-established and have provided a wealth of sound and important results. Today, their evolution consists essentially in their transformation into "strand" models, and so a collection of them describes a proper loop. Moreover, loops are now seen much more dynamic than they were in the past, either as the site of flows or of wave perturbations, or of heat pulses. So they need more and more time-dependent modeling to address, for instance, the importance of flows and the relative weight between evaporation-draining flows and siphon flows. The modeling is, therefore, becoming more and more demanding, although computing resources are now much more powerful than in the past and although some approaches are able to squeeze the spatial dimension, yet maintaining the temporal description. At the same time, new data seem to require other model refinements, such as the description of loop expansion in the transition region. The improvement of numerical and computing resources is also allowing more complex and complete modeling of whole loop regions including the 3-D magnetic field structure "ab initio". This approach is very promising and will surely provide important results in

the next future, to complement those obtained with basic single loop models. We all look forward self-consistent descriptions including the generation of heat from magnetic field rearrangements and perturbations.

Special attention still deserves the problem of what heats coronal loops, which means basically what heats the whole corona. This problem has revealed to be particularly difficult, essentially because of intrinsic physical reasons and, in particular, i) the highly effective thermal conduction, which inhibits the identification of the heating site, and ii) the expected small scales of the heating processes, which require so far prohibitive spatial/temporal resolution. Nevertheless, coronal loops remain an obvious excellent laboratory to investigate coronal heating mechanisms, because the dense plasma confined therein make them bright and easy to observe. The most recent challenge offered by coronal loops is probably the increasing evidence that the thin strands they are made of are ignited by small scale, rapid, but intense pulses. Most current efforts are devoted to study this aspect both from the theoretical/modeling and from the observational point of view. However, alternative explanations are actively explored and strongly proposed lately.

The study of coronal loops is very alive and is the subject of Coronal Loop Workshops, taking place every two years, which are site of debate, inspiration of new investigations, and school for young investigators. We look forward further great improvements in our knowledge of coronal loops from the new mission Solar Dynamic Observatory.

7 Acknowledgements

The author thanks P. Testa, S. Orlando, G. Peres, J. Klimchuk, and the anonymous referees for suggestions. The author acknowledges support from the Italian Ministero dell'Università e della Ricerca. The Transition Region and Coronal Explorer, TRACE, is a mission of the Stanford-Lockheed Institute for Space Research, and part of the NASA Small Explorer program. The solar X-ray images of Figure 2 is from the Yohkoh mission of ISAS, Japan. The X-ray telescope was prepared by the Lockheed-Martin Solar and Astrophysics Laboratory, the National Astronomical Observatory of Japan, and the University of Tokyo with the support of NASA and ISAS.

References

Acton, L.W., Finch, M.L., Gilbreth, C.W., Culhane, J.L., Bentley, R.D., Bowles, J.A., Guttridge, P., Gabriel, A.H., Firth, J.G. and Hayes, R.W., 1980, "The soft X-ray polychromator for the Solar Maximum Mission", *Solar Phys.*, **65**, 53–71. [DOI], [ADS] (Cited on page 7.)

Antiochos, S.K., 1984, "A dynamic model for the solar transition region", *Astrophys. J.*, **280**, 416–422. [DOI], [ADS] (Cited on page 40.)

Antiochos, S.K. and Noci, G., 1986, "The structure of the static corona and transition region", *Astrophys. J.*, **301**, 440–447. [DOI], [ADS] (Cited on page 33.)

Antiochos, S.K., MacNeice, P.J., Spicer, D.S. and Klimchuk, J.A., 1999, "The Dynamic Formation of Prominence Condensations", *Astrophys. J.*, **512**, 985–991. [DOI], [ADS], [arXiv:astro-ph/9808199] (Cited on page 30.)

Antiochos, S.K., Karpen, J.T., DeLuca, E.E., Golub, L. and Hamilton, P., 2003, "Constraints on Active Region Coronal Heating", *Astrophys. J.*, **590**, 547–553. [DOI], [ADS] (Cited on pages 25 and 45.)

Antolin, P., Shibata, K., Kudoh, T., Shiota, D. and Brooks, D., 2008, "Predicting Observational Signatures of Coronal Heating by Alfvén Waves and Nanoflares", *Astrophys. J.*, **688**, 669–682. [DOI], [ADS] (Cited on page 47.)

Argiroffi, C., Peres, G., Orlando, S. and Reale, F., 2008, "The flaring and quiescent components of the solar corona", *Astron. Astrophys.*, **488**, 1069–1077. [DOI], [ADS], [arXiv:0805.2685] (Cited on page 49.)

Aschwanden, M.J., 1999, "Do EUV Nanoflares Account for Coronal Heating?", *Solar Phys.*, **190**, 233–247. [DOI], [ADS] (Cited on pages 44 and 45.)

Aschwanden, M.J., 2001, "Revisiting the Determination of the Coronal Heating Function from Yohkoh Data", *Astrophys. J. Lett.*, **559**, L171–L174. [DOI], [ADS] (Cited on pages 16, 39, and 43.)

Aschwanden, M.J., 2002, "The Differential Emission Measure Distribution in the Multiloop Corona", *Astrophys. J. Lett.*, **580**, L79–L83. [DOI], [ADS] (Cited on page 20.)

Aschwanden, M.J., 2004, *Physics of the Solar Corona: An Introduction*, Springer; Praxis, Berlin; New York; Chichester. [ADS], [Google Books] (Cited on page 5.)

Aschwanden, M.J. and Nightingale, R.W., 2005, "Elementary Loop Structures in the Solar Corona Analyzed from TRACE Triple-Filter Images", *Astrophys. J.*, **633**, 499–517. [DOI], [ADS] (Cited on pages 15, 16, and 24.)

Aschwanden, M.J. and Nitta, N., 2000, "The Effect of Hydrostatic Weighting on the Vertical Temperature Structure of the Solar Corona", *Astrophys. J. Lett.*, **535**, L59–L62. [DOI], [ADS], [arXiv:astro-ph/0004093] (Cited on page 33.)

Aschwanden, M.J., Fletcher, L., Schrijver, C.J. and Alexander, D., 1999a, "Coronal Loop Oscillations Observed with the Transition Region and Coronal Explorer", *Astrophys. J.*, **520**, 880–894. [DOI], [ADS] (Cited on page 46.)

Aschwanden, M.J., Newmark, J.S., Delaboudinière, J.-P., Neupert, W.M., Klimchuk, J.A., Gary, G.A., Portier-Fozzani, F. and Zucker, A., 1999b, "Three-dimensional Stereoscopic Analysis of Solar Active Region Loops. I. SOHO/EIT Observations at Temperatures of $(1.0-1.5)\times10^6$ K", *Astrophys. J.*, **515**, 842–867. [DOI], [ADS] (Cited on page 22.)

Aschwanden, M.J., Nightingale, R.W. and Alexander, D., 2000, "Evidence for Nonuniform Heating of Coronal Loops Inferred from Multithread Modeling of TRACE Data", *Astrophys. J.*, **541**, 1059–1077. [DOI], [ADS] (Cited on pages 10 and 22.)

Aschwanden, M.J., Poland, A.I. and Rabin, D.M., 2001, "The New Solar Corona", *Annu. Rev. Astron. Astrophys.*, **39**, 175–210. [DOI], [ADS] (Cited on page 5.)

Aschwanden, M.J., De Pontieu, B., Schrijver, C.J. and Title, A.M., 2002, "Transverse Oscillations in Coronal Loops Observed with TRACE II. Measurements of Geometric and Physical Parameters", *Solar Phys.*, **206**, 99–132. [DOI], [ADS] (Cited on page 12.)

Aschwanden, M.J., Nightingale, R.W. and Boerner, P., 2007, "A Statistical Model of the Inhomogeneous Corona Constrained by Triple-Filter Measurements of Elementary Loop Strands with TRACE", *Astrophys. J.*, **656**, 577–597. [DOI], [ADS] (Cited on page 15.)

Aschwanden, M.J., Nitta, N.V., Wuelser, J.-P. and Lemen, J.R., 2008a, "First 3D Reconstructions of Coronal Loops with the STEREO A+B Spacecraft. II. Electron Density and Temperature Measurements", *Astrophys. J.*, **680**, 1477–1495. [DOI], [ADS] (Cited on page 16.)

Aschwanden, M.J., Wülser, J.-P., Nitta, N.V. and Lemen, J.R., 2008b, "First Three-Dimensional Reconstructions of Coronal Loops with the STEREO A and B Spacecraft. I. Geometry", *Astrophys. J.*, **679**, 827–842. [DOI], [ADS] (Cited on page 12.)

Aschwanden, M.J., Wuelser, J.-P., Nitta, N.V., Lemen, J.R. and Sandman, A., 2009, "First Three-Dimensional Reconstructions of Coronal Loops with the STEREO A+B Spacecraft. III. Instant Stereoscopic Tomography of Active Regions", *Astrophys. J.*, **695**, 12–29. [DOI], [ADS] (Cited on pages 7, 12, and 23.)

Bartoe, J.-D.F., Brueckner, G.E., Purcell, J.D. and Tousey, R., 1977, "Extreme ultraviolet spectrograph ATM experiment S082B", *Appl. Optics*, **16**, 879–886. [ADS] (Cited on page 6.)

Beliën, A.J.C., Martens, P.C.H. and Keppens, R., 1999, "Coronal Heating by Resonant Absorption: The Effects of Chromospheric Coupling", *Astrophys. J.*, **526**, 478–493. [DOI], [ADS] (Cited on page 47.)

Benz, A.O., 2008, "Flare Observations", *Living Rev. Solar Phys.*, **5**, lrsp-2008-1. [ADS]. URL (accessed 26 October 2010):
http://www.livingreviews.org/lrsp-2008-1 (Cited on page 24.)

Berger, T.E., De Pontieu, B., Fletcher, L., Schrijver, C.J., Tarbell, T.D. and Title, A.M., 1999a, "What is Moss?", *Solar Phys.*, **190**, 409–418. [DOI], [ADS] (Cited on page 22.)

Berger, T.E., De Pontieu, B., Schrijver, C.J. and Title, A.M., 1999b, "High-resolution Imaging of the Solar Chromosphere/Corona Transition Region", *Astrophys. J. Lett.*, **519**, L97–L100. [DOI], [ADS] (Cited on page 25.)

Berghmans, D. and Clette, F., 1999, "Active region EUV transient brightenings: First Results by EIT of SOHO JOP 80", *Solar Phys.*, **186**, 207–229. [DOI], [ADS] (Cited on page 46.)

Berton, R. and Sakurai, T., 1985, "Stereoscopic determination of the three-dimensional geometry of coronal magnetic loops", *Solar Phys.*, **96**, 93–111. [DOI], [ADS] (Cited on page 12.)

Betta, R., Peres, G., Reale, F. and Serio, S., 1997, "An adaptive grid code for high resolution 1-D hydrodynamics of the solar and stellar transition region and corona", *Astron. Astrophys. Suppl.*, **122**, 585–592. [DOI], [ADS] (Cited on pages 30 and 31.)

Betta, R.M., Peres, G., Reale, F. and Serio, S., 2001, "Coronal loop hydrodynamics. The solar flare observed on November 12, 1980 revisited: The UV line emission", *Astron. Astrophys.*, **380**, 341–346. [DOI], [ADS], [arXiv:astro-ph/0110514] (Cited on page 34.)

Beveridge, C., Longcope, D.W. and Priest, E.R., 2003, "A model for elemental coronal flux loops", *Solar Phys.*, **216**, 27–40. [DOI], [ADS] (Cited on page 15.)

Bohlin, J.D., Frost, K.J., Burr, P.T., Guha, A.K. and Withbroe, G.L., 1980, "Solar Maximum Mission", *Solar Phys.*, **65**, 5–14. [DOI], [ADS] (Cited on page 6.)

Borrini, G. and Noci, G., 1982, "Non-equilibrium ionization in coronal loops", *Solar Phys.*, **77**, 153–166. [DOI], [ADS] (Cited on page 40.)

Bradshaw, S.J. and Cargill, P.J., 2005, "The cooling of coronal plasmas", *Astron. Astrophys.*, **437**, 311–317. [DOI], [ADS] (Cited on page 42.)

Bradshaw, S.J. and Cargill, P.J., 2006, "Explosive heating of low-density coronal plasma", *Astron. Astrophys.*, **458**, 987–995. [DOI], [ADS] (Cited on pages 30 and 31.)

Bradshaw, S.J. and Cargill, P.J., 2010, "The Cooling of Coronal Plasmas. III. Enthalpy Transfer as a Mechanism for Energy Loss", *Astrophys. J.*, **717**, 163–174. [DOI], [ADS] (Cited on pages 36 and 42.)

Bradshaw, S.J. and Mason, H.E., 2003, "The radiative response of solar loop plasma subject to transient heating", *Astron. Astrophys.*, **407**, 1127–1138. [DOI], [ADS] (Cited on page 30.)

Bray, R.J., Cram, L.E., Durrant, C. and Loughhead, R.E., 1991, *Plasma loops in the solar corona*, vol. 18 of Cambridge Astrophysics Series, Cambridge University Press, Cambridge, UK. [ADS] (Cited on pages 5 and 32.)

Brekke, P., 1993, "Observed redshifts in O V and downflows in the solar transition region", *Astrophys. J.*, **408**, 735–743. [DOI], [ADS] (Cited on page 27.)

Brekke, P., 1999, "Observations of Transition Region Plasma", *Solar Phys.*, **190**, 379–408. [DOI], [ADS] (Cited on page 27.)

Brekke, P., Kjeldseth-Moe, O. and Harrison, R.A., 1997, "High-Velocity Flows in an Active Region Loop System Observed with the Coronal Diagnostic Spectrometer (CDS) on SOHO", *Solar Phys.*, **175**, 511–521. [DOI], [ADS] (Cited on pages 8 and 27.)

Brickhouse, N.S. and Schmelz, J.T., 2006, "The Transparency of Solar Coronal Active Regions", *Astrophys. J. Lett.*, **636**, L53–L56. [DOI], [ADS], [arXiv:astro-ph/0511683] (Cited on page 20.)

Brković, A., Landi, E., Landini, M., Rüedi, I. and Solanki, S.K., 2002, "Models for solar magnetic loops. II. Comparison with SOHO-CDS observations on the solar disk", *Astron. Astrophys.*, **383**, 661–677. [DOI], [ADS] (Cited on page 34.)

Brooks, D.H., Ugarte-Urra, I. and Warren, H.P., 2008, "The Role of Transient Brightenings in Heating the Solar Corona", *Astrophys. J. Lett.*, **689**, L77–L80. [DOI], [ADS] (Cited on page 26.)

Brosius, J.W., Davila, J.M., Thomas, R.J. and Monsignori-Fossi, B.C., 1996, "Measuring Active and Quiet-Sun Coronal Plasma Properties with Extreme-Ultraviolet Spectra from SERTS", *Astrophys. J. Suppl. Ser.*, **106**, 143. [DOI], [ADS] (Cited on pages 17 and 23.)

Browning, P.K., Gerrard, C., Hood, A.W., Kevis, R. and van der Linden, R.A.M., 2008, "Heating the corona by nanoflares: simulations of energy release triggered by a kink instability", *Astron. Astrophys.*, **485**, 837–848. [DOI], [ADS] (Cited on page 48.)

Buchlin, E. and Velli, M., 2007, "Shell Models of RMHD Turbulence and the Heating of Solar Coronal Loops", *Astrophys. J.*, **662**, 701–714. [DOI], [ADS], [arXiv:astro-ph/0606610] (Cited on page 48.)

Buchlin, E., Cargill, P.J., Bradshaw, S.J. and Velli, M., 2007, "Profiles of heating in turbulent coronal magnetic loops", *Astron. Astrophys.*, **469**, 347–354. [DOI], [ADS], [arXiv:astro-ph/0702748] (Cited on page 48.)

Cargill, P.J., 1993, "The Fine Structure of a Nanoflare-Heated Corona", *Solar Phys.*, **147**, 263–268. [DOI], [ADS] (Cited on page 44.)

Cargill, P.J., 1994, "Some implications of the nanoflare concept", *Astrophys. J.*, **422**, 381–393. [DOI], [ADS] (Cited on pages 44 and 45.)

Cargill, P.J., 1995, "Diagnostics of Coronal Heating", in *Infrared Tools for Solar Astrophysics: What's Next?*, (Eds.) Kuhn, J.R., Penn, M.J., Proceedings of the Fifteenth NSO/Sac Peak Workshop, 19 – 23 September 1994, Sunspot, New Mexico, p. 17, World Scientific, Singapore. [ADS] (Cited on page 5.)

Cargill, P.J. and Klimchuk, J.A., 1997, "A Nanoflare Explanation for the Heating of Coronal Loops Observed by YOHKOH", *Astrophys. J.*, **478**, 799. [DOI], [ADS] (Cited on page 44.)

Cargill, P.J. and Klimchuk, J.A., 2004, "Nanoflare Heating of the Corona Revisited", *Astrophys. J.*, **605**, 911–920. [DOI], [ADS] (Cited on pages 15, 35, 38, and 44.)

Cargill, P.J. and Klimchuk, J.A., 2006, "On the Temperature-Emission Measure Distribution in Stellar Coronae", *Astrophys. J.*, **643**, 438–443. [DOI], [ADS] (Cited on page 49.)

Cargill, P.J. and Priest, E.R., 1980, "Siphon flows in coronal loops: I. Adiabatic flow", *Solar Phys.*, **65**, 251–269. [DOI], [ADS] (Cited on page 40.)

Cassak, P.A., Mullan, D.J. and Shay, M.A., 2008, "From Solar and Stellar Flares to Coronal Heating: Theory and Observations of How Magnetic Reconnection Regulates Coronal Conditions", *Astrophys. J. Lett.*, **676**, L69–L72. [DOI], [ADS], [arXiv:0710.3399] (Cited on page 48.)

Chae, J., Schühle, U. and Lemaire, P., 1998a, "SUMER Measurements of Nonthermal Motions: Constraints on Coronal Heating Mechanisms", *Astrophys. J.*, **505**, 957–973. [DOI], [ADS] (Cited on page 27.)

Chae, J., Wang, H., Lee, C.-Y., Goode, P.R. and Schuhle, U., 1998b, "Chromospheric Upflow Events Associated with Transition Region Explosive Events", *Astrophys. J. Lett.*, **504**, L123. [DOI], [ADS] (Cited on page 27.)

Cheng, C.-C., Oran, E.S., Doschek, G.A., Boris, J.P. and Mariska, J.T., 1983, "Numerical simulations of loops heated to solar flare temperatures. I", *Astrophys. J.*, **265**, 1090–1119. [DOI], [ADS] (Cited on page 34.)

Cirtain, J.W., Del Zanna, G., DeLuca, E.E., Mason, H.E., Martens, P.C.H. and Schmelz, J.T., 2007, "Active Region Loops: Temperature Measurements as a Function of Time from Joint TRACE and SOHO CDS Observations", *Astrophys. J.*, **655**, 598–605. [DOI], [ADS] (Cited on page 26.)

Craig, I.J.D., McClymont, A.N. and Underwood, J.H., 1978, "The Temperature and Density Structure of Active Region Coronal Loops", *Astron. Astrophys.*, **70**, 1. [ADS] (Cited on page 32.)

Culhane, L., Harra, L.K., Baker, D., van Driel-Gesztelyi, L., Sun, J., Doschek, G.A., Brooks, D.H., Lundquist, L.L., Kamio, S., Young, P.R. and Hansteen, V.H., 2007, "Hinode EUV Study of Jets in the Sun's South Polar Corona", *Publ. Astron. Soc. Japan*, **59**, S751–S756. [ADS] (Cited on page 7.)

Davila, J.M., 1987, "Heating of the solar corona by the resonant absorption of Alfvén waves", *Astrophys. J.*, **317**, 514–521. [DOI], [ADS] (Cited on page 46.)

De Groof, A., Berghmans, D., van Driel-Gesztelyi, L. and Poedts, S., 2004, "Intensity variations in EIT shutterless mode: Waves or flows?", *Astron. Astrophys.*, **415**, 1141–1151. [DOI], [ADS] (Cited on pages 27 and 42.)

De Moortel, I., Ireland, J., Walsh, R.W. and Hood, A.W., 2002, "Longitudinal intensity oscillations in coronal loops observed with TRACE I. Overview of Measured Parameters", *Solar Phys.*, **209**, 61–88. [DOI], [ADS] (Cited on page 46.)

De Pontieu, B., McIntosh, S.W., Carlsson, M., Hansteen, V.H., Tarbell, T.D., Schrijver, C.J., Title, A.M., Shine, R.A., Tsuneta, S., Katsukawa, Y., Ichimoto, K., Suematsu, Y., Shimizu, T. and Nagata, S., 2007, "Chromospheric Alfvénic Waves Strong Enough to Power the Solar Wind", *Science*, **318**, 1574–1577. [DOI], [ADS] (Cited on page 46.)

De Pontieu, B., McIntosh, S.W., Hansteen, V.H. and Schrijver, C.J., 2009, "Observing the roots of solar coronal heating – in the chromosphere", *Astrophys. J. Lett.*, **701**, L1–L6. [DOI], [ADS], [arXiv:0906.5434] (Cited on pages 28 and 48.)

DeForest, C.E., 2007, "On the Size of Structures in the Solar Corona", *Astrophys. J.*, **661**, 532–542. [DOI], [ADS], [arXiv:astro-ph/0610178] (Cited on page 14.)

Del Zanna, G., 2008, "Flows in active region loops observed by Hinode EIS", *Astron. Astrophys.*, **481**, L49–L52. [DOI], [ADS] (Cited on page 28.)

Del Zanna, G. and Mason, H.E., 2003, "Solar active regions: SOHO/CDS and TRACE observations of quiescent coronal loops", *Astron. Astrophys.*, **406**, 1089–1103. [DOI], [ADS] (Cited on pages 16, 20, and 23.)

Delaboudinière, J.-P., Artzner, G.E., Brunaud, J., Gabriel, A.H., Hochedez, J.F., Millier, F., Song, X.Y., Au, B., Dere, K.P., Howard, R.A., Kreplin, R., Michels, D.J., Moses, J.D., Defise, J.M., Jamar, C., Rochus, P., Chauvineau, J.P., Marioge, J.P., Catura, R.C., Lemen, J.R., Shing, L., Stern, R.A., Gurman, J.B., Neupert, W.M., Maucherat, A., Clette, F., Cugnon, P. and van Dessel, E.L., 1995, "EIT: Extreme-Ultraviolet Imaging Telescope for the SOHO Mission", *Solar Phys.*, **162**, 291–312. [DOI], [ADS] (Cited on page 7.)

Démoulin, P., van Driel-Gesztelyi, L., Mandrini, C.H., Klimchuk, J.A. and Harra, L., 2003, "The Long-Term Evolution of AR 7978: Testing Coronal Heating Models", *Astrophys. J.*, **586**, 592–605. [DOI], [ADS] (Cited on page 47.)

Dere, K.P., 1982, "Extreme ultraviolet spectra of solar active regions and their analysis", *Solar Phys.*, **77**, 77–93. [DOI], [ADS] (Cited on page 27.)

Dere, K.P., 2008, "The plasma filling factor of coronal bright points. Coronal bright points", *Astron. Astrophys.*, **491**, 561–566. [DOI], [ADS] (Cited on page 18.)

Dere, K.P., 2009, "The plasma filling factor of coronal bright points. II. Combined EIS and TRACE results", *Astron. Astrophys.*, **497**, 287–290. [DOI], [ADS] (Cited on page 18.)

Dere, K.P., Bartoe, J.-D.F. and Brueckner, G.E., 1986, "Outflows and ejections in the solar transition zone", *Astrophys. J.*, **310**, 456–462. [DOI], [ADS] (Cited on page 27.)

Dere, K.P., Bartoe, J.-D.F. and Brueckner, G.E., 1989, "Explosive events in the solar transition zone", *Solar Phys.*, **123**, 41–68. [DOI], [ADS] (Cited on page 27.)

DeRosa, M.L., Schrijver, C.J., Barnes, G., Leka, K.D., Lites, B.W., Aschwanden, M.J., Amari, T., Canou, A., McTiernan, J.M., Régnier, S., Thalmann, J.K., Valori, G., Wheatland, M.S., Wiegelmann, T., Cheung, M.C.M., Conlon, P.A., Fuhrmann, M., Inhester, B. and Tadesse, T., 2009, "A Critical Assessment of Nonlinear Force-Free Field Modeling of the Solar Corona for Active Region 10953", *Astrophys. J.*, **696**, 1780–1791. [DOI], [ADS], [arXiv:0902.1007] (Cited on page 12.)

Di Giorgio, S., Reale, F. and Peres, G., 2003, "CDS/SoHO multi-line observation of a solar active region: Detection of a hot stable loop and of a cool dynamic loop", *Astron. Astrophys.*, **406**, 323–335. [DOI], [ADS] (Cited on pages 20, 21, 24, 25, and 27.)

Di Matteo, V., Reale, F., Peres, G. and Golub, L., 1999, "Analysis and comparison of loop structures imaged with NIXT and Yohkoh/SXT", *Astron. Astrophys.*, **342**, 563–574. [ADS] (Cited on pages 14 and 19.)

Domingo, V., Fleck, B. and Poland, A.I., 1995, "The SOHO Mission: an Overview", *Solar Phys.*, **162**, 1–37. [DOI], [ADS] (Cited on page 7.)

Doschek, G.A., Bohlin, J.D. and Feldman, U., 1976, "Doppler wavelength shifts of transition zone lines measured in SKYLAB solar spectra", *Astrophys. J. Lett.*, **205**, L177–L180. [DOI], [ADS] (Cited on page 27.)

Doschek, G.A., Boris, J.P., Cheng, C.C., Mariska, J.T. and Oran, E.S., 1982, "A Numerical Simulation of Cooling Coronal Flare Plasma", *Astrophys. J.*, **258**, 373. [DOI], [ADS] (Cited on page 30.)

Doschek, G.A., Mariska, J.T., Warren, H.P., Brown, C.M., Culhane, J.L., Hara, H., Watanabe, T., Young, P.R. and Mason, H.E., 2007a, "Nonthermal Velocities in Solar Active Regions Observed with the Extreme-Ultraviolet Imaging Spectrometer on Hinode", *Astrophys. J. Lett.*, **667**, L109–L112. [DOI], [ADS] (Cited on page 28.)

Doschek, G.A., Mariska, J.T., Warren, H.P., Culhane, L., Watanabe, T., Young, P.R., Mason, H.E. and Dere, K.P., 2007b, "The Temperature and Density Structure of an Active Region Observed with the Extreme-Ultraviolet Imaging Spectrometer on Hinode", *Publ. Astron. Soc. Japan*, **59**, 707. [ADS] (Cited on page 23.)

Doschek, G.A., Warren, H.P., Mariska, J.T., Muglach, K., Culhane, J.L., Hara, H. and Watanabe, T., 2008, "Flows and Nonthermal Velocities in Solar Active Regions Observed with the EUV Imaging Spectrometer on Hinode: A Tracer of Active Region Sources of Heliospheric Magnetic Fields?", *Astrophys. J.*, **686**, 1362–1371. [DOI], [ADS], [arXiv:0807.2860] (Cited on page 28.)

Dudok de Wit, T. and Auchère, F., 2007, "Multispectral analysis of solar EUV images: linking temperature to morphology", *Astron. Astrophys.*, **466**, 347–355. [DOI], [ADS], [arXiv:astro-ph/0702052] (Cited on page 14.)

Dymova, M.V. and Ruderman, M.S., 2006, "The geometry effect on transverse oscillations of coronal loops", *Astron. Astrophys.*, **459**, 241–244. [DOI], [ADS] (Cited on page 12.)

Favata, F., Reale, F., Micela, G., Sciortino, S., Maggio, A. and Matsumoto, H., 2000, "An extreme X-ray flare observed on EV Lac by ASCA in July 1998", *Astron. Astrophys.*, **353**, 987–997. [ADS], [arXiv:astro-ph/9909491] (Cited on page 37.)

Favata, F., Flaccomio, E., Reale, F., Micela, G., Sciortino, S., Shang, H., Stassun, K.G. and Feigelson, E.D., 2005, "Bright X-Ray Flares in Orion Young Stars from COUP: Evidence for Star-Disk Magnetic Fields?", *Astrophys. J. Suppl. Ser.*, **160**, 469–502. [DOI], [ADS], [arXiv:astro-ph/0506134] (Cited on page 49.)

Feldman, U., Doschek, G.A. and Mariska, J.T., 1979, "On the structure of the solar transition zone and lower corona", *Astrophys. J.*, **229**, 369–374. [DOI], [ADS] (Cited on page 16.)

Feldman, U., Doschek, G.A. and Cohen, L., 1982, "Doppler wavelength shifts of ultraviolet spectral lines in solar active regions", *Astrophys. J.*, **255**, 325–328. [DOI], [ADS] (Cited on page 27.)

Feng, L., Inhester, B., Solanki, S.K., Wiegelmann, T., Podlipnik, B., Howard, R.A. and Wuelser, J.-P., 2007, "First Stereoscopic Coronal Loop Reconstructions from STEREO SECCHI Images", *Astrophys. J. Lett.*, **671**, L205–L208. [DOI], [ADS], [arXiv:0802.0773] (Cited on page 12.)

Fisher, G.H., Canfield, R.C. and McClymont, A.N., 1985a, "Flare loop radiative hydrodynamics. V. Response to thick-target heating", *Astrophys. J.*, **289**, 414–424. [DOI], [ADS] (Cited on pages 30 and 34.)

Fisher, G.H., Canfield, R.C. and McClymont, A.N., 1985b, "Flare loop radiative hydrodynamics. VI. Chromospheric evaporation due to heating by nonthermal electrons", *Astrophys. J.*, **289**, 425–433. [DOI], [ADS] (Cited on pages 30 and 34.)

Fisher, G.H., Canfield, R.C. and McClymont, A.N., 1985c, "Flare loop radiative hydrodynamics. VII. Dynamics of the thick-target heated chromosphere", *Astrophys. J.*, **289**, 434–441. [DOI], [ADS] (Cited on pages 30 and 34.)

Fletcher, L. and De Pontieu, B., 1999, "Plasma Diagnostics of Transition Region 'Moss' using SOHO/CDS and TRACE", *Astrophys. J. Lett.*, **520**, L135–L138. [DOI], [ADS] (Cited on page 22.)

Foukal, P., 1975, "The temperature structure and pressure balance of magnetic loops in active regions", *Solar Phys.*, **43**, 327–336. [DOI], [ADS] (Cited on page 6.)

Foukal, P.V., 1976, "The pressure and energy balance of the cool corona over sunspots", *Astrophys. J.*, **210**, 575–581. [DOI], [ADS] (Cited on pages 6, 8, 25, and 27.)

Gabriel, A.H., 1976, "A magnetic model of the solar transition region", *Philos. Trans. R. Soc. London, Ser. A*, **281**, 339–352. [ADS] (Cited on pages 8 and 32.)

Gabriel, A.H. and Jordan, C., 1975, "Analysis of EUV observations of regions of the quiet and active corona at the time of the 1970 March 7 eclipse", *Mon. Not. R. Astron. Soc.*, **173**, 397–418. [ADS] (Cited on page 17.)

Galeev, A.A., Rosner, R., Serio, S. and Vaiana, G.S., 1981, "Dynamics of coronal structures: Magnetic field-related heating and loop energy balance", *Astrophys. J.*, **243**, 301–308. [DOI], [ADS] (Cited on page 43.)

Gan, W.Q., Zhang, H.Q. and Fang, C., 1991, "A hydrodynamic model of the impulsive phase of a solar flare loop", *Astron. Astrophys.*, **241**, 618–624. [ADS] (Cited on page 30.)

Gebbie, K.B., Hill, F., November, L.J., Gurman, J.B., Shine, R.A., Woodgate, B.E., Athay, R.G., Tandberg-Hanssen, E.A., Toomre, J. and Simon, G.W., 1981, "Steady flows in the solar transition region observed with SMM", *Astrophys. J. Lett.*, **251**, L115–L118. [DOI], [ADS] (Cited on page 27.)

Getman, K.V., Feigelson, E.D., Micela, G., Jardine, M.M., Gregory, S.G. and Garmire, G.P., 2008, "X-Ray Flares in Orion Young Stars. II. Flares, Magnetospheres, and Protoplanetary Disks", *Astrophys. J.*, **688**, 437–455. [DOI], [ADS], [arXiv:0807.3007] (Cited on page 49.)

Giacconi, R., Reidy, W.P., Zehnpfennig, T., Lindsay, J.C. and Muney, W.S., 1965, "Solar X-Ray Image Obtained Using Grazing-Incidence Optics", *Astrophys. J.*, **142**, 1274–1278. [DOI], [ADS] (Cited on page 6.)

Golub, L., 1996, "The Solar X-Ray Corona", *Astrophys. J. Suppl. Ser.*, **237**, 33–48. [DOI], [ADS] (Cited on page 5.)

Golub, L. and Herant, M., 1989, "Analysis of the 23 June 1988 flare using NIXT multilayer X-ray images", in *X-Ray/EUV Optics for Astronomy and Microscopy*, (Ed.) Hoover, R.B., San Diego, CA, August 7 – 11, 1989, vol. 1160 of Proc. SPIE, pp. 629–635, SPIE, Bellingham, WA. [ADS] (Cited on page 7.)

Golub, L. and Pasachoff, J.M., 1997, *The Solar Corona*, Cambridge University Press, Cambridge, UK. [ADS], [Google Books] (Cited on page 5.)

Golub, L. and Pasachoff, J.M., 2001, *Nearest Star: The Surprising Science of Our Sun*, Harvard University Press, Cambridge, MA (Cited on page 5.)

Golub, L., Maxson, C., Rosner, R., Vaiana, G.S. and Serio, S., 1980, "Magnetic fields and coronal heating", *Astrophys. J.*, **238**, 343–348. [DOI], [ADS] (Cited on page 43.)

Golub, L., Noci, G., Poletto, G. and Vaiana, G.S., 1982, "Active region coronal evolution", *Astrophys. J.*, **259**, 359–365. [DOI], [ADS] (Cited on pages 6 and 43.)

Golub, L., Hartquist, T.W. and Quillen, A.C., 1989, "Comments on the observability of coronal variations", *Solar Phys.*, **122**, 245–261. [DOI], [ADS] (Cited on page 40.)

Golub, L., Deluca, E., Austin, G., Bookbinder, J., Caldwell, D., Cheimets, P., Cirtain, J., Cosmo, M., Reid, P., Sette, A., Weber, M., Sakao, T., Kano, R., Shibasaki, K., Hara, H., Tsuneta, S., Kumagai, K., Tamura, T., Shimojo, M., McCracken, J., Carpenter, J., Haight, H., Siler, R., Wright, E., Tucker, J., Rutledge, H., Barbera, M., Peres, G. and Varisco, S., 2007, "The X-Ray Telescope (XRT) for the Hinode Mission", *Solar Phys.*, **243**, 63–86. [DOI], [ADS] (Cited on page 7.)

Gomez, D.O., Martens, P.C.H. and Golub, L., 1993, "Normal incidence X-ray telescope power spectra of X-ray emission from solar active regions. I. Observations. II. Theory", *Astrophys. J.*, **405**, 767–781. [DOI], [ADS] (Cited on page 14.)

Gontikakis, C., Contopoulos, I. and Dara, H.C., 2008, "Distribution of coronal heating in a solar active region", *Astron. Astrophys.*, **489**, 441–447. [DOI], [ADS] (Cited on page 34.)

Grappin, R., Léorat, J. and Ofman, L., 2003, "Flows in coronal loops driven by Alfvén waves: 1.5 MHD simulations with transparent boundary conditions", in *Solar Wind Ten*, (Eds.) Velli, M., Bruno, R., Malara, F., Proceedings of the Tenth International Solar Wind Conference, Pisa, Italy, 17 – 21 June 2002, vol. 679 of AIP Conference Proceedings, pp. 750–753, American Institute of Physics, Melville, NY. [DOI], [ADS] (Cited on page 42.)

Grappin, R., Léorat, J. and Habbal, S.R., 2005, "Siphon flows and oscillations in long coronal loops due to Alfvén waves", *Astron. Astrophys.*, **437**, 1081–1092. [DOI], [ADS] (Cited on page 42.)

Griffiths, N.W., Fisher, G.H., Woods, D.T., Acton, L.W. and Siegmund, O.H.W., 2000, "Simultaneous SOHO and Yohkoh Observations of a Small Solar Active Region", *Astrophys. J.*, **537**, 481–494. [DOI], [ADS] (Cited on page 19.)

Guarrasi, M., Reale, F. and Peres, G., 2010, "Coronal Fuzziness Modeled with Pulse-heated Multi-stranded Loop Systems", *Astrophys. J.*, **719**, 576–582. [DOI], [ADS] (Cited on pages 39 and 40.)

Güdel, M., 2004, "X-ray astronomy of stellar coronae", *Annu. Rev. Astron. Astrophys.*, **12**, 71–237. [DOI], [ADS], [arXiv:astro-ph/0406661] (Cited on page 49.)

Gudiksen, B.V. and Nordlund, Å., 2005, "An Ab Initio Approach to the Solar Coronal Heating Problem", *Astrophys. J.*, **618**, 1020–1030. [DOI], [ADS], [arXiv:astro-ph/0407266] (Cited on pages 32, 43, 47, and 48.)

Habbal, S.R., Ronan, R. and Withbroe, G.L., 1985, "Spatial and temporal variations of solar coronal loops", *Solar Phys.*, **98**, 323–340. [DOI], [ADS] (Cited on page 24.)

Haisch, B.M., Strong, K.T., Harrison, R.A. and Gary, G.A., 1988, "Active region coronal loops: Structure and variability", *Astrophys. J. Suppl. Ser.*, **68**, 371–405. [DOI], [ADS] (Cited on page 24.)

Handy, B.N., Acton, L.W., Kankelborg, C.C., Wolfson, C.J., Akin, D.J., Bruner, M.E., Caravalho, R., Catura, R.C., Chevalier, R., Duncan, D.W., Edwards, C.G., Feinstein, C.N., Freeland, S.L., Friedlaender, F.M., Hoffmann, C.H., Hurlburt, N.E., Jurcevich, B.K., Katz, N.L., Kelly, G.A., Lemen, J.R., Levay, M., Lindgren, R.W., Mathur, D.P., Meyer, S.B., Morrison, S.J., Morrison, M.D., Nightingale, R.W., Pope, T.P., Rehse, R.A., Schrijver, C.J., Shine, R.A., Shing, L., Strong, K.T., Tarbell, T.D., Title, A.M., Torgerson, D.D., Golub, L., Bookbinder, J.A., Caldwell, D., Cheimets, P.N., Davis, W.N., DeLuca, E.E., McMullen, R.A., Warren, H.P., Amato, D., Fisher, R., Maldonado, H. and Parkinson, C., 1999, "The transition region and coronal explorer", *Solar Phys.*, **187**, 229–260. [DOI], [ADS] (Cited on page 7.)

Hansteen, V., 1993, "A new interpretation of the redshift observed in optically thin transition region lines", *Astrophys. J.*, **402**, 741–755. [DOI], [ADS] (Cited on pages 27, 30, and 40.)

Hansteen, V.H., Carlsson, M. and Gudiksen, B., 2007, "3D Numerical Models of the Chromosphere, Transition Region, and Corona", in *The Physics of Chromospheric Plasmas*, (Eds.) Heinzel, P., Dorotovič, I., Rutten, R.J., Proceedings of the conference held 9 – 13 October, 2006 at the University of Coimbra, Portugal, vol. 368 of ASP Conference Series, pp. 107–114, Astronomical Society of the Pacific, San Francisco. [ADS], [arXiv:0704.1511] (Cited on page 32.)

Hara, H., Tsuneta, S., Lemen, J.R., Acton, L.W. and McTiernan, J.M., 1992, "High-temperature plasmas in active regions observed with the Soft X-ray Telescope aboard YOHKOH", *Publ. Astron. Soc. Japan*, **44**, L135–L140. [ADS] (Cited on page 7.)

Hara, H., Watanabe, T., Harra, L.K., Culhane, J.L., Young, P.R., Mariska, J.T. and Doschek, G.A., 2008, "Coronal Plasma Motions near Footpoints of Active Region Loops Revealed from Spectroscopic Observations with Hinode EIS", *Astrophys. J. Lett.*, **678**, L67–L71. [DOI], [ADS] (Cited on page 28.)

Harrison, R.A., Sawyer, E.C., Carter, M.K., Cruise, A.M., Cutler, R.M., Fludra, A., Hayes, R.W., Kent, B.J., Lang, J., Parker, D.J., Payne, J., Pike, C.D., Peskett, S.C., Richards, A.G., Gulhane, J.L., Norman, K., Breeveld, A.A., Breeveld, E.R., Al Janabi, K.F., McCalden, A.J., Parkinson, J.H., Self, D.G., Thomas, P.D., Poland, A.I., Thomas, R.J., Thompson, W.T., Kjeldseth-Moe, O., Brekke, P., Karud, J., Maltby, P., Aschenbach, B., Bräuninger, H., Kühne, M., Hollandt, J., Siegmund, O.H.W., Huber, M.C.E., Gabriel, A.H., Mason, H.E. and Bromage, B.J.I., 1995, "The Coronal Diagnostic Spectrometer for the Solar and Heliospheric Observatory", *Solar Phys.*, **162**, 233–290. [DOI], [ADS] (Cited on page 7.)

Haynes, M., Arber, T.D. and Verwichte, E., 2008, "Coronal loop slow mode oscillations driven by the kink instability", *Astron. Astrophys.*, **479**, 235–239. [DOI], [ADS] (Cited on page 48.)

Hollweg, J.V., 1981, "Alfvén waves in the solar atmosphere II: Open and closed magnetic flux tubes", *Solar Phys.*, **70**, 25–66. [DOI], [ADS] (Cited on page 46.)

Hollweg, J.V., 1984, "Resonances of coronal loops", *Astrophys. J.*, **277**, 392–403. [DOI], [ADS] (Cited on page 46.)

Hollweg, J.V., 1985, "Viscosity in a Magnetized Plasma: Physical Interpretation", *J. Geophys. Res.*, **90**, 7620–7622. [DOI], [ADS] (Cited on page 46.)

Hollweg, J.V., 1986, "Transition region, corona, and solar wind in coronal holes", *J. Geophys. Res.*, **91**, 4111–4125. [DOI], [ADS] (Cited on page 46.)

Hollweg, J.V. and Yang, G., 1988, "Resonance absorption of compressible magnetohydrodynamic waves at thin 'surfaces"', *J. Geophys. Res.*, **93**, 5423–5436. [DOI], [ADS] (Cited on page 46.)

Hood, A.W. and Priest, E.R., 1979, "The equilibrium of solar coronal magnetic loops", *Astron. Astrophys.*, **77**, 233–251. [ADS] (Cited on page 32.)

Hori, K., Yokoyama, T., Kosugi, T. and Shibata, K., 1997, "Pseudo–Two-dimensional Hydrodynamic Modeling of Solar Flare Loops", *Astrophys. J.*, **489**, 426. [DOI], [ADS] (Cited on page 34.)

Hori, K., Yokoyama, T., Kosugi, T. and Shibata, K., 1998, "Single and Multiple Solar Flare Loops: Hydrodynamics and Ca XIX Resonance Line Emission", *Astrophys. J.*, **500**, 492–510. [DOI], [ADS] (Cited on page 34.)

Hudson, H.S., 1991, "Solar flares, microflares, nanoflares, and coronal heating", *Solar Phys.*, **133**, 357–369. [DOI], [ADS] (Cited on page 45.)

Ignatiev, A.P., Kolachevsky, N.N., Korneev, V.V., Krutov, V.V., Kuzin, S.V., Mitrofanov, A.V., Pertsov, A., Ragozin, E.N., Slemzin, V.A., Tindo, I.P., Zhitnik, I.A., Salashchenko, N.N. and Thomas, R.J., 1998, "Manufacture and testing of x-ray optical elements for the TEREK-C and RES-C instruments on the CORONAS-I mission", in *Current Russian Research in Optics and Photonics: New Methods and Instruments for Space- and Earth-based Spectroscopy in XUV, UV, IR, and Millimeter Waves*, (Eds.) Sobelman, I.I., Slemzin, V.A., vol. 3406 of Proc. SPIE, pp. 20–34, SPIE, Bellingham, WA. [DOI], [ADS] (Cited on page 7.)

Ionson, J.A., 1978, "Resonant absorption of Alfvénic surface waves and the heating of solar coronal loops", *Astrophys. J.*, **226**, 650–673. [DOI], [ADS] (Cited on page 45.)

Ionson, J.A., 1982, "Resonant electrodynamic heating of stellar coronal loops: an LRC circuit analog", *Astrophys. J.*, **254**, 318–334. [DOI], [ADS] (Cited on page 46.)

Ionson, J.A., 1983, "Electrodynamic coupling in magnetically confined X-ray plasmas of astrophysical origin", *Astrophys. J.*, **271**, 778–792. [DOI], [ADS] (Cited on page 46.)

Jakimiec, J., Sylwester, B., Sylwester, J., Serio, S., Peres, G. and Reale, F., 1992, "Dynamics of flaring loops II. Flare evolution in the density-temperature diagram", *Astron. Astrophys.*, **253**, 269–276. [ADS] (Cited on pages 34 and 37.)

Jordan, C., 1976, "The structure and energy balance of solar active regions", *Philos. Trans. R. Soc. London, Ser. A*, **281**, 391–404. [ADS] (Cited on page 32.)

Jordan, C., 1980, "The energy balance of the solar transition region", *Astron. Astrophys.*, **86**, 355–363. [ADS] (Cited on pages 32 and 44.)

Jordan, C., Ayres, T.R., Brown, A., Linsky, J.L. and Simon, T., 1987, "The chromospheres and coronae of five G-K main-sequence stars", *Mon. Not. R. Astron. Soc.*, **225**, 903–937. [ADS] (Cited on page 17.)

Judge, P.G., Hansteen, V., Wikstol, O., Wilhelm, K., Schuehle, U. and Moran, T., 1998, "Evidence in Support of the 'Nanoflare' Picture of Coronal Heating from SUMER Data", *Astrophys. J.*, **502**, 981. [DOI], [ADS] (Cited on page 44.)

Kaiser, M.L., Kucera, T.A., Davila, J.M., St Cyr, O.C., Guhathakurta, M. and Christian, E., 2008, "The STEREO Mission: An Introduction", *Space Sci. Rev.*, **136**, 5–16. [DOI], [ADS] (Cited on page 7.)

Kano, R. and Tsuneta, S., 1995, "Scaling Law of Solar Coronal Loops Obtained with YOHKOH", *Astrophys. J.*, **454**, 934. [DOI], [ADS] (Cited on pages 18 and 32.)

Kashyap, V. and Drake, J.J., 1998, "Markov-Chain Monte Carlo Reconstruction of Emission Measure Distributions: Application to Solar Extreme-Ultraviolet Spectra", *Astrophys. J.*, **503**, 450. [DOI], [ADS] (Cited on page 17.)

Katsukawa, Y. and Tsuneta, S., 2001, "Small Fluctuation of Coronal X-Ray Intensity and a Signature of Nanoflares", *Astrophys. J.*, **557**, 343–350. [DOI], [ADS] (Cited on pages 44 and 45.)

Katsukawa, Y. and Tsuneta, S., 2005, "Magnetic Properties at Footpoints of Hot and Cool Loops", *Astrophys. J.*, **621**, 498–511. [DOI], [ADS] (Cited on page 13.)

Klimchuk, J.A., 1987, "On the large-scale dynamics and magnetic structure of solar active regions", *Astrophys. J.*, **323**, 368–379. [DOI], [ADS] (Cited on page 27.)

Klimchuk, J.A., 2000, "Cross-Sectional Properties of Coronal Loops", *Solar Phys.*, **193**, 53–75. [ADS] (Cited on page 13.)

Klimchuk, J.A., 2006, "On Solving the Coronal Heating Problem", *Solar Phys.*, **234**, 41–77. [DOI], [ADS], [arXiv:astro-ph/0511841] (Cited on pages 5, 18, 34, 43, and 45.)

Klimchuk, J.A. and Gary, D.E., 1995, "A Comparison of Active Region Temperatures and Emission Measures Observed in Soft X-Rays and Microwaves and Implications for Coronal Heating", *Astrophys. J.*, **448**, 925. [DOI], [ADS] (Cited on page 18.)

Klimchuk, J.A. and Porter, L.J., 1995, "Scaling of heating rates in solar coronal loops", *Nature*, **377**, 131–133. [DOI], [ADS] (Cited on page 18.)

Klimchuk, J.A., Lemen, J.R., Feldman, U., Tsuneta, S. and Uchida, Y., 1992, "Thickness variations along coronal loops observed by the Soft X-ray Telescope on YOHKOH", *Publ. Astron. Soc. Japan*, **44**, L181–L185. [ADS] (Cited on page 13.)

Klimchuk, J.A., Patsourakos, S. and Cargill, P.J., 2008, "Highly Efficient Modeling of Dynamic Coronal Loops", *Astrophys. J.*, **682**, 1351–1362. [DOI], [ADS], [arXiv:0710.0185] (Cited on page 31.)

Ko, Y.-K., Doschek, G.A., Warren, H.P. and Young, P.R., 2009, "Hot Plasma in Nonflaring Active Regions Observed by the Extreme-Ultraviolet Imaging Spectrometer on Hinode", *Astrophys. J.*, **697**, 1956–1970. [DOI], [ADS], [arXiv:0903.3029] (Cited on page 18.)

Kopp, R.A. and Poletto, G., 1993, "Coronal Heating by Nanoflares: Individual Events and Global Energetics", *Astrophys. J.*, **418**, 496. [DOI], [ADS] (Cited on page 44.)

Kopp, R.A., Poletto, G., Noci, G. and Bruner, M., 1985, "Analysis of loop flows observed on 27 March, 1980 by the UVSP instrument during the solar maximum mission", *Solar Phys.*, **98**, 91–118. [DOI], [ADS] (Cited on page 25.)

Kosugi, T., Matsuzaki, K., Sakao, T., Shimizu, T., Sone, Y., Tachikawa, S., Hashimoto, T., Minesugi, K., Ohnishi, A., Yamada, T., Tsuneta, S., Hara, H., Ichimoto, K., Suematsu, Y., Shimojo, M., Watanabe, T., Shimada, S., Davis, J.M., Hill, L.D., Owens, J.K., Title, A.M., Culhane, J.L., Harra, L.K., Doschek, G.A. and Golub, L., 2007, "The Hinode (Solar-B) Mission: An Overview", *Solar Phys.*, **243**, 3–17. [DOI], [ADS] (Cited on page 7.)

Kramar, M., Jones, S., Davila, J., Inhester, B. and Mierla, M., 2009, "On the Tomographic Reconstruction of the 3D Electron Density for the Solar Corona from STEREO COR1 Data", *Solar Phys.*, **259**, 109–121. [DOI], [ADS] (Cited on page 7.)

Krieger, A., Paolini, F., Vaiana, G.S. and Webb, D., 1972, "Results from OSO-IV: the Long Term Behavior of X-Ray Emitting Regions", *Solar Phys.*, **22**, 150–177. [DOI], [ADS] (Cited on page 6.)

Krieger, A.S., 1978, "The decay of coronal loops brightened by flares and transients", *Solar Phys.*, **56**, 107–120. [DOI], [ADS] (Cited on page 24.)

Landi, E. and Feldman, U., 2004, "Models for Solar Magnetic Loops. IV. On the Relation between Coronal and Footpoint Plasma in Active Region Loops", *Astrophys. J.*, **611**, 537–544. [DOI], [ADS] (Cited on pages 20 and 34.)

Landi, E. and Feldman, U., 2008, "The Thermal Structure of an Active Region Observed Outside the Solar Disk", *Astrophys. J.*, **672**, 674–683. [DOI], [ADS] (Cited on page 20.)

Landi, E. and Landini, M., 2004, "Models for Solar Magnetic Loops. III. Dynamic Models and Coronal Diagnostic Spectrometer Observations", *Astrophys. J.*, **608**, 1133–1147. [DOI], [ADS] (Cited on pages 20, 24, and 34.)

Landi, E. and Landini, M., 2005, "Models for Solar Magnetic Loops. V. A New Diagnostic Technique to Compare Loop Models and Observations", *Astrophys. J.*, **618**, 1039–1043. [DOI], [ADS] (Cited on page 44.)

Landi, E., Miralles, M.P., Curdt, W. and Hara, H., 2009, "Physical Properties of Cooling Plasma in Quiescent Active Region Loops", *Astrophys. J.*, **695**, 221–237. [DOI], [ADS] (Cited on page 23.)

Landini, M. and Landi, E., 2002, "Models for solar magnetic loops. I. A simple theoretical model and diagnostic procedure", *Astron. Astrophys.*, **383**, 653–660. [DOI], [ADS] (Cited on page 34.)

Landini, M. and Monsignori Fossi, B.C., 1975, "A loop model of active coronal regions", *Astron. Astrophys.*, **42**, 213–220. [ADS] (Cited on page 32.)

Lenz, D.D., 2004, "Effects of Flow on Structure and Abundances in Multispecies Solar Coronal Loops", *Astrophys. J.*, **604**, 433–441. [DOI], [ADS] (Cited on page 42.)

Lenz, D.D., DeLuca, E.E., Golub, L., Rosner, R. and Bookbinder, J.A., 1999, "Temperature and Emission-Measure Profiles along Long-lived Solar Coronal Loops Observed with the Transition Region and Coronal Explorer", *Astrophys. J. Lett.*, **517**, L155–L158. [DOI], [ADS], [arXiv:astro-ph/9903491] (Cited on pages 8, 22, 23, 24, 32, and 39.)

Litwin, C. and Rosner, R., 1998, "Alfvén Wave Transmission and Heating of Solar Coronal Loops", *Astrophys. J.*, **499**, 945. [DOI], [ADS] (Cited on pages 44 and 46.)

López Fuentes, M.C., Klimchuk, J.A. and Démoulin, P., 2006, "The Magnetic Structure of Coronal Loops Observed by TRACE", *Astrophys. J.*, **639**, 459–474. [DOI], [ADS], [arXiv:astro-ph/0507462] (Cited on page 13.)

López Fuentes, M.C., Klimchuk, J.A. and Mandrini, C.H., 2007, "The Temporal Evolution of Coronal Loops Observed by GOES SXI", *Astrophys. J.*, **657**, 1127–1136. [DOI], [ADS], [arXiv:astro-ph/0611338] (Cited on page 25.)

Lundquist, L.L., Fisher, G.H. and McTiernan, J.M., 2008a, "Forward Modeling of Active Region Coronal Emissions. I. Methods and Testing", *Astrophys. J. Suppl. Ser.*, **179**, 509–533. [DOI], [ADS] (Cited on page 47.)

Lundquist, L.L., Fisher, G.H., Metcalf, T.R., Leka, K.D. and McTiernan, J.M., 2008b, "Forward Modeling of Active Region Coronal Emissions. II. Implications for Coronal Heating", *Astrophys. J.*, **689**, 1388–1405. [DOI], [ADS] (Cited on page 47.)

MacNeice, P., 1986, "A numerical hydrodynamic model of a heated coronal loop", *Solar Phys.*, **103**, 47–66. [DOI], [ADS] (Cited on pages 30 and 34.)

MacNeice, P., Pallavicini, R., Mason, H.E., Simnett, G.M., Antonucci, E., Shine, R.A. and Dennis, B.R., 1985, "Multiwavelength analysis of a well observed flare from SMM", *Solar Phys.*, **99**, 167–188. [DOI], [ADS] (Cited on page 7.)

Maggio, A., Pallavicini, R., Reale, F. and Tagliaferri, G., 2000, "Twin X-ray flares and the active corona of AB Dor observed with BeppoSAX", *Astron. Astrophys.*, **356**, 627–642. [ADS] (Cited on page 37.)

Mandrini, C.H., Démoulin, P. and Klimchuk, J.A., 2000, "Magnetic Field and Plasma Scaling Laws: Their Implications for Coronal Heating Models", *Astrophys. J.*, **530**, 999–1015. [DOI], [ADS] (Cited on page 47.)

Mariska, J.T., Feldman, U. and Doschek, G.A., 1980, "Physical conditions in the solar atmosphere above an active region", *Astrophys. J.*, **240**, 300–305. [DOI], [ADS] (Cited on page 16.)

Martens, P.C.H., Kankelborg, C.C. and Berger, T.E., 2000, "On the Nature of the 'Moss' Observed by TRACE", *Astrophys. J.*, **537**, 471–480. [DOI], [ADS] (Cited on page 22.)

Martens, P.C.H., Cirtain, J.W. and Schmelz, J.T., 2002, "The Inadequacy of Temperature Measurements in the Solar Corona through Narrowband Filter and Line Ratios", *Astrophys. J. Lett.*, **577**, L115–L117. [DOI], [ADS] (Cited on page 20.)

Mason, H.E., Landi, E., Pike, C.D. and Young, P.R., 1999, "Electron density and temperature structure of two limb active regions observed by SOHO-CDS", *Solar Phys.*, **189**, 129–146. [ADS] (Cited on page 19.)

McLaughlin, J.A. and Ofman, L., 2008, "Three-dimensional Magnetohydrodynamic Wave Behavior in Active Regions: Individual Loop Density Structure", *Astrophys. J.*, **682**, 1338–1350. [DOI], [ADS] (Cited on page 31.)

McTiernan, J.M., 2009, "RHESSI/GOES Observations of the Nonflaring Sun from 2002 to 2006", *Astrophys. J.*, **697**, 94–99. [DOI], [ADS] (Cited on page 19.)

Mitra-Kraev, U. and Benz, A.O., 2001, "A nanoflare heating model for the quiet solar corona", *Astron. Astrophys.*, **373**, 318–328. [DOI], [ADS], [arXiv:astro-ph/0104218] (Cited on page 44.)

Montesinos, B. and Thomas, J.H., 1989, "Siphon flows in isolated magnetic flux tubes. II. Adiabatic flows", *Astrophys. J.*, **337**, 977–988. [DOI], [ADS] (Cited on page 40.)

Montesinos, B. and Thomas, J.H., 1993, "Siphon flows in isolated magnetic flux tubes. V. Radiative flows with variable ionization", *Astrophys. J.*, **402**, 314–325. [DOI], [ADS] (Cited on page 40.)

Morales, L. and Charbonneau, P., 2008, "Self-organized Critical Model of Energy Release in an Idealized Coronal Loop", *Astrophys. J.*, **682**, 654–666. [DOI], [ADS] (Cited on page 48.)

Müller, D.A.N., Hansteen, V.H. and Peter, H., 2003, "Dynamics of solar coronal loops. I. Condensation in cool loops and its effect on transition region lines", *Astron. Astrophys.*, **411**, 605–613. [DOI], [ADS] (Cited on page 30.)

Müller, D.A.N., Peter, H. and Hansteen, V.H., 2004, "Dynamics of solar coronal loops. II. Catastrophic cooling and high-speed downflows", *Astron. Astrophys.*, **424**, 289–300. [DOI], [ADS], [arXiv:astro-ph/0405538] (Cited on pages 42 and 44.)

Müller, D.A.N., De Groof, A., Hansteen, V.H. and Peter, H., 2005, "High-speed coronal rain", *Astron. Astrophys.*, **436**, 1067–1074. [DOI], [ADS] (Cited on page 42.)

Muller, R., Roudier, T., Vigneau, J. and Auffret, H., 1994, "The proper motion of network bright points and the heating of the solar corona", *Astron. Astrophys.*, **283**, 232–240. [ADS] (Cited on page 46.)

Nagai, F., 1980, "A model of hot loops associated with solar flares I. Gasdynamics in the loops", *Solar Phys.*, **68**, 351–379. [ADS] (Cited on pages 30 and 34.)

Nagai, F. and Emslie, A.G., 1984, "Gas dynamics in the impulsive phase of solar flares. I Thick-target heating by nonthermal electrons", *Astrophys. J.*, **279**, 896–908. [DOI], [ADS] (Cited on pages 30 and 34.)

Nagata, S., Hara, H., Kano, R., Kobayashi, K., Sakao, T., Shimizu, T., Tsuneta, S., Yoshida, T. and Gurman, J.B., 2003, "Spatial and Temporal Properties of Hot and Cool Coronal Loops", *Astrophys. J.*, **590**, 1095–1110. [DOI], [ADS] (Cited on pages 14 and 15.)

Nakariakov, V.M. and Ofman, L., 2001, "Determination of the coronal magnetic field by coronal loop oscillations", *Astron. Astrophys.*, **372**, L53–L56. [DOI], [ADS] (Cited on page 11.)

Nakariakov, V.M. and Verwichte, E., 2005, "Coronal Waves and Oscillations", *Living Rev. Solar Phys.*, **2**, lrsp-2005-3. [ADS]. URL (accessed 26 October 2010): http://www.livingreviews.org/lrsp-2005-3 (Cited on page 45.)

Nakariakov, V.M., Ofman, L., DeLuca, E.E., Roberts, B. and Davila, J.M., 1999, "TRACE observation of damped coronal loop oscillations: Implications for coronal heating", *Science*, **285**, 862–864. [DOI], [ADS] (Cited on pages 11 and 46.)

Nakariakov, V.M., Verwichte, E., Berghmans, D. and Robbrecht, E., 2000, "Slow magnetoacoustic waves in coronal loops", *Astron. Astrophys.*, **362**, 1151–1157. [ADS] (Cited on page 47.)

Narain, U. and Ulmschneider, P., 1996, "Chromospheric and Coronal Heating Mechanisms II", *Space Sci. Rev.*, **75**, 453–509. [DOI], [ADS] (Cited on page 45.)

Nigro, G., Malara, F., Carbone, V. and Veltri, P., 2004, "Nanoflares and MHD Turbulence in Coronal Loops: A Hybrid Shell Model", *Phys. Rev. Lett.*, **92**(19), 194501. [DOI], [ADS] (Cited on page 48.)

Nitta, N., 2000, "The relation between hot and cool loops", *Solar Phys.*, **195**, 123–133. [ADS] (Cited on page 19.)

Noci, G., 1981, "Siphon flows in the solar corona", *Solar Phys.*, **69**, 63–76. [DOI], [ADS] (Cited on page 40.)

Noci, G., Spadaro, D., Zappala, R.A. and Antiochos, S.K., 1989, "Mass flows and the ionization states of coronal loops", *Astrophys. J.*, **338**, 1131–1138. [DOI], [ADS] (Cited on page 40.)

Noglik, J.B., Walsh, R.W. and Cirtain, J., 2008, "Comparison of High-Resolution TRACE Data to Spectroscopic CDS Data for Temperature Determination", *Astrophys. J.*, **674**, 1191–1200. [DOI], [ADS] (Cited on pages 23 and 24.)

Ofman, L., 2009, "Three-Dimensional Magnetohydrodynamic Models of Twisted Multithreaded Coronal Loop Oscillations", *Astrophys. J.*, **694**, 502–511. [DOI], [ADS] (Cited on pages 31 and 47.)

Ofman, L. and Aschwanden, M.J., 2002, "Damping Time Scaling of Coronal Loop Oscillations Deduced from Transition Region and Coronal Explorer Observations", *Astrophys. J. Lett.*, **576**, L153–L156. [DOI], [ADS] (Cited on page 47.)

Ofman, L. and Wang, T., 2002, "Hot Coronal Loop Oscillations Observed by SUMER: Slow Magnetosonic Wave Damping by Thermal Conduction", *Astrophys. J. Lett.*, **580**, L85–L88. [DOI], [ADS] (Cited on page 30.)

Ofman, L. and Wang, T.J., 2008, "Hinode observations of transverse waves with flows in coronal loops", *Astron. Astrophys.*, **482**, L9–L12. [DOI], [ADS] (Cited on pages 28 and 47.)

Ofman, L., Davila, J.M. and Steinolfson, R.S., 1995, "Coronal heating by the resonant absorption of Alfvén waves: Wavenumber scaling laws", *Astrophys. J.*, **444**, 471–477. [DOI], [ADS] (Cited on page 46.)

Ofman, L., Klimchuk, J.A. and Davila, J.M., 1998, "A Self-consistent Model for the Resonant Heating of Coronal Loops: The Effects of Coupling with the Chromosphere", *Astrophys. J.*, **493**, 474–479. [DOI], [ADS] (Cited on page 46.)

Ogawara, Y., Takano, T., Kato, T., Kosugi, T., Tsuneta, S., Watanabe, T., Kondo, I. and Uchida, Y., 1991, "The SOLAR-A Mission: An Overview", *Solar Phys.*, **136**, 1–16. [DOI], [ADS] (Cited on page 7.)

O'Neill, I. and Li, X., 2005, "Coronal loops heated by turbulence-driven Alfvén waves: A two fluid model", *Astron. Astrophys.*, **435**, 1159–1167. [DOI], [ADS] (Cited on pages 42 and 46.)

Oraevsky, V.N. and Sobelman, I.I., 2002, "Comprehensive studies of solar activity on the CORONAS-F satellite", *Astron. Lett.*, **28**, 401–410. [DOI], [ADS] (Cited on page 7.)

Orlando, S. and Peres, G., 1999, "Effects on UV lines observations of stationary plasma flows confined in coronal loops", *Phys. Chem. Earth*, **24**, 401–406. [DOI], [ADS] (Cited on pages 40 and 41.)

Orlando, S., Peres, G. and Serio, S., 1995a, "Models of stationary siphon flows in stratified, thermally conducting coronal loops I. Regular solutions", *Astron. Astrophys.*, **294**, 861–873. [ADS] (Cited on page 40.)

Orlando, S., Peres, G. and Serio, S., 1995b, "Models of stationary siphon flows in stratified, thermally conducting coronal loops II. Shocked solutions", *Astron. Astrophys.*, **300**, 549. [ADS] (Cited on page 40.)

Orlando, S., Peres, G. and Reale, F., 2000, "The Sun as an X-Ray Star. I. Deriving the Emission Measure Distribution versus Temperature of the Whole Solar Corona from the Yohkoh/Soft X-Ray Telescope Data", *Astrophys. J.*, **528**, 524–536. [DOI], [ADS] (Cited on pages 44 and 49.)

Orlando, S., Peres, G. and Reale, F., 2001, "The Sun as an X-Ray Star. IV. The Contribution of Different Regions of the Corona to Its X-Ray Spectrum", *Astrophys. J.*, **560**, 499–513. [DOI], [ADS] (Cited on page 49.)

Orlando, S., Peres, G. and Reale, F., 2004, "The Sun as an X-ray star: Active region evolution, rotational modulation, and implications for stellar X-ray variability", *Astron. Astrophys.*, **424**, 677–689. [DOI], [ADS] (Cited on page 49.)

O'Shea, E., Banerjee, D. and Doyle, J.G., 2007, "Plasma condensation in coronal loops", *Astron. Astrophys.*, **475**, L25–L28. [DOI], [ADS] (Cited on page 25.)

Parenti, S. and Young, P.R., 2008, "On the ultraviolet signatures of small scale heating in coronal loops", *Astron. Astrophys.*, **492**, 857–862. [DOI], [ADS] (Cited on page 45.)

Parenti, S., Buchlin, E., Cargill, P.J., Galtier, S. and Vial, J.-C., 2006, "Modeling the Radiative Signatures of Turbulent Heating in Coronal Loops", *Astrophys. J.*, **651**, 1219–1228. [DOI], [ADS] (Cited on page 43.)

Parker, E.N., 1988, "Nanoflares and the solar X-ray corona", *Astrophys. J.*, **330**, 474–479. [DOI], [ADS] (Cited on pages 39, 44, and 47.)

Parker, E.N., 1991, "Heating solar coronal holes", *Astrophys. J.*, **372**, 719–727. [DOI], [ADS] (Cited on page 46.)

Pascoe, D.J., de Moortel, I. and McLaughlin, J.A., 2009, "Impulsively generated oscillations in a 3D coronal loop", *Astron. Astrophys.*, **505**, 319–327. [DOI], [ADS] (Cited on page 31.)

Patsourakos, S. and Klimchuk, J.A., 2005, "Coronal Loop Heating by Nanoflares: The Impact of the Field-aligned Distribution of the Heating on Loop Observations", *Astrophys. J.*, **628**, 1023–1030. [DOI], [ADS] (Cited on page 44.)

Patsourakos, S. and Klimchuk, J.A., 2006, "Nonthermal Spectral Line Broadening and the Nanoflare Model", *Astrophys. J.*, **647**, 1452–1465. [DOI], [ADS] (Cited on pages 40 and 46.)

Patsourakos, S. and Klimchuk, J.A., 2007, "The Cross-Field Thermal Structure of Coronal Loops from Triple-Filter TRACE Observations", *Astrophys. J.*, **667**, 591–601. [DOI], [ADS] (Cited on pages 16, 23, and 24.)

Patsourakos, S. and Klimchuk, J.A., 2008, "Static and Impulsive Models of Solar Active Regions", *Astrophys. J.*, **689**, 1406–1411. [DOI], [ADS], [arXiv:0808.2745] (Cited on page 44.)

Patsourakos, S. and Klimchuk, J.A., 2009, "Spectroscopic Observations of Hot Lines Constraining Coronal Heating in Solar Active Regions", *Astrophys. J.*, **696**, 760–765. [DOI], [ADS], [arXiv:0903.3880] (Cited on page 18.)

Patsourakos, S., Klimchuk, J.A. and MacNeice, P.J., 2004, "The Inability of Steady-Flow Models to Explain the Extreme-Ultraviolet Coronal Loops", *Astrophys. J.*, **603**, 322–329. [DOI], [ADS] (Cited on pages 39 and 42.)

Pekünlü, E.R., Çakırlı, Ö. and Özetken, E., 2001, "Solar coronal heating by magnetosonic waves", *Mon. Not. R. Astron. Soc.*, **326**, 675–685. [DOI], [ADS] (Cited on page 47.)

Peres, G. and Vaiana, G.S., 1990, "X-ray observations, scaling laws and magnetic fields", *Mem. Soc. Astron. Ital.*, **61**, 401–430. [ADS] (Cited on pages 5 and 6.)

Peres, G., Serio, S., Vaiana, G.S. and Rosner, R., 1982, "Coronal closed structures. IV. Hydrodynamical stability and response to heating perturbations", *Astrophys. J.*, **252**, 791–799. [DOI], [ADS] (Cited on pages 30, 34, and 48.)

Peres, G., Spadaro, D. and Noci, G., 1992, "Steady siphon flows in closed coronal structures: Comparison with extreme-ultraviolet observations", *Astrophys. J.*, **389**, 777–783. [DOI], [ADS] (Cited on page 40.)

Peres, G., Reale, F. and Serio, S., 1993, "Hydrodynamics and Diagnostics of Coronal Loops Subject to Dynamic Heating", in *Physics of Solar and Stellar Coronae: G.S. Vaiana Memorial Symposium*, (Eds.) Linsky, J.L., Serio, S., Proceedings of a conference of the IAU, held in Palermo, Italy, 22 – 26 June, vol. 183 of Astrophysics and Space Science Library, p. 151, Kluwer, Dordrecht; Boston. [ADS] (Cited on page 44.)

Peres, G., Reale, F. and Golub, L., 1994, "Loop models of low coronal structures observed by the Normal Incidence X-Ray Telescope (NIXT)", *Astrophys. J.*, **422**, 412–415. [DOI], [ADS] (Cited on pages 19 and 22.)

Peres, G., Orlando, S., Reale, F., Rosner, R. and Hudson, H., 2000, "The Sun as an X-Ray Star. II. Using the Yohkoh/Soft X-Ray Telescope-derived Solar Emission Measure versus Temperature to Interpret Stellar X-Ray Observations", *Astrophys. J.*, **528**, 537–551. [DOI], [ADS] (Cited on pages 8, 22, and 49.)

Peres, G., Orlando, S., Reale, F. and Rosner, R., 2001, "The Distribution of the Emission Measure, and of the Heating Budget, among the Loops in the Corona", *Astrophys. J.*, **563**, 1045–1054. [DOI], [ADS], [arXiv:astro-ph/0111192] (Cited on page 44.)

Peres, G., Orlando, S. and Reale, F., 2004, "Are Coronae of Late-Type Stars Made of Solar-like Structures? The X-Ray Surface Flux versus Hardness Ratio Diagram and the Pressure-Temperature Correlation", *Astrophys. J.*, **612**, 472–480. [DOI], [ADS], [arXiv:astro-ph/0405281] (Cited on page 49.)

Peter, H., 1999, "Analysis of Transition-Region Emission-Line Profiles from Full-Disk Scans of the Sun Using the SUMER Instrument on SOHO", *Astrophys. J.*, **516**, 490–504. [DOI], [ADS] (Cited on page 27.)

Poletto, G., Vaiana, G.S., Zombeck, M.V., Krieger, A.S. and Timothy, A.F., 1975, "A comparison of coronal X-ray structures of active regions with magnetic fields computed from photospheric observations", *Solar Phys.*, **44**, 83–99. [DOI], [ADS] (Cited on page 6.)

Porter, L.J. and Klimchuk, J.A., 1995, "Soft X-Ray Loops and Coronal Heating", *Astrophys. J.*, **454**, 499. [DOI], [ADS] (Cited on pages 10 and 18.)

Porter, L.J., Klimchuk, J.A. and Sturrock, P.A., 1994, "The possible role of MHD waves in heating the solar corona", *Astrophys. J.*, **435**, 482–501. [DOI], [ADS] (Cited on page 46.)

Priest, E.R., 1978, "The structure of coronal loops", *Solar Phys.*, **58**, 57–87. [DOI], [ADS] (Cited on page 29.)

Priest, E.R., 1981, "Theory of loop flows and instability", in *Solar Active Regions*, (Ed.) Orrall, F.Q., A Monograph from Skylab Solar Workshop III, pp. 213–275, Colorado Associated University Press, Boulder, CO. [ADS] (Cited on page 40.)

Priest, E.R., Foley, C.R., Heyvaerts, J., Arber, T.D., Mackay, D., Culhane, J.L. and Acton, L.W., 2000, "A Method to Determine the Heating Mechanisms of the Solar Corona", *Astrophys. J.*, **539**, 1002–1022. [DOI], [ADS] (Cited on pages 16 and 43.)

Rappazzo, A.F., Velli, M., Einaudi, G. and Dahlburg, R.B., 2007, "Coronal Heating, Weak MHD Turbulence, and Scaling Laws", *Astrophys. J. Lett.*, **657**, L47–L51. [DOI], [ADS], [arXiv:astro-ph/0701872] (Cited on page 48.)

Raymond, J.C., Cox, D.P. and Smith, B.W., 1976, "Radiative cooling of a low-density plasma", *Astrophys. J.*, **204**, 290–292. [DOI], [ADS] (Cited on page 30.)

Reale, F., 1999, "Inclination of large coronal loops observed by TRACE", *Solar Phys.*, **190**, 139–144. [DOI], [ADS] (Cited on page 33.)

Reale, F., 2002a, "Stellar Flare Modeling", in *Stellar Coronae in the Chandra and XMM-NEWTON Era*, (Eds.) Favata, F., Drake, J.J., Proceedings of a symposium held at ESTEC, Noordwijk, The Netherlands, 25 – 29 June 2001, vol. 277 of ASP Conference Series, p. 103, Astronomical Society of the Pacific, San Francisco. [ADS] (Cited on page 49.)

Reale, F., 2002b, "More on the Determination of the Coronal Heating Function from Yohkoh Data", *Astrophys. J.*, **580**, 566–573. [DOI], [ADS], [arXiv:astro-ph/0207550] (Cited on pages 16 and 44.)

Reale, F., 2003, "Modeling solar and stellar flares", *Adv. Space Res.*, **32**, 1057–1066. [DOI], [ADS] (Cited on page 49.)

Reale, F., 2005, "Sub-Structuring Dynamics and Heating in Dense Coronal Structures", in *The Dynamic Sun: Challenges for Theory and Observations*, (Eds.) Danesy, D., Poedts, S., De Groof, A., Andries, J., Proceedings of the 11th European Solar Physics Meeting, 11 – 16 September 2005, Leuven, Belgium, vol. SP-600 of ESA Special Publications, ESA Publications Division, Noordwijk. [ADS] (Cited on page 5.)

Reale, F., 2007, "Diagnostics of stellar flares from X-ray observations: from the decay to the rise phase", *Astron. Astrophys.*, **471**, 271–279. [DOI], [ADS], [arXiv:0705.3254] (Cited on pages 34, 35, 36, 37, and 38.)

Reale, F. and Ciaravella, A., 2006, "Analysis of a multi-wavelength time-resolved observation of a coronal loop", *Astron. Astrophys.*, **449**, 1177–1192. [DOI], [ADS], [arXiv:astro-ph/0512397] (Cited on pages 16, 20, and 24.)

Reale, F. and Orlando, S., 2008, "Nonequilibrium of Ionization and the Detection of Hot Plasma in Nanoflare-heated Coronal Loops", *Astrophys. J.*, **684**, 715–724. [DOI], [ADS], [arXiv:0805.3512] (Cited on pages 31 and 34.)

Reale, F. and Peres, G., 2000, "TRACE-derived Temperature and Emission Measure Profiles along Long-lived Coronal Loops: The Role of Filamentation", *Astrophys. J. Lett.*, **528**, L45–L48. [DOI], [ADS], [arXiv:astro-ph/9911096] (Cited on pages 31 and 39.)

Reale, F., Peres, G., Serio, S., Rosner, R. and Schmitt, J.H.M.M., 1988, "Hydrodynamic modeling of an X-ray flare on Proxima Centauri observed by the Einstein telescope", *Astrophys. J.*, **328**, 256–264. [DOI], [ADS] (Cited on page 49.)

Reale, F., Serio, S. and Peres, G., 1993, "Dynamics of the decay of confined stellar X-ray flares", *Astron. Astrophys.*, **272**, 486. [ADS] (Cited on page 36.)

Reale, F., Peres, G. and Serio, S., 1996, "Radiatively-driven downdrafts and redshifts in transition region lines. I. Reference model", *Astron. Astrophys.*, **316**, 215–228. [ADS] (Cited on pages 27 and 40.)

Reale, F., Betta, R., Peres, G., Serio, S. and McTiernan, J., 1997a, "Determination of the length of coronal loops from the decay of X-ray flares I. Solar flares observed with YOHKOH SXT", *Astron. Astrophys.*, **325**, 782–790. [ADS] (Cited on page 36.)

Reale, F., Peres, G. and Serio, S., 1997b, "Radiatively driven downdrafts and redshifts in transition region lines. II. Exploring the parameter space", *Astron. Astrophys.*, **318**, 506–520. [ADS] (Cited on pages 27 and 40.)

Reale, F., Peres, G., Serio, S., Betta, R.M., DeLuca, E.E. and Golub, L., 2000a, "A Brightening Coronal Loop Observed by TRACE. II. Loop Modeling and Constraints on Heating", *Astrophys. J.*, **535**, 423–437. [DOI], [ADS] (Cited on pages 12, 25, 30, and 43.)

Reale, F., Peres, G., Serio, S., DeLuca, E.E. and Golub, L., 2000b, "A Brightening Coronal Loop Observed by TRACE. I. Morphology and Evolution", *Astrophys. J.*, **535**, 412–422. [DOI], [ADS] (Cited on pages 12, 25, and 43.)

Reale, F., Peres, G. and Orlando, S., 2001, "The Sun as an X-Ray Star. III. Flares", *Astrophys. J.*, **557**, 906–920. [DOI], [ADS], [arXiv:astro-ph/0104021] (Cited on page 49.)

Reale, F., Bocchino, F. and Peres, G., 2002, "Modeling non-confined coronal flares: Dynamics and X-ray diagnostics", *Astron. Astrophys.*, **383**, 952–971. [DOI], [ADS], [arXiv:astro-ph/0112333] (Cited on page 49.)

Reale, F., Güdel, M., Peres, G. and Audard, M., 2004, "Modeling an X-ray flare on Proxima Centauri: Evidence of two flaring loop components and of two heating mechanisms at work", *Astron. Astrophys.*, **416**, 733–747. [DOI], [ADS], [arXiv:astro-ph/0312267] (Cited on page 49.)

Reale, F., Nigro, G., Malara, F., Peres, G. and Veltri, P., 2005, "Modeling a Coronal Loop Heated by Magnetohydrodynamic Turbulence Nanoflares", *Astrophys. J.*, **633**, 489–498. [DOI], [ADS], [arXiv:astro-ph/0506694] (Cited on pages 43, 44, and 48.)

Reale, F., Parenti, S., Reeves, K.K., Weber, M., Bobra, M.G., Barbera, M., Kano, R., Narukage, N., Shimojo, M., Sakao, T., Peres, G. and Golub, L., 2007, "Fine Thermal Structure of a Coronal Active Region", *Science*, **318**, 1582–. [DOI], [ADS] (Cited on page 19.)

Reale, F., McTiernan, J.M. and Testa, P., 2009a, "Comparison of Hinode/XRT and RHESSI Detection of Hot Plasma in the Non-Flaring Solar Corona", *Astrophys. J. Lett.*, **704**, L58–L61. [DOI], [ADS], [arXiv:0909.2529] (Cited on pages 8 and 19.)

Reale, F., Testa, P., Klimchuk, J.A. and Parenti, S., 2009b, "Evidence of Widespread Hot Plasma in a Nonflaring Coronal Active Region from Hinode/X-Ray Telescope", *Astrophys. J.*, **698**, 756–765. [DOI], [ADS], [arXiv:0904.0878] (Cited on pages 16, 19, and 22.)

Reeves, E.M., Timothy, J.G. and Huber, M.C.E., 1977, "Extreme UV spectroheliometer on the Apollo Telescope Mount", *Appl. Optics*, **16**, 837–848. [ADS] (Cited on page 6.)

Reeves, K.K. and Warren, H.P., 2002, "Modeling the Cooling of Postflare Loops", *Astrophys. J.*, **578**, 590–597. [DOI], [ADS] (Cited on page 34.)

Reidy, W.P., Vaiana, G.S., Zehnpfennig, T. and Giacconi, R., 1968, "Study of X-Ray Images of the Sun at Solar Minimum", *Astrophys. J.*, **151**, 333. [DOI], [ADS] (Cited on page 6.)

Rosner, R., Tucker, W.H. and Vaiana, G.S., 1978, "Dynamics of the quiescent solar corona", *Astrophys. J.*, **220**, 643–665. [DOI], [ADS] (Cited on pages 6, 24, 29, and 32.)

Rosner, R., Golub, L. and Vaiana, G.S., 1985, "On stellar X-ray emission", *Annu. Rev. Astron. Astrophys.*, **23**, 413–452. [DOI], [ADS] (Cited on page 49.)

Rottman, G.J., Hassler, D.D., Jones, M.D. and Orrall, F.Q., 1990, "The systematic radial downflow in the transition region of the quiet sun from limb-to-limb observations of the C IV resonance lines", *Astrophys. J.*, **358**, 693–697. [DOI], [ADS] (Cited on page 27.)

Saito, K. and Billings, D.E., 1964, "Polarimetric Observations of a Coronal Condensation", *Astrophys. J.*, **140**, 760. [DOI], [ADS] (Cited on page 12.)

Sakamoto, Y., Tsuneta, S. and Vekstein, G., 2008, "Observational Appearance of Nanoflares with SXT and TRACE", *Astrophys. J.*, **689**, 1421–1432. [DOI], [ADS] (Cited on pages 26 and 45.)

Sakamoto, Y., Tsuneta, S. and Vekstein, G., 2009, "A Nanoflare Heating Model and Comparison with Observations", *Astrophys. J.*, **703**, 2118–2130. [DOI], [ADS] (Cited on page 45.)

Sakurai, T., 1981, "Calculation of force-free magnetic field with non-constant α", *Solar Phys.*, **69**, 343–359. [DOI], [ADS] (Cited on page 6.)

Sandman, A.W., Aschwanden, M.J., DeRosa, M.L., Wülser, J.P. and Alexander, D., 2009, "Comparison of STEREO/EUVI Loops with Potential Magnetic Field Models", *Solar Phys.*, **259**, 1–11. [DOI], [ADS] (Cited on page 12.)

Sanz-Forcada, J., Brickhouse, N.S. and Dupree, A.K., 2003, "The Structure of Stellar Coronae in Active Binary Systems", *Astrophys. J. Suppl. Ser.*, **145**, 147–179. [DOI], [ADS], [arXiv:astro-ph/0210652] (Cited on page 49.)

Scelsi, L., Maggio, A., Peres, G. and Pallavicini, R., 2005, "Coronal properties of G-type stars in different evolutionary phases", *Astron. Astrophys.*, **432**, 671–685. [DOI], [ADS], [arXiv:astro-ph/0501631] (Cited on page 49.)

Schmelz, J.T., 2002, "Are Coronal Loops Isothermal?", *Astrophys. J. Lett.*, **578**, L161–L164. [DOI], [ADS] (Cited on page 20.)

Schmelz, J.T., Scopes, R.T., Cirtain, J.W., Winter, H.D. and Allen, J.D., 2001, "Observational Constraints on Coronal Heating Models Using Coronal Diagnostics Spectrometer and Soft X-Ray Telescope Data", *Astrophys. J.*, **556**, 896–904. [DOI], [ADS] (Cited on pages 19 and 22.)

Schmelz, J.T., Beene, J.E., Nasraoui, K., Blevins, H.T., Martens, P.C.H. and Cirtain, J.W., 2003, "The Effect of Background Subtraction on the Temperature of EIT Coronal Loops", *Astrophys. J.*, **599**, 604–614. [DOI], [ADS] (Cited on pages 16 and 20.)

Schmelz, J.T., Nasraoui, K., Richardson, V.L., Hubbard, P.J., Nevels, C.R. and Beene, J.E., 2005, "All Coronal Loops Are the Same: Evidence to the Contrary", *Astrophys. J. Lett.*, **627**, L81–L84. [DOI], [ADS], [arXiv:astro-ph/0505593] (Cited on pages 20 and 21.)

Schmelz, J.T., Kashyap, V.L. and Weber, M.A., 2007a, "Coronal Heat: Solar Loop Temperatures from TRACE Triple-Filter Data", *Astrophys. J. Lett.*, **660**, L157–L160. [DOI], [ADS] (Cited on page 22.)

Schmelz, J.T., Nasraoui, K., Del Zanna, G., Cirtain, J.W., DeLuca, E.E. and Mason, H.E., 2007b, "Coronal Diagnostic Spectrometer Observations of Isothermal and Multithermal Coronal Loops", *Astrophys. J. Lett.*, **658**, L119–L122. [DOI], [ADS] (Cited on page 20.)

Schmelz, J.T., Scott, J. and Rightmire, L.A., 2008, "May Day! Coronal Loop Temperatures from the Hinode EUV Imaging Spectrometer", *Astrophys. J. Lett.*, **684**, L115–L118. [DOI], [ADS] (Cited on page 23.)

Schmelz, J.T., Nasraoui, K., Rightmire, L.A., Kimble, J.A., Del Zanna, G., Cirtain, J.W., DeLuca, E.E. and Mason, H.E., 2009a, "Are Coronal Loops Isothermal or Multithermal?", *Astrophys. J.*, **691**, 503–515. [DOI], [ADS], [arXiv:0901.3281] (Cited on page 23.)

Schmelz, J.T., Saar, S.H., DeLuca, E.E., Golub, L., Kashyap, V.L., Weber, M.A. and Klimchuk, J.A., 2009b, "Hinode X-Ray Telescope Detection of Hot Emission from Quiescent Active Regions: A Nanoflare Signature?", *Astrophys. J. Lett.*, **693**, L131–L135. [DOI], [ADS], [arXiv:0901.3122] (Cited on page 19.)

Schmidt, H.U., 1964, "On the Observable Effects of Magnetic Energy Storage and Release Connected With Solar Flares", in *The Physics of Solar Flares*, (Ed.) Hess, W.N., Proceedings of the AAS-NASA Symposium held 28 – 30 October, 1963 at the Goddard Space Flight Center, Greenbelt, MD, vol. SP-50 of NASA Special Publication, p. 107, NASA, Washington, DC. [ADS] (Cited on page 6.)

Schmieder, B., Rust, D.M., Georgoulis, M.K., Démoulin, P. and Bernasconi, P.N., 2004, "Emerging Flux and the Heating of Coronal Loops", *Astrophys. J.*, **601**, 530–545. [DOI], [ADS] (Cited on page 14.)

Schmitt, J.H.M.M., Collura, A., Sciortino, S., Vaiana, G.S., Harnden Jr, F.R. and Rosner, R., 1990, "Einstein Observatory coronal temperatures of late-type stars", *Astrophys. J.*, **365**, 704–728. [DOI], [ADS] (Cited on page 49.)

Schrijver, C.J., 2007, "Braiding-induced Interchange Reconnection of the Magnetic Field and the Width of Solar Coronal Loops", *Astrophys. J. Lett.*, **662**, L119–L122. [DOI], [ADS] (Cited on page 13.)

Schrijver, C.J., Sandman, A.W., Aschwanden, M.J. and DeRosa, M.L., 2004, "The Coronal Heating Mechanism as Identified by Full-Sun Visualizations", *Astrophys. J.*, **615**, 512–525. [DOI], [ADS] (Cited on page 47.)

Seaton, D.B., Winebarger, A.R., DeLuca, E.E., Golub, L., Reeves, K.K. and Gallagher, P.T., 2001, "Active Region Transient Events Observed with TRACE", *Astrophys. J. Lett.*, **563**, L173–L177. [DOI], [ADS] (Cited on page 25.)

Selwa, M. and Ofman, L., 2009, "3-D numerical simulations of coronal loops oscillations", *Ann. Geophys.*, **27**, 3899–3908. [DOI], [ADS] (Cited on page 31.)

Serio, S., Peres, G., Vaiana, G.S., Golub, L. and Rosner, R., 1981, "Closed coronal structures. II. Generalized hydrostatic model", *Astrophys. J.*, **243**, 288–300. [DOI], [ADS] (Cited on pages 30 and 33.)

Serio, S., Reale, F., Jakimiec, J., Sylwester, B. and Sylwester, J., 1991, "Dynamics of flaring loops I. Thermodynamic decay scaling laws", *Astron. Astrophys.*, **241**, 197–202. [ADS] (Cited on pages 36 and 37.)

Sheeley Jr, N.R., 1980, "Temporal variations of loop structures in the solar atmosphere", *Solar Phys.*, **66**, 79–87. [DOI], [ADS] (Cited on page 24.)

Shimizu, T., 1995, "Energetics and Occurrence Rate of Active-Region Transient Brightenings and Implications for the Heating of the Active-Region Corona", *Publ. Astron. Soc. Japan*, **47**, 251–263. [ADS] (Cited on page 44.)

Shimizu, T. and Tsuneta, S., 1997, "Deep Survey of Solar Nanoflares with YOHKOH", *Astrophys. J.*, **486**, 1045. [DOI], [ADS] (Cited on page 45.)

Shimizu, T., Tsuneta, S., Acton, L.W., Lemen, J.R., Ogawara, Y. and Uchida, Y., 1994, "Morphology of active region transient brightenings with the YOHKOH Soft X-ray Telescope", *Astrophys. J.*, **422**, 906–911. [DOI], [ADS] (Cited on page 25.)

Shimojo, M., Kurokawa, H. and Yoshimura, K., 2002, "Dynamical Features and Evolutional Characteristics of Brightening Coronal Loops", *Solar Phys.*, **206**, 133–142. [DOI], [ADS] (Cited on page 25.)

Spadaro, D., Noci, G., Zappala, R.A. and Antiochos, S.K., 1990, "The effect of nonequilibrium ionization on ultraviolet line shifts in the solar transition region", *Astrophys. J.*, **355**, 342–347. [DOI], [ADS] (Cited on page 40.)

Spadaro, D., Lanza, A.F., Lanzafame, A.C., Karpen, J.T., Antiochos, S.K., Klimchuk, J.A. and MacNeice, P.J., 2003, "A Transient Heating Model for Coronal Structure and Dynamics", *Astrophys. J.*, **582**, 486–494. [DOI], [ADS] (Cited on page 44.)

Spitzer Jr, L., 1962, *Physics of Fully Ionized Gases*, vol. 3 of Interscience Tracts on Physics and Astronomy, Interscience, New York, 2nd rev. edn. (Cited on page 30.)

Steinolfson, R.S. and Davila, J.M., 1993, "Coronal heating by the resonant absorption of Alfvén waves: Importance of the global mode and scaling laws", *Astrophys. J.*, **415**, 354–363. [DOI], [ADS] (Cited on page 46.)

Stelzer, B., Burwitz, V., Audard, M., Güdel, M., Ness, J.-U., Grosso, N., Neuhäuser, R., Schmitt, J.H.M.M., Predehl, P. and Aschenbach, B., 2002, "Simultaneous X-ray spectroscopy of YY Gem with Chandra and XMM-Newton", *Astron. Astrophys.*, **392**, 585–598. [DOI], [ADS], [arXiv:astro-ph/0206429] (Cited on page 37.)

Strong, K.T., Harvey, K., Hirayama, T., Nitta, N., Shimizu, T. and Tsuneta, S., 1992, "Observations of the variability of coronal bright points by the Soft X-ray Telescope on YOHKOH", *Publ. Astron. Soc. Japan*, **44**, L161–L166. [ADS] (Cited on page 25.)

Sylwester, B., Sylwester, J., Serio, S., Reale, F., Bentley, R.D. and Fludra, A., 1993, "Dynamics of flaring loops III. Interpretation of flare evolution in the emission measure-temperature diagram", *Astron. Astrophys.*, **267**, 586–594. [ADS] (Cited on pages 36 and 37.)

Sylwester, J., Gaicki, I., Kordylewski, Z., Nowak, M., Kowalinski, S., Sjarkowski, M., Bentley, W., Trzebinski, R.D., Whyndham, M.W., Guttridge, P.R., Culhane, J.L., Lang, J., Phillips, K.J.H., Brown, C.M., Doschek, G.A., Oraevsky, V.N., Boldyrev, S.I., Kopaev, I.M., Stepanov, A.I. and Klepikov, V.Y., 1998, "RESIK: High Sensitivity Soft X-ray Spectrometer for the Study of Solar Flare Plasma", in *A Crossroads for European Solar and Heliospheric Physics: Recent Achievements and Future Mission Possibilities*, (Eds.) Priest, E.R., Moreno-Insertis, F., Harris, R.A., Proceedings of the ESA/IAC Conference, Puerto de la Cruz, Tenerife, Canary Islands, Spain, March 23 – 27 1998, vol. SP-417 of ESA Special Publications, p. 313, ESA Publications Division, Noordwijk. [ADS] (Cited on page 7.)

Sylwester, J., Kuzin, S., Kotov, Y.D., Farnik, F. and Reale, F., 2008, "SphinX: A fast solar Photometer in X-rays", *J. Astrophys. Astron.*, **29**, 339–343. [DOI], [ADS] (Cited on page 7.)

Tanaka, Y., 1983, "Introduction to HINOTORI", *Solar Phys.*, **86**, 3–6. [DOI], [ADS] (Cited on page 7.)

Taroyan, Y., 2009, "Alfvén Instability in Coronal Loops With Siphon Flows", *Astrophys. J.*, **694**, 69–75. [DOI], [ADS] (Cited on page 42.)

Taroyan, Y., Erdélyi, R., Doyle, J.G. and Bradshaw, S.J., 2005, "Footpoint excitation of standing acoustic waves in coronal loops", *Astron. Astrophys.*, **438**, 713–720. [DOI], [ADS] (Cited on page 42.)

Telleschi, A., Güdel, M., Briggs, K., Audard, M., Ness, J.-U. and Skinner, S.L., 2005, "Coronal Evolution of the Sun in Time: High-Resolution X-Ray Spectroscopy of Solar Analogs with Different Ages", *Astrophys. J.*, **622**, 653–679. [DOI], [ADS], [arXiv:astro-ph/0503546] (Cited on page 49.)

Teriaca, L., Banerjee, D. and Doyle, J.G., 1999a, "SUMER observations of Doppler shift in the quiet Sun and in an active region", *Astron. Astrophys.*, **349**, 636–648. [ADS] (Cited on page 27.)

Teriaca, L., Doyle, J.G., Erdélyi, R. and Sarro, L.M., 1999b, "New insight into transition region dynamics via SUMER observations and numerical modelling", *Astron. Astrophys.*, **352**, L99–L102. [ADS] (Cited on pages 27 and 40.)

Teriaca, L., Madjarska, M.S. and Doyle, J.G., 2002, "Transition region explosive events: Do they have a coronal counterpart?", *Astron. Astrophys.*, **392**, 309–317. [DOI], [ADS] (Cited on page 27.)

Teriaca, L., Banerjee, D., Falchi, A., Doyle, J.G. and Madjarska, M.S., 2004, "Transition region small-scale dynamics as seen by SUMER on SOHO", *Astron. Astrophys.*, **427**, 1065–1074. [DOI], [ADS] (Cited on page 27.)

Terzo, S. and Reale, F., 2010, "On the importance of background subtraction in the analysis of coronal loops observed with TRACE", *Astron. Astrophys.*, **515**, A7. [DOI], [ADS], [arXiv:1002.2121 [astro-ph.SR]] (Cited on page 16.)

Testa, P., Peres, G., Reale, F. and Orlando, S., 2002, "Temperature and Density Structure of Hot and Cool Loops Derived from the Analysis of TRACE Data", *Astrophys. J.*, **580**, 1159–1171. [DOI], [ADS] (Cited on pages 14 and 16.)

Testa, P., Peres, G. and Reale, F., 2005, "Emission Measure Distribution in Loops Impulsively Heated at the Footpoints", *Astrophys. J.*, **622**, 695–703. [DOI], [ADS], [arXiv:astro-ph/0412482] (Cited on pages 44 and 45.)

Thomas, J.H., 1988, "Siphon flows in isolated magnetic flux tubes", *Astrophys. J.*, **333**, 407–419. [DOI], [ADS] (Cited on page 40.)

Thomas, J.H. and Montesinos, B., 1990, "Siphon flows in isolated magnetic flux tubes. III. The equilibrium path of the flux-tube arch", *Astrophys. J.*, **359**, 550–559. [DOI], [ADS] (Cited on page 40.)

Thomas, J.H. and Montesinos, B., 1991, "Siphon flows in isolated magnetic flux tubes. IV. Critical flows with standing tube shocks", *Astrophys. J.*, **375**, 404–413. [DOI], [ADS] (Cited on page 40.)

Title, A.M., 2010, "AIA on SDO", 216th AAS Meeting, 23 – 27 May 2010, Miami, FL, conference paper. [ADS] (Cited on page 45.)

Tomczyk, S., McIntosh, S.W., Keil, S.L., Judge, P.G., Schad, T., Seeley, D.H. and Edmondson, J., 2007, "Alfvén Waves in the Solar Corona", *Science*, **317**, 1192–1196. [DOI], [ADS] (Cited on page 46.)

Tousey, R., Bartoe, J.-D.F., Brueckner, G.E. and Purcell, J.D., 1977, "Extreme ultraviolet spectroheliograph ATM experiment S082A", *Appl. Optics*, **16**, 870–878. [ADS] (Cited on page 6.)

Tripathi, D., Mason, H.E., Young, P.R. and Del Zanna, G., 2008, "Density structure of an active region and associated moss using Hinode/EIS", *Astron. Astrophys.*, **481**, L53–L56. [DOI], [ADS], [arXiv:0802.3311] (Cited on page 23.)

Tripathi, D., Mason, H.E., Dwivedi, B.N., Del Zanna, G. and Young, P.R., 2009, "Active Region Loops: Hinode/Extreme-Ultraviolet Imaging Spectrometer Observations", *Astrophys. J.*, **694**, 1256–1265. [DOI], [ADS], [arXiv:0901.0095] (Cited on pages 20, 24, 28, and 40.)

Tsuneta, S., Acton, L., Bruner, M., Lemen, J., Brown, W., Caravalho, R., Catura, R., Freeland, S., Jurcevich, B. and Owens, J., 1991, "The soft X-ray telescope for the SOLAR-A mission", *Solar Phys.*, **136**, 37–67. [DOI], [ADS] (Cited on page 7.)

Tsuneta, S., Hara, H., Shimizu, T., Acton, L.W., Strong, K.T., Hudson, H.S. and Ogawara, Y., 1992, "Observation of a solar flare at the limb with the YOHKOH Soft X-ray Telescope", *Publ. Astron. Soc. Japan*, **44**, L63–L69. [ADS] (Cited on page 18.)

Uchida, Y., 1970, "Diagnosis of Coronal Magnetic Structure by Flare-Associated Hydromagnetic Disturbances", *Publ. Astron. Soc. Japan*, **22**, 341–364. [ADS] (Cited on page 11.)

Ugarte-Urra, I., Doyle, J.G., Walsh, R.W. and Madjarska, M.S., 2005, "Electron density along a coronal loop observed with CDS/SOHO", *Astron. Astrophys.*, **439**, 351–359. [DOI], [ADS] (Cited on page 15.)

Ugarte-Urra, I., Warren, H.P. and Brooks, D.H., 2009, "Active Region Transition Region Loop Populations and Their Relationship to the Corona", *Astrophys. J.*, **695**, 642–651. [DOI], [ADS], [arXiv:0901.1075] (Cited on page 20.)

Ulrich, R.K., 1996, "Observations of Magnetohydrodynamic Oscillations in the Solar Atmosphere with Properties of Alfvén Waves", *Astrophys. J.*, **465**, 436. [DOI], [ADS] (Cited on page 46.)

Uzdensky, D.A., 2007, "The Fast Collisionless Reconnection Condition and the Self-Organization of Solar Coronal Heating", *Astrophys. J.*, **671**, 2139–2153. [DOI], [ADS], [arXiv:0707.1316] (Cited on page 48.)

Vaiana, G.S. and Rosner, R., 1978, "Recent advances in coronal physics", *Annu. Rev. Astron. Astrophys.*, **16**, 393–428. [DOI], [ADS] (Cited on pages 5 and 6.)

Vaiana, G.S., Reidy, W.P., Zehnpfennig, T., Vanspeybroeck, L. and Giacconi, R., 1968, "X-ray Structures of the Sun during the Importance 1N Flare of 8 June 1968", *Science*, **161**, 564–567. [DOI], [ADS] (Cited on page 6.)

Vaiana, G.S., Krieger, A.S. and Timothy, A.F., 1973, "Identification and Analysis of Structures in the Corona from X-Ray Photography", *Solar Phys.*, **32**, 81–116. [DOI], [ADS] (Cited on pages 6, 8, 10, and 15.)

van Ballegooijen, A.A., 1986, "Cascade of magnetic energy as a mechanism of coronal heating", *Astrophys. J.*, **311**, 1001–1014. [DOI], [ADS] (Cited on page 47.)

van den Oord, G.H.J. and Mewe, R., 1989, "The X-ray flare and the quiescent emission from Algol as detected by EXOSAT", *Astron. Astrophys.*, **213**, 245–260. [ADS] (Cited on page 37.)

van den Oord, G.H.J., Mewe, R. and Brinkman, A.C., 1988, "An EXOSAT observation of an X-ray flare and quiescent emission from the RS CVn binary σ^2 CrB", *Astron. Astrophys.*, **205**, 181–196. [ADS] (Cited on page 37.)

Vekstein, G., 2009, "Probing nanoflares with observed fluctuations of the coronal EUV emission", *Astron. Astrophys.*, **499**, L5–L8. [DOI], [ADS] (Cited on pages 14, 15, and 44.)

Vekstein, G. and Katsukawa, Y., 2000, "Scaling Laws for a Nanoflare-Heated Solar Corona", *Astrophys. J.*, **541**, 1096–1103. [DOI], [ADS] (Cited on page 45.)

Vekstein, G.E. and Jain, R., 2003, "Signatures of a nanoflare heated solar corona", *Plasma Phys. Control. Fusion*, **45**, 535–545. [DOI], [ADS] (Cited on page 45.)

Vernazza, J.E., Avrett, E.H. and Loeser, R., 1981, "Structure of the Solar Chromosphere. III. Models of the EUV Brightness Components of the Quiet Sun", *Astrophys. J. Suppl. Ser.*, **45**, 635–725. [DOI], [ADS] (Cited on page 30.)

Vesecky, J.F., Antiochos, S.K. and Underwood, J.H., 1979, "Numerical modeling of quasi-static coronal loops. I. Uniform energy input", *Astrophys. J.*, **233**, 987–997. [DOI], [ADS] (Cited on pages 29 and 32.)

Wang, J., Shibata, K., Nitta, N., Slater, G.L., Savy, S.K. and Ogawara, Y., 1997, "Shrinkage of Coronal X-Ray Loops", *Astrophys. J. Lett.*, **478**, L41. [DOI], [ADS] (Cited on page 25.)

Wang, T.J., Ofman, L. and Davila, J.M., 2009, "Propagating Slow Magnetoacoustic Waves in Coronal Loops Observed by Hinode/EIS", *Astrophys. J.*, **696**, 1448–1460. [DOI], [ADS], [arXiv:0902.4480 [astro-ph.SR]] (Cited on page 47.)

Warren, H.P., 2006, "Multithread Hydrodynamic Modeling of a Solar Flare", *Astrophys. J.*, **637**, 522–530. [DOI], [ADS], [arXiv:astro-ph/0507328] (Cited on page 34.)

Warren, H.P. and Winebarger, A.R., 2006, "Hydrostatic Modeling of the Integrated Soft X-Ray and Extreme Ultraviolet Emission in Solar Active Regions", *Astrophys. J.*, **645**, 711–719. [DOI], [ADS], [arXiv:astro-ph/0602052] (Cited on pages 31 and 39.)

Warren, H.P. and Winebarger, A.R., 2007, "Static and Dynamic Modeling of a Solar Active Region", *Astrophys. J.*, **666**, 1245–1255. [DOI], [ADS], [arXiv:astro-ph/0609023] (Cited on page 45.)

Warren, H.P., Winebarger, A.R. and Hamilton, P.S., 2002, "Hydrodynamic Modeling of Active Region Loops", *Astrophys. J. Lett.*, **579**, L41–L44. [DOI], [ADS] (Cited on pages 23, 31, 39, and 44.)

Warren, H.P., Winebarger, A.R. and Mariska, J.T., 2003, "Evolving Active Region Loops Observed with the Transition Region and Coronal explorer. II. Time-dependent Hydrodynamic Simulations", *Astrophys. J.*, **593**, 1174–1186. [DOI], [ADS] (Cited on pages 23, 39, and 44.)

Warren, H.P., Ugarte-Urra, I., Doschek, G.A., Brooks, D.H. and Williams, D.R., 2008a, "Observations of Active Region Loops with the EUV Imaging Spectrometer on Hinode", *Astrophys. J. Lett.*, **686**, L131–L134. [DOI], [ADS], [arXiv:0808.3227] (Cited on pages 23 and 24.)

Warren, H.P., Winebarger, A.R., Mariska, J.T., Doschek, G.A. and Hara, H., 2008b, "Observation and Modeling of Coronal 'Moss' With the EUV Imaging Spectrometer on Hinode", *Astrophys. J.*, **677**, 1395–1400. [DOI], [ADS], [arXiv:0709.0396] (Cited on page 23.)

Warren, H.P., Winebarger, A.R. and Brooks, D.H., 2010, "Evidence for Steady Heating: Observations of an Active Region Core with Hinode and TRACE", *Astrophys. J.*, **711**, 228–238. [DOI], [ADS], [arXiv:0910.0458 [astro-ph.SR]] (Cited on pages 19, 25, 45, and 48.)

Watanabe, T., Hara, H., Yamamoto, N., Kato, D., Sakaue, H.A., Murakami, I., Kato, T., Nakamura, N. and Young, P.R., 2009, "Fe XIII Density Diagnostics in the EIS Observing Wavelengths", *Astrophys. J.*, **692**, 1294–1304. [DOI], [ADS] (Cited on page 18.)

Weber, M.A., Schmelz, J.T., DeLuca, E.E. and Roames, J.K., 2005, "Isothermal Bias of the 'Filter Ratio' Method for Observations of Multithermal Plasma", *Astrophys. J. Lett.*, **635**, L101–L104. [DOI], [ADS] (Cited on page 22.)

West, M.J., Bradshaw, S.J. and Cargill, P.J., 2008, "On the Lifetime of Hot Coronal Plasmas Arising from Nanoflares", *Solar Phys.*, **252**, 89–100. [DOI], [ADS] (Cited on page 32.)

White, S.M., Kundu, M.R. and Gopalswamy, N., 1991, "Strong magnetic fields and inhomogeneity in the solar corona", *Astrophys. J. Lett.*, **366**, L43–L46. [DOI], [ADS] (Cited on page 11.)

Wilhelm, K., Curdt, W., Marsch, E., Schühle, U., Lemaire, P., Gabriel, A., Vial, J.-C., Grewing, M., Huber, M.C.E., Jordan, S.D., Poland, A.I., Thomas, R.J., Kühne, M., Timothy, J.G., Hassler, D.M. and Siegmund, O.H.W., 1995, "SUMER – Solar Ultraviolet Measurements of Emitted Radiation", *Solar Phys.*, **162**, 189–231. [DOI], [ADS] (Cited on page 7.)

Winebarger, A.R. and Warren, H.P., 2004, "Can TRACE Extreme-Ultraviolet Observations of Cooling Coronal Loops Be Used to Determine the Heating Parameters?", *Astrophys. J. Lett.*, **610**, L129–L132. [DOI], [ADS] (Cited on page 44.)

Winebarger, A.R. and Warren, H.P., 2005, "Cooling Active Region Loops Observed with SXT and TRACE", *Astrophys. J.*, **626**, 543–550. [DOI], [ADS], [arXiv:astro-ph/0502270] (Cited on pages 15 and 32.)

Winebarger, A.R., Emslie, A.G., Mariska, J.T. and Warren, H.P., 1999, "Analyzing the Energetics of Explosive Events Observed by SUMER on SOHO", *Astrophys. J.*, **526**, 471–477. [DOI], [ADS] (Cited on page 27.)

Winebarger, A.R., DeLuca, E.E. and Golub, L., 2001, "Apparent Flows above an Active Region Observed with the Transition Region and Coronal Explorer", *Astrophys. J. Lett.*, **553**, L81–L84. [DOI], [ADS] (Cited on pages 27 and 39.)

Winebarger, A.R., Emslie, A.G., Mariska, J.T. and Warren, H.P., 2002a, "Energetics of Explosive Events Observed with SUMER", *Astrophys. J.*, **565**, 1298–1311. [DOI], [ADS] (Cited on page 27.)

Winebarger, A.R., Updike, A.C. and Reeves, K.K., 2002b, "Correlating Transition Region Explosive Events with Extreme-Ultraviolet Brightenings", *Astrophys. J. Lett.*, **570**, L105–L108. [DOI], [ADS] (Cited on page 27.)

Winebarger, A.R., Warren, H., van Ballegooijen, A., DeLuca, E.E. and Golub, L., 2002c, "Steady Flows Detected in Extreme-Ultraviolet Loops", *Astrophys. J. Lett.*, **567**, L89–L92. [DOI], [ADS] (Cited on pages 27, 39, and 42.)

Winebarger, A.R., Warren, H.P. and Mariska, J.T., 2003a, "Transition Region and Coronal Explorer and Soft X-Ray Telescope Active Region Loop Observations: Comparisons with Static Solutions of the Hydrodynamic Equations", *Astrophys. J.*, **587**, 439–449. [DOI], [ADS] (Cited on pages 23, 24, 32, and 39.)

Winebarger, A.R., Warren, H.P. and Seaton, D.B., 2003b, "Evolving Active Region Loops Observed with the Transition Region and Coronal Explorer. I. Observations", *Astrophys. J.*, **593**, 1164–1173. [DOI], [ADS] (Cited on pages 39 and 44.)

Winebarger, A.R., Warren, H.P. and Falconer, D.A., 2008, "Modeling X-Ray Loops and EUV 'Moss' in an Active Region Core", *Astrophys. J.*, **676**, 672–679. [DOI], [ADS], [arXiv:0712.0756] (Cited on page 34.)

Wragg, M.A. and Priest, E.R., 1981, "The temperature-density structure of coronal loops in hydrostatic equilibrium", *Solar Phys.*, **70**, 293–313. [DOI], [ADS] (Cited on page 33.)

Yokoyama, T. and Shibata, K., 2001, "Magnetohydrodynamic Simulation of a Solar Flare with Chromospheric Evaporation Effect Based on the Magnetic Reconnection Model", *Astrophys. J.*, **549**, 1160–1174. [DOI], [ADS] (Cited on page 32.)

Yoshida, T. and Tsuneta, S., 1996, "Temperature Structure of Solar Active Regions", *Astrophys. J.*, **459**, 342. [DOI], [ADS] (Cited on page 18.)

Yoshida, T., Tsuneta, S., Golub, L., Strong, K. and Ogawara, Y., 1995, "Temperature Structure of the Solar Corona: Comparison of the NIXT and YOHKOH X-Ray Images", *Publ. Astron. Soc. Japan*, **47**, L15–L19. [ADS] (Cited on page 19.)

Young, P.R., Watanabe, T., Hara, H. and Mariska, J.T., 2009, "High-precision density measurements in the solar corona. I. Analysis methods and results for Fe XII and Fe XIII", *Astron. Astrophys.*, **495**, 587–606. [DOI], [ADS], [arXiv:0805.0958] (Cited on page 18.)

Zhitnik, I.A., Bugaenko, O.I., Ignat'ev, A.P., Krutov, V.V., Kuzin, S.V., Mitrofanov, A.V., Oparin, S.N., Pertsov, A.A., Slemzin, V.A., Stepanov, A.I. and Urnov, A.M., 2003, "Dynamic 10 MK plasma structures observed in monochromatic full-Sun images by the SPIRIT spectroheliograph on the CORONAS-F mission", *Mon. Not. R. Astron. Soc.*, **338**, 67–71. [DOI], [ADS] (Cited on page 7.)

Zirker, J.B., 1993, "Coronal heating", *Solar Phys.*, **148**, 43–60. [DOI], [ADS] (Cited on page 5.)